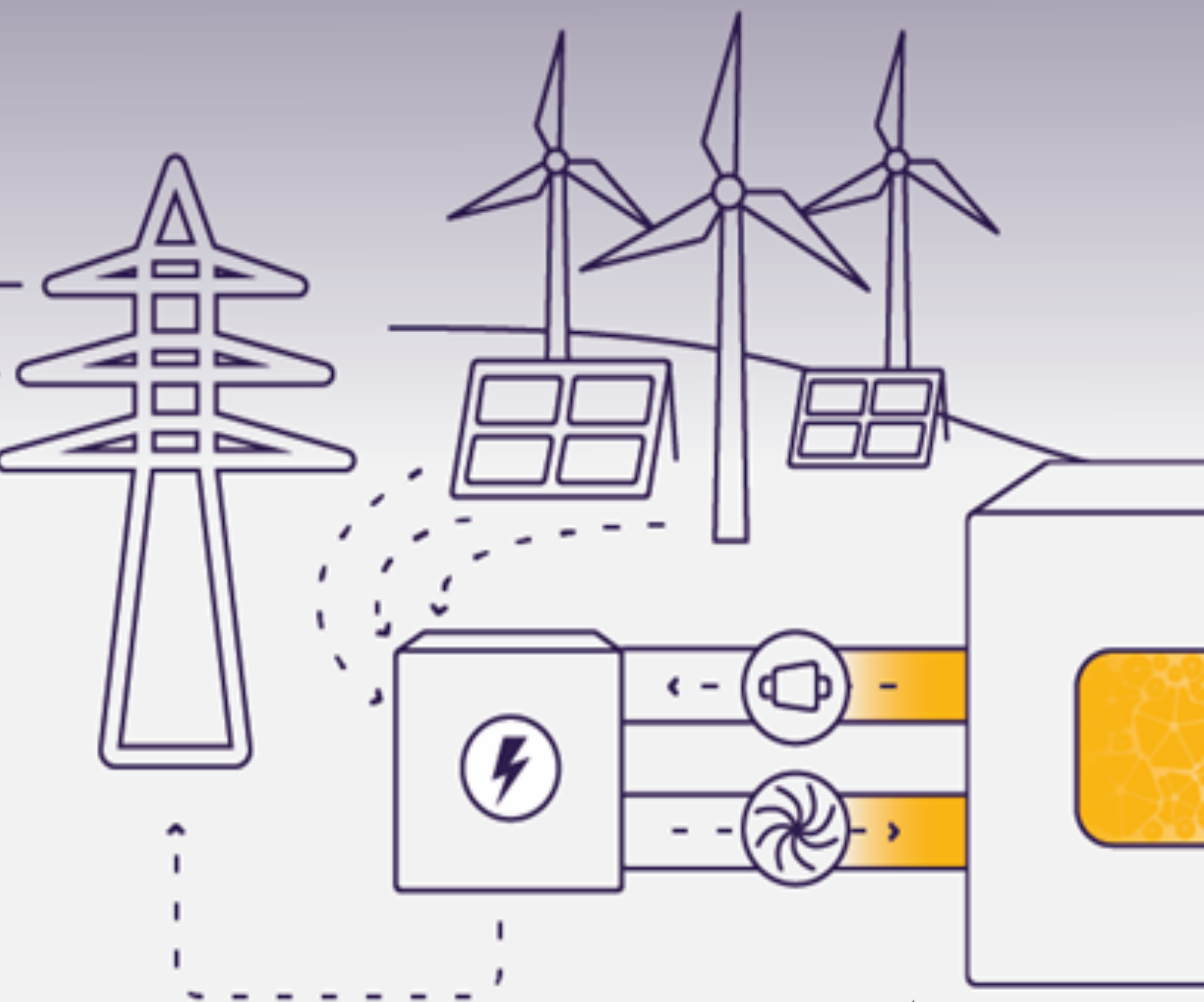


ENERGY SYSTEM INTEGRATION AND MARKET MODELLING OF AN INNOVATIVE ELECTRIC THERMAL ENERGY STORAGE

María de la Esperanza Mata Pérez

January, 2020



ENERGY SYSTEM INTEGRATION AND MARKET
MODELLING OF AN INNOVATIVE ELECTRIC
THERMAL ENERGY STORAGE (ETES)

A thesis submitted to the Delft University of Technology in partial
fulfillment of the requirements for the degree of

Master of Science in Sustainable Energy Technology

by

María de la Esperanza Mata Pérez

January 2020

María de la Esperanza Mata Pérez: *Energy System Integration and Market Modelling of an Innovative Electric Thermal Energy Storage (ETES)* (2020)

The work in this thesis was made in collaboration with:



Faculty of Electrical Engineering, Mathematics and
Computer Science, and Faculty of Technology Policy
and Management
Delft University of Technology

Thesis Committee: Prof.dr.ir. P.M. Herder
Dr.ir. R.A. Verzijlbergh
Dr.ir. L.J. de Vries
Siemens Gamesa Supervisor: Jennifer Verena Wagner

EXECUTIVE SUMMARY

The increasing penetration of renewable energy sources is challenging the current state of affairs of the energy system. As a result of their fluctuating nature, high renewable power shares will require the introduction of flexible assets in the power generation fleet, as well as in the power transmission and distribution networks.

Large-scale thermal energy storage offers a cost-effective solution to increase the flexibility of the future energy system and to avoid the need for extensive fossil backup capacities. In addition, the storage of electric power into thermal energy will facilitate the coupling of the electricity and heat sectors, which will be an important contribution for the decarbonization of all energy vectors. With this aim, Siemens Gamesa Renewable Energy has developed an innovative Electric Thermal Energy Storage (ETES) and is now evaluating its commercial positioning. The goal of this thesis is to identify under which boundary conditions there is a business opportunity for the technology, with regards to the future electricity and heat markets. To meet this target, a novel optimization model has been developed as the main tool for the analysis of the storage and its profitability under different situations.

The model integrates the versatility of the technology, which can be designed to charge and discharge electricity or heat by virtue of its modular structure. As regards the boundary conditions, three revenue streams have been included: discharge of electricity to the day-ahead market, discharge of heat to a district heating network, and discharge of high-temperature heat to an energy-intensive industry. The model allows the isolation and combination of each of the aforementioned applications in order to test different conditions. Additionally, it has been developed from a detailed engineering perspective and includes the most relevant components' mechanical limitations and thermodynamic losses. The developed model is one of the first to investigate the operation of an electric thermal energy storage technology in detail, and its integration in the heat and power markets. Thus, the provided formulation greatly contributes to the study of the technology and to the understanding of its potential.

Regarding the analysis of the boundary conditions, it has been conducted in a systematic way in order to isolate the impacts of each of the input variables on the system. The electricity price and the heat demand input curves have been modelled as the addition of periodic sinusoidal curves. This approach has enabled to vary the magnitude and frequency of the components in an structured manner. The frequencies have been obtained from the spectral density analysis of actual data by means of the Fast Fourier Transform algorithm. The remaining input variables, namely the supply power and the heat prices, have been modelled with real wind generation data and with constant values respectively. As regards the storage capacity, the analysis have been carried out for two different

storage capacities (i.e. 834 MWh and 3.34 GWh), to evaluate the impact of the storage scale.

The results have shown that high-temperature heat sale to an energy-intensive industry is the application with the largest revenue potential due to several reasons. Firstly, the volatility of prices should be very large to justify a business model based exclusively on electricity arbitrage. This condition is aggravated by the low discharging efficiency of the steam cycle, compared to the high efficiency of the heat-discharging cycle. Secondly, the investment costs of the system without the Rankine cycle are lower and therefore the break-even price is also lower. Notwithstanding, the break-even price for district heating supply could be achieved under a very ambitious scenario of reduction of emissions, with support schemes in place. Likewise, the electricity arbitrage application would benefit from increasingly recurrent conditions such as high renewable power curtailment or imbalance penalties.

The analysis has also exhibited the great importance of the electricity and heat prices for the business case. Regarding the day-ahead electricity price, the results show that the average is the component with the largest impact on the revenue generation, being lower values more advantageous when heat sales are available. As regards the volatility, the component of the smallest period results in the highest variations in the revenues, as well as in the storage cycles. Lastly, with respect to the variable heat demands, it has been demonstrated that the concurrence of heating load peaks and electricity prices is positive for the business case for district heating, and the opposite effect takes place for the sale of heat to an energy-intensive industry.

ACKNOWLEDGEMENTS

Foremost, I would like to express my sincere gratitude to the people who have made this thesis possible. I would like to thank my supervisor from Siemens Gamesa, Jennifer, for her personal support and continuous trust during the whole project. Her guidance, sometimes beyond what was demanded from her, and her constructive comments have been invaluable for keeping the broader perspective in mind. I would also like to thank Remco and Paulien, my supervisors from TU Delft, whose advice and academic standpoint have been essential to conduct this research. I would like to extend my special thanks to my family and friends, from Spain and abroad, who have always encouraged me to pursue a career in sustainable energy. Last but not least, a big thanks to Jose for his continuous patience and care during these nine months.

Esperanza Mata
Madrid, 01.01.2020

CONTENTS

1	INTRODUCTION	1
1.1	Problem in context	1
1.2	Research objectives and methodology	2
1.3	Literature review	4
1.3.1	Energy storage modelling techniques	5
1.3.2	Trends in the Literature on the role of ETES in the future energy system	8
1.3.3	Academic contribution of this thesis	9
1.4	Outline and structure of the report	10
2	ETES TECHNOLOGY EXPLAINED	11
2.1	Thermal Energy Storage	11
2.1.1	Main thermodynamic principles of Sensible Heat Storage	12
2.1.2	State-of-the-art of Sensible Heat Storage systems	13
2.2	Fundamentals of the ETES concept under research	16
2.2.1	System configuration	16
2.2.2	Charging and discharging mechanisms	18
2.2.3	Technical limitations of the system	20
2.3	Critical comparison to other storage technologies	23
3	POTENTIAL APPLICATIONS	25
3.1	Increased control over fluctuating renewable power generation	25
3.2	Energy arbitrage and grid services	27
3.3	Heat supply to a nearby district heating network	29
3.4	Heat supply to an energy-intensive industry	32
3.5	Flexibility source for thermal power plants	34
4	MODEL FORMULATION	37
4.1	Layout of the system	37
4.2	Nomenclature	38
4.3	Objective function: maximizing the revenue	40
4.4	Constraints	42
4.4.1	System constraints	42
4.4.2	Demand constraints	45
4.4.3	Technical and operational constraints	46
4.5	Rolling horizon framework	49
4.6	Model verification	49
4.7	Financial evaluation	51
5	ANALYSIS APPROACH	53
5.1	Signal processing in the frequency domain	53

5.2	Input signals modelling	54
5.2.1	District heating demand (D_{dhn})	55
5.2.2	High-temperature heat demand (D_{th})	57
5.2.3	Day-ahead market price (R_{el})	59
5.3	Case studies	63
5.3.1	Case 1: Power-to-Power	63
5.3.2	Case 2: Power-to-Power and district heating	64
5.3.3	Case 3: Power-to-Heat	65
5.3.4	Case 4: Power-to-Heat-and-Power	66
5.3.5	Summary of cases	67
6	RESULTS AND DISCUSSION	69
6.1	Case 1: Power-to-Power	69
6.1.1	Rankine cycle efficiency	69
6.1.2	Electricity prices	71
6.2	Case 2: Power-to-Power and district heating	74
6.2.1	District heating price	74
6.2.2	District heating demand profile	75
6.2.3	Rankine cycle efficiency	77
6.2.4	Electricity prices	78
6.3	Case 3: Power-to-Heat	81
6.3.1	High-temperature heat price	81
6.3.2	High-temperature demand profile	83
6.3.3	Electricity prices	88
6.4	Case 4: Power-to-Heat-and-Power	90
6.4.1	District heating price	91
6.4.2	District heating demand	92
6.4.3	High-temperature heat price	93
6.4.4	High-temperature demand profile	95
6.4.5	Rankine cycle efficiency	96
6.4.6	Competitiveness of ETES with natural gas	97
7	CONCLUSIONS	99
7.1	Research findings	99
7.2	Recommendations for future work	103
A	REFERENCE CASE	111
B	FOURIER ANALYSIS	113
C	ADDITIONAL SIMULATION RESULTS	115
C.1	Power-to-Heat	115
C.2	Power-to-Heat-and-Power	117

LIST OF FIGURES

Figure 1.1	A simplified schematic and examples of the optimization approach	6
Figure 1.2	A simplified schematic and examples of the simulation approach	7
Figure 2.1	Basic configuration of the ETES technology	16
Figure 2.2	Dynamics of the charging and discharging of the storage .	19
Figure 2.3	Rankine cycle T-S diagram	21
Figure 2.4	Electricity storage technologies displayed according to their power rating and cost per kWh. Based on [1]	24
Figure 3.1	General timing of electricity markets	27
Figure 3.2	District heating and electricity network example. Adapted from [2]	30
Figure 3.3	Energy industries by heat temperature requirements. Adapted from [3]	33
Figure 4.1	Layout of the system with thermal demand, power generation, and access to a district heat network (DHN)	37
Figure 4.2	Start-up and shut-down energy losses of the Rankine cycle	41
Figure 4.3	Example of the energy, exergy, and exergy loss curves . . .	44
Figure 4.4	Power and thermal losses of the Rankine cycle with steam extraction	46
Figure 4.5	Rolling horizon scheme	49
Figure 4.6	Simulation results of different variables	50
Figure 5.1	Spectral density of the hourly district heating demand of Hamburg	55
Figure 5.2	Real district heating demand and its equivalent artificial signal consisting of the sum of three sines (with periods of a year, a day, and half a day)	57
Figure 5.3	Spectral density of the steam daily demand of an industry	57
Figure 5.4	Real steam demand and its equivalent artificial signal for a random week	58
Figure 5.5	(a) Real annual heat demand data and (b) its equivalent artificial signal consisting of the sum of three sines (with periods of a year, a week and half a week) and white noise	59
Figure 5.6	Spectral density of the 2018 day ahead markets prices of (a) Germany and (b) Spain	60
Figure 5.7	Evolution of the natural gas and carbon dioxide (CO ₂) prices in the Iberian peninsula in 2018	61
Figure 5.8	Real weekly electricity price of Germany and its equivalent artificial signal	62

Figure 5.9	Real weekly electricity price of Spain and its equivalent artificial signal	62
Figure 5.10	Layout of the system for a Power to Power application . . .	63
Figure 5.11	Layout of the system for a Power to Power and district heating application	64
Figure 5.12	Layout of the system for a Power to Heat application . . .	65
Figure 5.13	Layout of the system with the three applications	66
Figure 5.14	Summary of the case studies and their pertinent variables.	67
Figure 6.1	P2P: sensitivity of the net present value (NPV) to changes in the Rankine cycle efficiency, for two different storage capacities	70
Figure 6.2	P2P: comparison of the NPV of electric thermal energy storage (ETES) to other storage technologies with higher efficiencies, for two different storage capacities	71
Figure 6.3	P2P: sensitivity of the NPV to changes in the electricity price coefficients	73
Figure 6.4	P2P and DHN: Sensitivity of the NPV to changes in the district heating price, for two different storage capacities .	75
Figure 6.5	P2P and DHN: sensitivity of the NPV to changes in the district heating price, for a 24h storage and two different demand profiles	76
Figure 6.6	P2P and DHN: sensitivity of NPV to changes in the daily district heating demand fluctuations for a 24h storage . . .	76
Figure 6.7	P2P and DHN: one week simulation of the electricity prices, district heating demand, and district heating sales, for two different demand spreads	77
Figure 6.8	P2P and DHN: sensitivity of the NPV to changes in the Rankine cycle efficiency for two different district heating prices	78
Figure 6.9	P2P and DHN: sensitivity of the NPV to changes in the electricity price coefficients, for a 24h storage	79
Figure 6.10	P2P and DHN: sensitivity of the heat sales to changes in the electricity price coefficients, for a 24h storage	79
Figure 6.11	P2P and DHN: sensitivity of the storage cycles to changes in the electricity price coefficients, for a 24h storage	80
Figure 6.12	P2H: sensitivity of the NPV to changes in the heat price, for two different storage capacities	82
Figure 6.13	P2H: sensitivity analysis of the NPV to changes in the constant heat demand level, for two different storage capacities	84
Figure 6.14	P2H: sensitivity of the NPV to changes in the variability of the heat demand, for two different storage capacities . .	85
Figure 6.15	Yearly plot of the demand moving average, the electricity prices moving average, and a constant demand of 70 MW	85

Figure 6.16	P2H: weekly plot of the heat demand, heat sold, charged power and electricity prices, and the corresponding state of charge of the storage, for oh phase difference between the demand and the electricity prices	86
Figure 6.17	P2H: weekly plot of the heat demand, heat sold, charged power and electricity prices, and the corresponding state of charge of the storage, for 6h phase difference between the demand and the electricity prices	87
Figure 6.18	P2H: sensitivity of the NPV to the phase shift between the heat demand and the electricity price, for a 6h storage . . .	88
Figure 6.19	P2H: sensitivity of the NPV to changes in the electricity price coefficients, for a 6h storage	88
Figure 6.20	P2H: sensitivity of the heat sales to changes in the electricity price coefficients, for a 6h storage	89
Figure 6.21	P2H: sensitivity of the number of cycles to changes in the electricity price coefficients, for a 6h storage	89
Figure 6.22	P2H&P: sensitivity analysis of the NPV to changes in the DHN price, for two different storage capacities	91
Figure 6.23	P2H&P: sensitivity analysis of the electric and thermal discharged powers to changes in the DHN price	92
Figure 6.24	P2H&P: sensitivity analysis of the NPV to changes in the DHN demand, for two different storage capacities	93
Figure 6.25	P2H&P: sensitivity analysis of the electric and thermal discharged powers to changes in the DHN demand	93
Figure 6.26	P2H&P: sensitivity analysis of the NPV to changes in the high-temperature heat price, for two different storage capacities	94
Figure 6.27	P2H&P: sensitivity analysis of the electric and thermal discharged powers to changes in the high-temperature heat price	94
Figure 6.28	P2H&P: sensitivity analysis of the NPV to changes in the high-temperature heat demand, for two different storage capacities	95
Figure 6.29	P2H&P: sensitivity analysis of the electric and thermal discharged powers to changes in the high-temperature heat demand	95
Figure 6.30	P2H&P: sensitivity analysis of the NPV to changes in the Rankine cycle efficiency, for two different storage capacities	96
Figure 6.31	P2H&P: sensitivity analysis of the electric and thermal discharged powers to changes in the Rankine cycle efficiency	97
Figure 6.32	Maximum heat price to be competitive with natural gas considering CO ₂ prices, for three different natural gas scenarios	97
Figure A.1	Flow chart with the process calculation of the revenues of the reference case	112

Figure B.1	Spectral density of the day-ahead market prices of Germany and Spain, from 2014 to 2018	113
Figure C.1	P2H: sensitivity analysis of the heat sales to changes in the constant heat demand level, for two different storage capacities	115
Figure C.2	P2H: sensitivity of the number of cycles to changes in the constant heat demand level, for two different storage capacities	115
Figure C.3	P2H: sensitivity of the heat sales to the variability of the heat demand, for two different storage capacities	116
Figure C.4	P2H: sensitivity of the number of cycles to the variability of the heat demand, for two different storage capacities	116
Figure C.5	P2H: sensitivity of the heat sales to the phase shift between the heat demand and the electricity price, for a 6h storage	117
Figure C.6	P2H: sensitivity of the number of storage cycles to the phase shift between the heat demand and the electricity price, for a 6h storage	117
Figure C.7	P2H&P: sensitivity analysis of the NPV to changes in the Rankine cycle efficiency, for a higher DHN price	118
Figure C.8	P2H&P: sensitivity analysis of the electric and thermal discharged powers to changes in the Rankine cycle efficiency, for a higher DHN price	118
Figure C.9	P2H&P: sensitivity analysis of the NPV to changes in the Rankine cycle efficiency, for a higher industrial heat price	119
Figure C.10	P2H&P: sensitivity analysis of the electric and thermal discharged powers to changes in the Rankine cycle efficiency, for a higher industrial heat price	119

LIST OF TABLES

Table 2.1	Typical applications of different types of TES [4]	12
Table 2.2	Properties of common SHS materials at 20°C [5]	13
Table 2.3	Different possible charging and discharging configurations	17
Table 3.1	Clustering of energy-intensive manufacturing industries, listed by expected decreasing energy consumption levels in 2040. Extracted from [6]	32
Table 3.2	Technical characteristics of different gas-fired and coal-fired power generation technologies. Extracted from [7] .	35
Table 5.1	Results from the spectral density analysis of the 2012 district heating demand of Hamburg	56
Table 5.2	Results from the spectral density analysis of the steam demand of an industry	58
Table 5.3	Results from the spectral density analysis of the DA market prices of Germany and Spain	60
Table 5.4	Summary of the storage power and capacity ratings used in the simulations	63
Table A.1	Revenue calculation for the reference case without storage	111

ACRONYMS

aFRR	frequency restoration reserves with automatic activation	28
ANR	annual net revenue	40
CAES	compressed air energy storage	23
CAPEX	capital expenditure	23
CHP	combined heat and power	8
CO ₂	carbon dioxide	xi
CSP	concentrated solar power	8
DA	day-ahead	27
DFT	discrete Fourier transform	53
DHN	district heat network	xi
ETES	electric thermal energy storage	xii
FCR	frequency containment reserves	28
FFT	fast Fourier transform	53
GHG	greenhouse gas	1
H ₂ P	Heat-to-Power	8
IEA	International Energy Agency	15
LCOE	levelised cost of electricity	1
LHS	latent heat storage	11
LP	linear programming	7
mFRR	frequency restoration reserves with manual activation	28
MILP	mixed-integer linear programming	7
NLP	non-linear programming	7
NPV	net present value	xii
OCGT	open cycle gas turbines	34
PPA	power purchase agreement	27
PV	photovoltaic	1
P ₂ G	Power-to-Gas	2
P ₂ H	Power-to-Heat	2
P ₂ H ₂ P	Power-to-Heat-to-Power	8
P ₂ H&P	Power-to-Heat-and-Power	69
P ₂ L	Power-to-Liquid	2

P2P	Power-to-Power	69
P2X	Power-to-X	2
RES	renewable energy sources	1
RR	replacement reserves	28
SGRE	Siemens Gamesa Renewable Energy	2
SHS	sensible heat storage	11
SoC	state of charge	18
TCS	thermochemical storage	11
TES	thermal energy storage	8

1 | INTRODUCTION

The purpose of this chapter is to give an overview to the reader of the importance of this work. With this aim, firstly the research objectives are placed in context and the research questions are presented. Secondly, the followed strategy to meet such objectives is briefly introduced. A Literature review of previous investigations is then performed in order to assess the academic knowledge on the area of study. Lastly, the contributions of this thesis to the research field are highlighted.

1.1 PROBLEM IN CONTEXT

In the past decades, the global energy scenario has started a pathway to decarbonization. The European Union commitment to reduce its greenhouse gas (GHG) emissions by 80-95% by 2050 with respect to 1990 levels [8] is an illustrative example of the amount of effort that will be required on a structural and social level to reach such target. The roadmap to decarbonization is still unclear, nevertheless, all scenarios certainly present challenges and opportunities to modernize and transform all energy sectors.

In the electricity sector, renewable energy sources (RES) are leading the transition away from fossil fuel generation technologies. Thanks to significant regulatory incentives, the electricity mix of many countries has already seen an increased share of solar photovoltaic (PV) and wind.

Despite the environmental benefits of RES, a scenario with a large share of these sources will pose significant challenges to many market players. To begin with, renewable energy assets operators will need to introduce flexibility options as a means to adjust their power generation to demand levels. As the levelised cost of electricity (LCOE) of sustainable energy technologies decreases, market mechanisms such as feed-in tariffs or curtailment payments will eventually be replaced by other schemes that will require producers to respond to real market signals [9]. These market changes will translate into a need for higher control over renewable power production. With respect to thermal power plants whose traditional application has been to provide baseload power, they will need to flexibilize their operation and decrease their ramping times. Such fast power response will become a requisite to meet sudden demand peaks when renewable sources are not available. Additionally, the most polluting conventional plants may turn unprofitable before the end of their lifetime due to carbon penalties such as high CO₂ prices. Lastly, a large RES penetration will entail a loss of inertia

in the grid, which will require the implementation of power control mechanisms by grid transmission operators to avoid costly damages.

The flexibility necessary to solve many of the foregoing issues will be provided by different cost-effective options, *inter alia*, energy storage. Many technologies and mechanisms for the storage of renewable power have already been developed for different purposes. The most extended of them is hydropower storage, which was introduced as a way to exploit onsite geographical elevations. More recently, electrochemical batteries such as Li-Ion batteries are entering the market to solve the increasingly recurrent power and voltage quality issues. Notwithstanding, batteries alone are not enough to solve most of the future energy system challenges due to their high cost and short discharge times. Storage with large power and capacity ratings will also be essential to achieve the full decarbonization of the power sector. Technologies with such power and capacity properties are being developed based on Power-to-X (P2X) mechanisms, that is, Power-to-Heat (P2H), Power-to-Gas (P2G), and Power-to-Liquid (P2L).

The electricity market share for P2X technologies will significantly increase under a high RES penetration scenario [10]. Additionally, it is foreseen that they will contribute to the complete transformation of the energy system by the integration of the three most polluting sectors: heat, power, and transport, by means of coupling the low-carbon energy carriers, heat, electricity, hydrogen, and natural gas. Many studies have shown that a highly-electrified scenario would be very costly due to the large investment required to extend the grid infrastructure, and difficult to achieve in industrial activities where energy is used as a feedstock [11]. It is therefore anticipated that the integration of the energy networks by P2X technologies, together with some level of electrification, will eventually increase the flexibility of the energy system in the most cost-efficient way.

The potential and still unexploited market for large scale and sector-coupling storage technologies has led Siemens Gamesa Renewable Energy (SGRE) to research and develop a new Electric Thermal Energy Storage (ETES) concept. The innovative storage technology has been developed as a multi-function means to make renewables baseload capable, to decarbonize the heat sector, and to eliminate the need for extensive fossil backup capacities. As the proofs of concept and of system have now been finalized, the implementation of the technology in a commercial-scale project becomes a requisite for the continuous generation of knowledge on the various applications. However, despite the versatility of the technology, the ETES solution might not be optimal under all system and market conditions and requirements. The goal of this thesis is therefore to evaluate what are the boundary conditions, dictated by the electricity and heat sectors, under which the ETES technology can best serve the energy system.

1.2 RESEARCH OBJECTIVES AND METHODOLOGY

As described in the previous section, the economies pursuit of decarbonization and the increased penetration of renewable energy sources is challenging the en-

ergy market *status quo*. The new global scenario has driven energy technology developers to create new storage concepts to capture new market opportunities that will unfold in the upcoming years. One of these market players is SGRE, which has developed and tested a new Electric Thermal Energy Storage technology (ETES). The main challenge that ETES designers are currently facing is the assessment of different power and heat markets around the globe to determine which one is optimal for the commercial installation of the technology. This is a complex task as the energy market is becoming more volatile and the economic performance of the storage depends greatly on its operational needs. Consequently, such assessment requires a tool or model that enables to quantitatively evaluate the technology under very different conditions and situations. Following this rationale, the next research questions and sub-questions are proposed.

Research question

Under which boundary conditions is there a business opportunity for ETES, with regards to the future electricity and heat markets?

Research sub-questions

1. How should a programming-based model be formulated to evaluate the thermodynamic performance of ETES and its implementation for different applications?
2. Which is the most promising energy market for the integration of ETES into the future energy system, and what future developments will have to take place to open up new markets?
3. Which are the most relevant boundary conditions of the heat and electricity sectors that SGRE developers should consider for the commercial positioning of ETES?

Research methodology

Answering the research question and sub-questions requires the analysis of the dynamics of the system and its adequacy to different price and demand set-ups. In order to develop a comprehensive model of the technology and test its performance under different boundary conditions, the following research steps have been identified:

1. *Scope of research*: the first milestone is the identification of the boundaries of the study as well as the desired outcomes. This is done via the research questions, which structure the overarching goal of the study (Chapter 1).
2. *Literature review and evaluation of the state-of-the-art of thermal storage*: the second milestone is the review of previous studies and the compilation of the last thermal storage technology developments. This work allows to

find the missing elements in the Literature and to place the technology in context (Chapters 1 and 2).

3. *Conceptual design of the model*: the third step consists of the identification of the main components of the model. To that end, firstly, the main thermodynamic principles and the main features of the ETES concept under study have to be defined. Secondly, after the thermodynamics of the technology have been disclosed, the potential end-uses have to be listed and the most relevant have to be selected (Chapters 2 and 3).
4. *Model formulation and verification*: the formulation of the working principles of the technology along with the most relevant applications is the following research milestone. Such exercise has to be performed in parallel to the verification of the model equations ensure the validity of the results (Chapter 4).
5. *Development of demand and price input curves*: once the model has been constructed, the following step is the development of a systematic methodology to compare different demand and price signals. This is done by means of the construction of artificial signals from actual data, in order to isolate the impacts of different input parameters on the business model (Chapter 5).
6. *Analysis of results and discussion*: lastly, the results are presented and evaluated against the research questions, in order to answer them and to meet the overarching goal of the thesis (Chapters 6 and 7).

1.3 LITERATURE REVIEW

ETES is defined by Cao, et al. [12] as the integration of several innovative and cutting edge technologies (e.g. thermal storage, heat engines, and heat storage mediums). Each of these technologies has been extensively studied and analyzed in the Literature, however, a comprehensive model that includes a detailed formulation of ETES' working principles and its behaviour under different boundary conditions has not been found.

The need to better understand the impact of renewables in the energy system and the need for flexibility resources, has nevertheless led to the development of a broad spectrum of models of several energy storage technologies. In order to build upon such studies, this section explores some of their modelling techniques. Additionally, it gives an overview of the current trends in the Literature on the role of ETES in the future energy system, and the applications that have been most extensively studied. It concludes by assessing the academic value of this thesis and the knowledge gap it aims to fill.

1.3.1 Energy storage modelling techniques

Multiple energy storage modelling techniques can be found in the Literature. These can be classified according to the scale, the boundary conditions, the level of detail, and so on, which are designed after the desired outcomes of the model. Because of the relevance for this study and the need to understand its scope and limitations, two different archetypes of models have been further researched: system and engineering models on the one hand, and optimization and simulation models on the other. The design of the first two mainly differs on whether a 'top-down' or a 'bottom-up' approach is used, whereas the construction of the last two follows different methodologies.

System models and engineering models

According to Grünewald, et al. [13] [14], the main distinction between 'system models' and 'engineering models' is the boundary drawn around the storage system. On the one hand, system models focus on the entire energy system, set spatial boundaries (e.g. regional, national, European, etc.), and search for the benefits that storage will bring to the overall system. They usually determine the value of the technology following a cost-minimization logic. On the other hand, engineering models consider a given system context and focus on the techno-economic assessment of a specific storage asset. They aim at monitoring and optimizing the asset operation and at determining its profitability [15]. Because system models consider macroeconomic changes caused by energy storage, they are sometimes called top-down models, whereas engineering models, which give a detailed description of the storage system, are called bottom-up models [16].

The majority of the reviewed articles that include thermal storage and cover both the electricity and heat sectors were system models. A widely used system model that includes the power and heat sectors is the EnergyPLAN model, which gives the optimal energy assets combination and calculates the heat and electricity generation costs. This model is used by many researchers but does not consider ETES for power applications [17]. Another example is the REMod-D model used by Henning and Palzer [18] to model the electricity and heat sectors of Germany. In this case, thermal energy storage is used to store renewable power but the re-conversion of heat back to electricity is not considered. Different types of optimization techniques and constraints for the integration of storage and RES into district heating systems are discussed in [19] and [20], also from a system model perspective. Lastly, a combined analysis of the electricity and heat networks is performed in [21] based on an hydraulic-thermal model of the heat network and an electrical power flow model. Similarly to the models mentioned above, in this study ETES systems can only discharge heat.

The aforementioned articles and system models do not focus on electric thermal storage specifically, but rather offer thermal storage as a flexibility source for thermal loads. Additionally, the working principles of thermal storage are

greatly simplified and reduced to power and capacity capabilities and round-trip efficiencies. Such modeling methodology is not robust in depicting the limitations and losses caused by the thermodynamics of the ETES technology. Therefore, it is gathered that there is an academic knowledge gap regarding the detailed engineering formulation of the technology and its performance under different system conditions.

Optimization models and simulation models

Models can also be classified into ‘optimization’ or ‘simulation’ models, depending on the nature of the solving techniques. The former try to provide the optimal trajectory and solution to a problem, based on system parameters and criteria. The latter provide plausible future trajectories with evolving parameters and hypotheses [22]. Some models have a purely optimization or simulation nature, whereas other models combine both approaches to meet different purposes.

The optimization approach requires the selection of an overarching goal, expressed by means of an objective function, and the selection of the problem’s parameters. The goal is usually related to economic optimization, but can also consist of maximizing welfare, minimizing CO₂ emissions, or maximizing security of supply, to give some examples (see Figure 1.1). Some authors such as Lund, et al. [23], point out the significant impact of model choices on the results. Some important parameters in optimization models are the discount rate, the system boundaries, and the monetization of emissions’ negative effects. As the authors mention, the magnitude of their impact is usually damped by sensitivity tests.

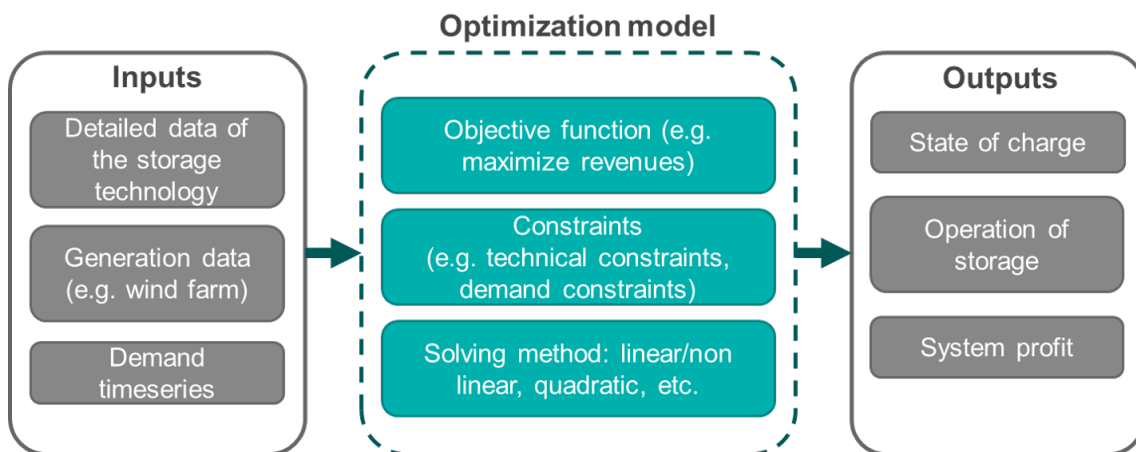


Figure 1.1: A simplified schematic and examples of the optimization approach

As regards simulation models, they aim at envisaging the behaviour of a system under certain established conditions, without necessarily searching for the optimal solution. They usually analyse the system under different situations or scenarios and compare the results against relevant criteria (see Figure 1.2). As mentioned in [23], because of this reason, in simulation models the different options of the future become more relevant than the details of the current sys-

tem. In order to mitigate the uncertainty of the assumptions about the future system conditions (e.g. fuel prices, energy demand, etc.), different conditions are compared.

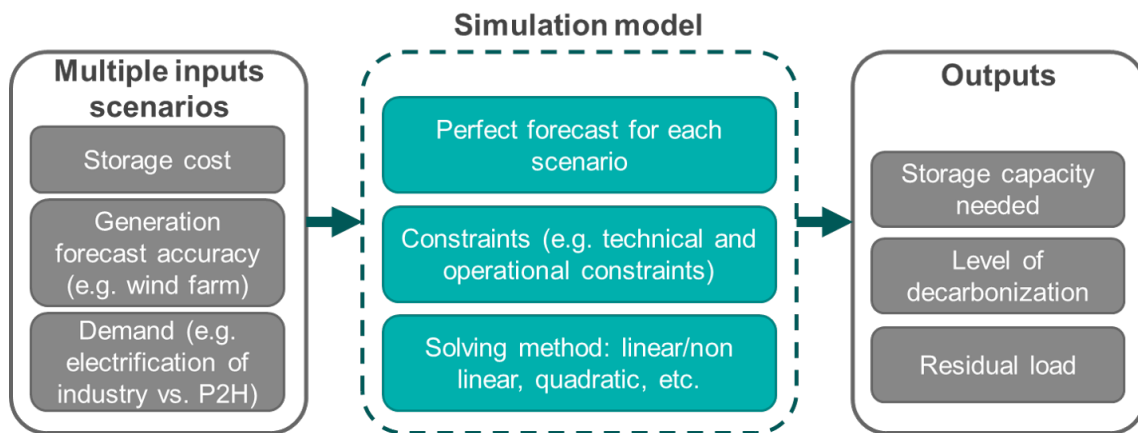


Figure 1.2: A simplified schematic and examples of the simulation approach

Likewise the model of this thesis, the majority of energy storage models are optimization models that seek to support investment and operation decisions [16]. Consequently, the optimization tools used in the Literature to deliver robust results, e.g. sensitivity tests on the inputs, have been carefully considered in this work. Notwithstanding, some characteristics of the simulation approach have also been included in the research. These mainly include the analysis of the system under different market conditions in order to mitigate the uncertainties of future developments.

Optimization techniques

Apart from the scope and approach, the trade-off between computational time and complexity should be also taken into account in the construction of the mathematical optimization. Mathematical optimization problems are classified according to several factors, such as the linearity of the objective functions and constraints, the presence of integer variables, quadratic terms, and so on.

Each category of solving technique is needed to solve different mathematical problems and has a different computational complexity [24]. For instance, in a study carried by Ommen, et al. [25], the computational time of a model with thermal power plants, thermal energy storage, boilers, and heat pumps is compared for different optimization methods. Their results show that the solving time of the linear programming (LP) was the shortest, half of that of the mixed-integer linear programming (MILP), and that the time requirement of the non-linear programming (NLP) approach was more than 4,000 times larger. Similarly, Bloess, et al. [2] carry out a Literature review of P2H technologies and modelling approaches and conclude that most optimization models apply either LP or MILP, due to the lower computational requirements.

A short computational time is always a desired criterion, and it is more related to the solving technique than to the simulation or optimization nature of the

model. Based on the findings of the Literature and in order to be able to carry out multiple simulations, it was decided to formulate the model in linear terms in order to minimize the computational burden.

1.3.2 Trends in the Literature on the role of ETES in the future energy system

The investigation of electric thermal storage in the Literature can be presented according to the applications considered. Many of these papers also refer to the technology as *electrothermal energy storage* or *Carnot battery*.

Concerning the use of ETES for the integration of renewable power, the attention of the vast majority of the reviewed studies resides on P₂H applications. Among the different RES, most of the publications refer to the integration of wind-generated electricity for space heating [26] [27]. Many authors allude to heat storage as a cost-effective solution to avoid wind curtailment due to the strong coupling between power and heat generation of combined heat and power (CHP) plants during heating seasons [28] [29]. Some works focus on the value of the technology for providing grid services by using surplus power for heating. For example, in [30] the technology is called ‘grid-interactive electric thermal storage’, and its effectiveness for grid management and heat provision is presented. Several authors also perform capacity and operational optimization of the technology’s integration into a heating system. For instance, Renaldi, et al. [31] design a model to compare conventional domestic heating with a small-scale, low-carbon alternative technology, consisting of a water-based thermal storage and heat pumps.

Thermal storage for Power-to-Heat-to-Power (P₂H₂P) is often out of consideration, presumably due to the low round-trip efficiency. The first economic model of ETES to reduce wind power curtailment and provide electricity was carried out by Okazaki, et al. [32]. They conclude that wind-powered ETES has an economic advantage over other systems since grid extension and thermal backup costs are avoided. Optimization of P₂H₂P based on thermal storage concepts with PV plants and the use of transcritical CO₂ cycles are performed in [33], and with thermal collectors in [34]. These studies focus on the performance of the system rather than on its integration into the power sector. Because molten salts in concentrated solar power (CSP) plants account for around three-quarters of the total global thermal energy storage (TES) used for Heat-to-Power (H₂P) [1], many authors have attempted to optimize their operation for providing baseload generation [35] [36]. However the scope of these studies is the storage of surplus solar heat, while electricity storage is left aside.

The search for Literature regarding the integration of ETES into thermal power plants to increase their flexibility yielded the largest number of results. The financial viability of a heat pump and an ETES concept in large-scale thermal power plants is assessed by Risthaus and Madlener in [37]. They analyse three types of thermal power plants, namely a coal-fired plant, a combined cycle, and a CSP, and calculate the net present value for each of them. Among other con-

clusions, they determine that energy arbitrage is not enough to have net gains and that the largest revenues stem from offering tertiary control power. Nevertheless, they estimate the costs of the thermal storage unit in a conservative way (according to the authors). More studies and dynamic models that assess the capability of thermal storage to support the flexible operation of conventional power plants can be found in [38] [39] [40]. The integration of thermal storage into different types of power plants is also studied in [41]. In this case, the focus is on the round-trip efficiency and the economic aspects are disregarded.

Another relevant study to this thesis is that of Gibb, et al. [42]. The authors develop a general methodology to evaluate the process integration of an ETES concept based on three steps. The first step is the process analysis to address the technical requirements for the integration of ETES. Then, the system boundary is delimited and the technical and economic parameters of the storage are disclosed. These results are finally used to determine the benefit of an ETES to an application, and to spot the difference in perspective among the stakeholders. The paper does not develop a model per se, but offers a systematic approach that can be used for that end.

1.3.3 Academic contribution of this thesis

Modelling of storage has become a topic of interest in the Literature. Most of the models have an optimisation nature and aim to define the benefits that different storage technologies will bring to the increasingly-volatile energy system. This thesis builds upon existing modelling techniques for optimizing the storage operation under different boundary conditions, and contributes to the knowledge expansion about the potential of ETES in the future energy system.

The model of this thesis can be classified under the 'engineering model' and 'optimization model' categories. It is an 'engineering model' because it deals with operational challenges while paying detailed attention to the technical and economic aspects of the storage. It is an 'optimization model' because the analysis is carried out by means of optimizing the operation of the plant to maximize the profit. There are multiple engineering optimization models for a wide range of energy storage systems. All of them include operational constraints, such as power balance or ramp constraints, that are technology-agnostic and can be used by the present study as a modelling base. Each of the optimization approaches has advantages and drawbacks in terms of accuracy and computational time that have been taken into account. The optimization has also been followed by a sensitivity analysis on the key input data in order to mitigate the uncertainty of the assumptions.

Carrying out a complete Literature review is challenging as a model of ETES can potentially involve a wide range of scientific purposes. Nevertheless, a first screening using different terms and keywords has resulted in either case-specific models of electric thermal storage for heat applications only, or for power applications only. Aside from that, the found models do not describe ETES from a detailed engineering perspective but more as a thermal backup for the energy

system. For instance, most of the models formulate the technology in power and capacity terms, ignoring the thermodynamics of the storage. This approach prevents them from including important efficiency losses expressions, as well as the performance of the technology over different time horizons. Therefore it can be concluded that, despite the large number of energy storage models found in the Literature, none of them consisted of a comprehensive model of the performance of ETES under different market conditions, and this thesis aims to fill that gap.

As regards the evaluation of ETES for different applications, this thesis tests the technology in a novel systematic way instead of using real price and demand data. The approach consists on the creation of artificial sinusoidal curves based on the extraction of the most relevant frequencies by means of the Fast Fourier Transform. This methodology enables to tailor the input boundary signals in a structured way, as a means to isolate the impacts of different variations in the boundary conditions.

1.4 OUTLINE AND STRUCTURE OF THE REPORT

The report is structured as follows. Chapter 2 gives an overview of the state-of-the-art of thermal energy storage and explains the main working principles of the technology, in order to provide a knowledge basis for the model. The understanding of the working principles of the technology is necessary to comprehend its potential applications, displayed in Chapter 3. The model formulation is provided in Chapter 4 along with the proposed financial evaluation. The generation of the input curves for assessing different boundary conditions is explained in Chapter 5, together with a brief introduction to the case studies. Lastly, the main results and conclusions are given in Chapters 6 and 7 respectively.

2 | ETES TECHNOLOGY EXPLAINED

This chapter introduces the working principles of the ETES technology, in order to set the knowledge base for the model formulation in Chapter 4. Firstly, the reader is introduced to the main thermodynamic principles of thermal energy storage and to state-of-the-art of sensible heat storage in order to place the ETES technology in context. Secondly, the main fundamentals of the technology are explained in more detail. The system configuration and its components are presented, as well as the charging and discharging mechanisms. The chapter ends by explaining the main limitations and energy losses of the system, and by briefly comparing ETES to other energy storage technologies.

2.1 THERMAL ENERGY STORAGE

As its name implies, ETES is based on thermal energy storage (TES). TES is the second most practised form of energy storage and, in its broadest meaning, consists of the storage of thermal energy by cooling or heating a storage medium to use it at a later time. More specifically, ETES comprises the stages of obtaining the heat, either directly or as a result of an electrothermal conversion, storing the heat in a thermal medium, and lastly, either withdrawing the heat or generating electricity.

Depending on the storage principle, TES can be classified into sensible heat storage (SHS), latent heat storage (LHS), and thermochemical storage (TCS). In storage systems based on SHS, the storage medium absorbs and releases the energy by means of temperature variations. The most common materials used in commercial projects are water and molten salts. They differ from LHS systems, which store thermal energy during the phase change process of the storing material (i.e. from liquid to solid, liquid to gas, solid to solid). These materials are also known as phase-change materials (PCMs) and can be organic and inorganic. Some examples are paraffin wax ($\text{CH}_3-(\text{CH}_2)_n-\text{CH}_3$), salts, metals, and salt hydrates [43]. Lastly, in TCS, the storage medium undergoes reversible endothermic and exothermic chemical reactions for heat storage and release. TCS materials are still under research and development and their commercial introduction is still limited.

The ETES technology is classified under SHS, which is at the same time the most used storing principle. Concretely, the most used technology is hot-water SHS due to its cost-effectiveness, followed by molten salts SHS, which are mainly used in CSP plants to generate controllable renewable power. LHS and TCS systems are

more expensive and not mature yet, however, there are many R&D activities to unlock their large energy density potential [44]. Common applications for each category of TES are presented in Table 2.1.

Table 2.1: Typical applications of different types of TES [4]

Sensible Heat Storage	Latent Heat Storage	Thermochemical Storage
Domestic hot water	Cold storage in buildings and industries	Cold storage (absorption)
Buildings heating	Waste heat in cement, steel, and glass industries	Process heat (industrial heating/drying appliances)
Waste heat in cement, steel, and glass industries	High temperature storage (>400 °C), for CSP and CAES	Waste heat in cement, steel, and glass industries (chemical reactions)
High temperature storage (>400 °C), for CSP and CAES		High temperature storage (>400 °C), for CSP and CAES
District Heating		

2.1.1 Main thermodynamic principles of Sensible Heat Storage

From underground water tanks to molten salts in CSP plants, all SHS systems operate under the same fundamental process: storing energy in a solid or liquid material by varying its temperature. The energy capacity of the system is therefore proportional to the temperature gradient and to the storage medium's mass and specific heat. It is expressed by the following equation:

$$E = m C_p (T_2 - T_1) \quad (2.1)$$

Where E is the energy [J], m is the mass of the storage medium [kg], C_p is the specific heat at constant pressure [J/kg K], and T_1 and T_2 are the initial and final temperatures [K]. If the mass m is substituted by a mass flow rate, i.e. \dot{m} , Equation 2.1 can be understood as an energy transfer rate.

A parameter of relevance for thermal storage is the thermal diffusivity (λ) of the storage medium. The thermal diffusivity measures the velocity at which heat

can be extracted from or injected to the material, and is, in turn, related to the specific heat as follows:

$$\lambda = \frac{k}{\rho C_p} \quad (2.2)$$

Where k is the thermal conductivity of the material [W/(mK)] and ρ the mass density [kg/m³].

For a TES to be effective, the storage material must have particular properties. It should have a high thermal capacity, that is, a high mass density ρ and a high specific heat C_p . The thermal capacity, or ρC_p , determines the amount of heat the material will be able to store. It should also have a good thermal conductivity k in order to maximize the heat transfer to and from the material. Nevertheless, a high k also implies higher losses [45]. As seen in Equation 2.1.1, the amount of heat stored depends on the temperature gradient, therefore the insulation container plays a crucial role in TES to improve the performance of the storage and minimize such heat losses as much as possible. Additionally, in order to be commercially viable, low price and good environmental properties are also important advantages [46]. Table 2.2 shows the properties of some common materials.

Table 2.2: Properties of common SHS materials at 20°C [5]

Material	Mass Density [kg/m ³]	Specific Heat [J/(kgK)]	Thermal Capacity [J/(m ³ K)]
Water	988	4,182	4,131,816
Molten salts	1,549	1,530	2,369,970
Engine oil	888	1,880	1,669,440
Gravelly earth	2,050	1,840	3,772,000
Rock	2,560	879	2,250,240
Concrete	2,000	880	1,760,000
Sandstone	2,200	712	1,566,400
Brick	1,800	837	1,506,600
Clay	1,458	879	1,281,582
Sand	1,555	800	1,244,000

For high-temperature SHS, some materials' thermal properties are comparable to those of water per unit volume. The lower heat capacity of earthy materials is counterbalanced by the the large temperature gradients they can withstand without undergoing a change in phase and by their larger densities [47].

2.1.2 State-of-the-art of Sensible Heat Storage systems

SHS systems can be classified according to the operating temperature and according to the energy storage in liquids or solids. Storage in gas media is also

technically possible but the energy density is smaller and the volumes required for equivalent amounts of energy are extremely large. Underground thermal energy storage employing soil layers as a storage medium is also possible, more information can be found in [44].

SHS in liquids at low temperature

Water is the most used material for working temperatures below 100°C as it is inexpensive and non-toxic. It is usually combined with solar for end-use thermal energy applications, including distributed heating (e.g. domestic water boilers) and air heating and cooling. The latter application is especially significant considering that heating and cooling are responsible for a 39% of global CO₂ emissions and 48% of global energy consumption [48].

Water SHS systems can be distributed or centralized. Distributed systems have a power capacity usually around a few tens of kW. They often use solar energy from collectors to heat up water, which is then used in domestic or commercial appliances and cycle many times a day. Their potential impact is higher in countries where the buildings sector is growing since they are easier to integrate into new installations [44]. Water SHS is also deployed in centralized plants larger in capacity, ranging from hundreds of kWh up to several MWh or even GWh. These are mostly used to store waste or by-product heat to improve the efficiency of the energy-intensive industry. Heat from centralized CHP plants is also used to provide district heating and cooling by means of insulated pipes and large underground water tanks [44].

Water SHS technology has the advantages of being greatly mature – it has been in place for decades –, of having low installation costs, and of using a safe and affordable storage medium. Nevertheless, water can only be heated up to 100°C at ambient pressure without changing its phase so, despite its large thermal capacity, it presents low energy density as compared to other media and requires greater volumes for large-scale TES [49].

SHS in liquids at high temperature

High-temperature TES systems are mainly used for power generation in CSP plants. In 2017 there were 3.3 GW of TES for electricity installed, placing TES as the technology with the second largest power storage capacity deployed (1.9% of the global storage capacity) only after pumped-hydro [1].

The majority of high-temperature SHS plants are based on molten salts and installed in centralized CSP plants, where solar energy is stored and converted to electricity to reduce the fluctuation of the renewable power output. The heat is also sometimes used directly for district heating [44]. CSP plants use mirrors to concentrate solar rays in a receiver that heats up the molten nitrate salts to a temperature range of 250-620°C [50]. Whenever electricity is needed, the heat from the molten salts is transferred to a steam cycle to spin a turbine and generate power [51][52]. All industrial CSP plants are direct systems, that is, the molten salts are used both as the heat transfer fluid and as the storage medium. They

are also based on two storage tanks at different temperatures above the melting point of the nitrate salts.

Current research efforts are focused on the implementation of only one tank and on the use of other heat transfer fluids (e.g. oil) [52]. The maturity of the molten salts approach has also led to the development of new concepts for the storage of electric energy from wind or PV. In general terms, such systems collect surplus renewable power, store it in a two-tank molten salt storage system and convert it back to power through a heat engine.

Despite the wide implementation and the high energy density of molten salts storage, the cost and availability of the salts are disadvantages. They account for roughly 49% of the TES total cost that, in turn, accounts for about 9% of the total plant initial investment expenditure [31]. According to the International Energy Agency (IEA), in 2050 CSP plants will provide 10% of the global power generation. Most of these plants will be built with TES (an IEA report shows that 85% of all planned CSP plants until 2023 will include thermal storage [53]). Some studies have predicted that this increase in demand will create an important bottleneck in the availability of the mineral resources they include, leading to conflicts and tension [54].

SHS in solids at high temperature

Different advanced concepts for the storage of heat in solids up to 1,000°C are being developed. Among these, regenerators are the most common. They use a heat transfer fluid, usually a fluid medium like air, to transfer the heat from the source to the solid storage material that can be made of natural stones, ceramic bricks, concrete, or packed beds of pellets. These systems are called indirect systems as they use different mediums for heat transfer and storage [5].

As seen in Table 2.2, the solids used in high-temperature SHS generally have lower specific heat than the fluids, however, they have larger densities and can resist larger temperatures as compared to water and molten salts that are limited by their boiling points. Therefore, solid SHS mediums can reach higher temperatures and heat up the steam to very high levels, minimizing the losses of power generation. For instance, a common used material is concrete due to its low cost and good thermal properties. Concrete has a high specific heat, a good mechanical resistance to thermal cycling, and good compressive strength, as well as other mechanical properties [47]. Additionally, it has a similar thermal expansion coefficient to steel, which reduces the mechanical stress between the pipes and the storage.

Several high-temperature solid SHS concepts - like the one under study in this thesis - are under development and demonstration. The commercial potential of this technology has led to some leading energy companies to include practical research in their portfolios [55][56]. The ETES technology studied in this thesis is still in the research and development phase. Nevertheless, the proof of concept built with more than 1,000 tons of rocks as storage material, has already been developed achieving 24 hours of storage capacity, 25% round-trip cycle efficiency for power generation, 95% heat storage efficiency, and 480°C steam temperature

at 65 bar [57]. Future developments have the potential to reach higher discharge times, a 45% H₂P efficiency, and air temperatures up to 800°C. More details about the technology and the working principles are given in the following section.

2.2 FUNDAMENTALS OF THE ETES CONCEPT UNDER RESEARCH

The ETES technology under research – from now on referred to as ‘the system’ – falls under the SHS in solids at high temperature category. Similarly to the other technologies that belong to this group, the system uses different mediums for the storage and the heat transfer. The storage bulk material consists of a pebble bed of volcanic stones in an insulated container. The stones have diameters in the centimeter scale in order to optimize the heat transfer between the fluid energy carrier and the rocks. With respect to the heat transfer fluid, non-pressurized air is used.

The system configuration, the charging and discharging mechanisms, and the efficiency losses that are necessary to understand the operating principles of the storage, are described in the following lines.

2.2.1 System configuration

Similarly to any other storage technology, the architecture of the ETES system has three main parts: the charging cycle, the storage container, and the discharging cycle (Figure 2.1).

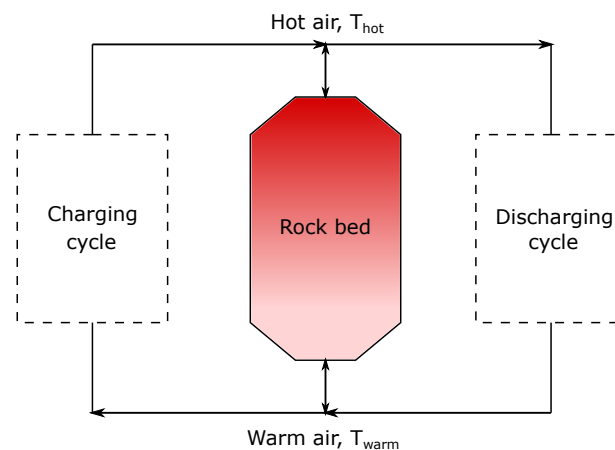


Figure 2.1: Basic configuration of the ETES technology

The ETES technology can be set up in order to charge heat or electricity, to be later discharged also as heat or electricity. Depending on the end use, the configuration is shaped in a different way and the components of the system vary. The different options are depicted in the diagrams below.

Table 2.3: Different possible charging and discharging configurations

Input / Output	Charging cycle	Discharging cycle
Heat		
Electricity		

Regarding the set-up of the charging cycle, if the system has been designed to store heat, the energy is introduced in the unit by means of a heat exchanger and a blower. If on the contrary the main application is the storage of electric power, the P₂H conversion takes place by means of an electric heater that heats up the air, and a blower that moves the heated medium through the pipes to the rock bed. The air can reach very high temperatures. In the model, a temperature of 750 °C is set at the outlet of the heater (T_{hot}), and around 200 °C at the inlet (T_{warm}).

As regards the discharging mechanism, when the storage is designed to meet a heat demand it does so by means of a heat exchanger. For certain specific applications, the ETES technology could also be designed to meet a heat demand by delivering hot air to, for instance, a nearby industry. In that case, in order to maintain the air mass flow balance through the pipes, ambient or heated up air should be reintroduced into the system. If the storage is used for the delivery of electric power, the H₂P conversion is carried out by means of a Rankine cycle, where the energy is transferred from the air to the steam by means of a heat recovery steam generator. The electric power is generated via a steam turbine and a condenser. Some applications also involve the withdrawal of heat in an intermediate phase between the high pressure and low pressure turbines. Further explanation on the efficiency of each component and cycle is provided in Section 2.2.3.

The system has a modular design and allows the decoupling of the charging power capability, the discharging power capability, and the energy storage capacity. Additionally, due to the large availability of the storage material (i.e. volcanic rocks), the storage can be scaled up without incurring a dramatic cost increase. All these characteristics result in a storage with a large power and capacity rating, in the MW and GWh scale.

2.2.2 Charging and discharging mechanisms

The charging and discharging of the rock bed process is based on the three heat transfer mechanisms:

- **Convection:** during the charging process, the hot air flows through the stones and heats them up due to the temperature difference between the mediums. The convective effect is maximized by the use of fans, which also counterbalance the pressure drop over the bed.
- **Conduction:** with respect to the conductive heat transfer, it mainly takes place within the stones and the container wall. As expressed earlier in Section 2.1.1, the larger the value of the thermal conductivity of a material, the faster the heat transfer. Following this logic, the insulation container is designed to maximize the transfer time with the ambient, in order to maintain the temperature gradient the longest time possible.
- **Radiation:** radiation also takes place and is mainly dependent on the surface area, the temperature, and the emissivity of the materials.

During the discharging process the same mechanisms come into play, but this time the heat is transferred from the hot rocks to the cold air. Among the three, convection is the predominant heat transfer process and is the only one considered in this thesis.

During the charging process, the hot air flows from the inlet to the outlet of the storage, cools down as it transfers thermal energy to the stones, and it forms a temperature gradient along the rock bed (see Figure 2.2). For simplicity, the end where the heated air enters the storage is referred to as the 'hot side', and the other one is referred to as the 'warm side'. Because of the large contact surface and the thermodynamic properties of the materials, the heat transfer process takes place in a relatively short distance. This creates a temperature transition region with a short depth and, consequently, a steep temperature gradient. Once the maximum temperature has been reached in the hot side, as the air continues to flow through the storage, the temperatures of both ends of the bed remain nearly constant. Further loading of hot air thus results in the vertical displacement of the temperature transition region towards the warm end of the storage tank. In practice, these temperatures vary with the state of charge (SoC) and operation mode of the storage, nevertheless, they are considered as constant in the present model in order to avoid non-linearities.

During the discharging process, the reverse process occurs. The cold air flows across the stones, being heated up as it removes the thermal energy from them. In this case, the warm side of the storage increases in volume, and the temperature gradient is displaced towards the hot side of the system. If the temperature transition zone reaches the outlet of the storage during the process (i.e. the hot side), the temperature of the air stream decreases and lowers the efficiency of the system. To avoid such temperature drop, a mode of operation is usually selected in which the rock bed is discharged down to a defined termination temperature

below the maximum. This means that the storage tank is not fully discharged and the capacity of the storage is not utterly used. Such termination temperature has already been taken into account in the model, thus the considered capacity can be entirely used.

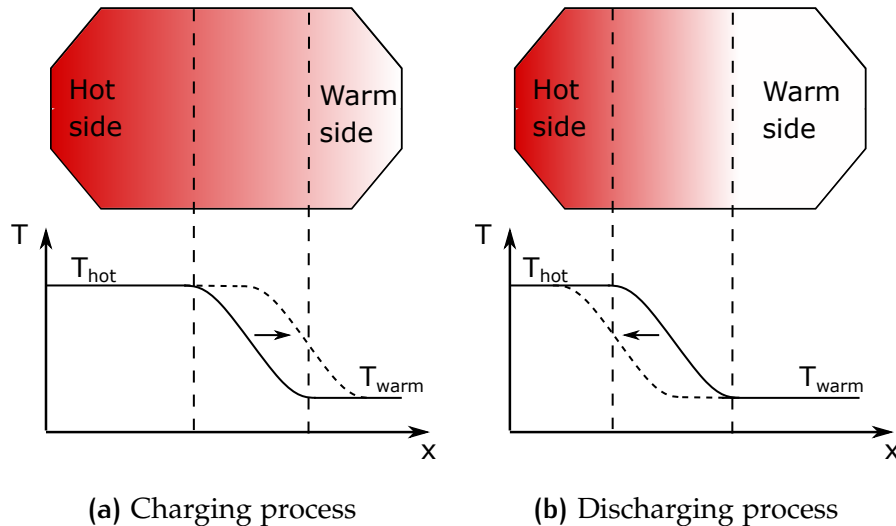


Figure 2.2: Dynamics of the charging and discharging of the storage

A steep temperature gradient is preferred over a flat one because it would mean the storage has a larger exergy content. Exergy is defined as:

"the amount of work possible to achieve from a system when it, through reversible processes, reaches thermodynamic equilibrium with the surroundings." [58]

Exergy is therefore an alternative means of determining the usable energy stored in the system. Such loss in the availability or quality of energy is caused by four primary factors [59]:

- heat losses to the environment,
- heat conduction from the hot end of the storage medium to the colder side,
- vertical conduction in the wall of the storage tank, and
- mixing of fluids at different temperatures during charging and discharging processes.

The first factor is mainly offset by the insulation material, which reduces the losses to the environment to negligible values for time horizons shorter than several days. Experimental results from the ETES system have shown that the second factor gains relevance when the storage tank does not undergo full charging cycles (the storage does not reach 100% SoC). Consequently, partial cycling results in exergy loss, which translates into smaller discharge depths and into loss of available energy. The quality of the energy can be restored by charging the storage to its maximum capacity. Only after this process the storage reaches

again the optimal temperature distribution and the maximum theoretical depth of discharge. Lastly, in order to minimize the mixing of fluids during charging and discharging, the storage is designed to achieve the appropriate temperature stratification.

The exergy content of a storage system can be modelled with thermodynamic expressions. Nevertheless, very accurate mathematical formulations are not included in the current study as they would add extra computational complexity and their added value towards the research objectives would be limited due to the high frequency of full charging cycles. The exergy loss is in any case approximated in the model by a linear function obtained from empirical observations. Such analytical expression is presented in the formulation in Chapter 4. The interested reader can find elaborate thermodynamic models of exergy in [59] and [60].

2.2.3 Technical limitations of the system

The limitations of the system are herein introduced into two different categories: energy losses and mechanical limitations. The most relevant energy losses are the efficiency losses of the H₂P and P₂H conversion, the heat losses to the ambient, and the exergy losses inside the tank. As regards the mechanical limitations, the present study touches upon those of the Rankine cycle.

Energy losses to the ambient and exergy losses

Two energy losses have already been introduced in Section 2.2.2, namely the energy losses to the ambient and the exergy losses inside the rock bed. The energy losses of the storage bed to the ambient are caused by the temperature gradient between the inside and the outside of the insulation material. These losses can be significant for a timespan of several days or longer, reason why the ETES technology under study is not considered appropriate for long-term seasonal storage. As regards the exergy losses, they arise when the storage does not undergo full charging cycles or stands inactive. They are mainly a consequence of heat conduction forces between the hot end of the storage and the warm end, which create a longer temperature stratification region and therefore a more moderate gradient. The energy content of the storage is not affected, notwithstanding, the usable energy content is decreased and therefore the efficiency of the storage as well.

Energy losses in the electric heater

Electric heaters produce heat as a result of an electric current flowing through a resistance (i.e. Joule Heating) and have been used for decades in common appliances such as radiators, electric cookers, electric irons, etc.

The heat generated can be calculated from the dissipated electric power as:

$$E(t) = RI^2t \tag{2.3}$$

Where R [$\Omega = J/(sA^2)$] is the resistance of the heater, I [A] is the electric current, and t [s] is the time the current is flowing. As seen in the equation above, it can be considered that all the electric power dissipated in the heater's resistance over time is converted into heat, in other words, it can be considered that the efficiency of an electric heater is almost 100%. This is because electricity is a 'high-quality' form of energy that can be converted into another type of useful energy almost entirely without losses.

Energy losses in the Rankine cycle

Contrary to electricity, thermal energy is the least useful form of energy. The conversion efficiency of heat into electric power is capped by the Carnot cycle efficiency and is lower than that of the electric heater. The Carnot efficiency depends on the temperatures of the cold and hot reservoirs of the circuit and is the maximum theoretical efficiency that a heat engine can reach, as it assumes that no new entropy is generated. In practice, it is not possible to achieve the Carnot efficiency and real steam engines efficiency can be better approximated by the non-ideal Rankine cycle.

The simple ideal Rankine cycle consists of four internally reversible processes shown in Figure 2.3: isentropic compression in a pump (1 - 2s), heat addition in a boiler at constant pressure (2s - 3), isentropic and isobaric expansion in a turbine (3 - 4s), and latent heat rejection in a condenser at constant temperature and pressure (4s - 1). The non-ideal steam cycle differs from the ideal cycle in the change in entropy in the pump and in the turbine (2 vs. 2s, and 4 vs. 4s), thus it considers the irreversibility, and in the pressure drop in the boiler and in the condenser. The enclosed area represents the net work produced throughout the time of the cycle [61].

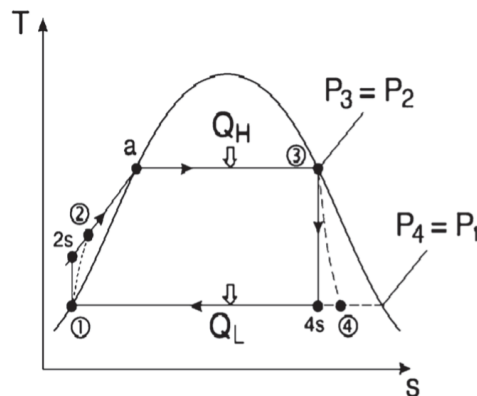


Figure 2.3: Rankine cycle T-S diagram

The model developed in this thesis takes into account the thermodynamic properties of the working fluid and the increase of entropy along the circuit by using real efficiency values. Real thermal power cycles are usually in the range of 30-45% [62], depending on the steam temperature and design of the plant. The higher the temperature, the lower the losses and the lower the content of

harmful moisture in the turbines, being these the reasons why TES systems for power generation work with high-temperature heat [12]. More sophisticated industrial plants usually adopt more complex configurations aimed at increasing the overall efficiency. These include additional steps like the use of high-pressure and low-pressure turbines with intermediate reheat, implementation of feedwater heaters, superheaters, and so on [63].

Steam at lower pressure can be extracted in an intermediate step and used for heat delivery to a district heating network or to an industrial process. The present research considers only the first application. The discharge of useful heat that could be instead used for electricity generation results in a loss of electric power. Such loss coefficient is denominated *power loss factor*, β , and represents the decrease in electricity generation ($\Delta P_{out,el,loss}$) per extracted heat unit ($Q_{out,dhn}$). If the real thermal power delivered to the district heat network ($P_{out,dhn}$) and the efficiency of the heat exchange process (η_{dhn}) are known, then β can be expressed as the following:

$$\beta = \frac{\text{Loss of electrical power}}{\text{Useful heat extracted}} = \frac{\Delta P_{out,el,loss}}{Q_{out,dhn}} = \frac{\Delta P_{out,el,loss}}{\frac{P_{out,dhn}}{\eta_{dhn}}} \quad (2.4)$$

District heating systems usually require low discharge pressures, which reduces the value of β . Common values range from 0.256 to 0.123, depending on the size of the steam turbine and the extraction pressure [64].

Mechanical limitations of the steam turbines

Lastly, it is important to mention the mechanical limitations of the Rankine cycle. In this study, the following parameters are considered: the load-following rate, the start-up and shut-down rates, and the minimum served load. They are briefly presented below:

- The load-following rate, or ramp rate, is the speed at which a steam turbine can change its output power. It is usually modelled as a maximum output power change between one time step and the following one.
- As regards the start-up rate, it indicates how fast the system can reach the minimum load and is limited by the thermal stress of the components. The start-up speed decreases with the time the system has not been operating, and can be classified as cold, warm, or hot start-up. Regarding the shut-down rate, it represents the time it takes to the system to stop generating power. A short start-up and shut-down times are desirable to minimize the system losses.
- The minimum load is the established minimum output power at which the system operates and it has a double functionality. Firstly, it reduces the system losses given that the electrical efficiency increases with the load and with an output power close to the nominal value. Secondly, it reduces the number of start-ups and shut-downs, which eventually decrease the lifetime of the system.

The three parameters above-stated have been simplified and included in the model formulation in Chapter 4.

2.3 CRITICAL COMPARISON TO OTHER STORAGE TECHNOLOGIES

Many storage technologies are emerging to increase the flexibility of the energy system. Most of them are sector-specific and have been designed to solve the mismatch between RES supply and demand in the electricity market. However, some cross-sectoral storage technologies like ETES are coming forward as an alternative to integrate and bridge two of the most polluting sectors, heating and power, to decarbonize them and increase their flexibility.

The most relevant energy storage technologies are introduced in the following paragraphs. They have been classified into sector-specific or cross-sectoral, and according to their power and energy rating:

- Sector-specific technologies of small power and capacity rating (i.e. up to few MW and few GWh respectively): flywheels, batteries, flow batteries, and electromagnetic storage. In general terms, these technologies have short discharge times (i.e. seconds to hours) and very high initial efficiencies, which make them especially suitable for grid stability applications like frequency control or voltage control. They are mostly used for small-scale and short-term storage due to the high investment costs they imply [1].
- Sector-specific technologies of large power and capacity rating (i.e. up to several GW and several GWh respectively): pumped-hydro and compressed air energy storage (CAES). Pumped-hydro accounts for 96% of all electricity storage installed in the world [1] mainly due to its low cost per installed capacity. However, and similarly to CAES, it is site-constrained as it can only be installed where the necessary geographical conditions are in place. The low cost of these technologies and low energy losses over time, make them suitable for large-scale storage of longer time horizons.
- Cross-sectoral energy storage technologies of very large power and capacity rating (i.e. up to several GW and TWh respectively): hydrogen and ETES. Hydrogen will play an essential role as a large-scale integrator of RES due to its high mass-energy density. Nevertheless, its largest potential resides in the coupling of the power and transport sectors (P₂G, P₂L) due to its low round-trip efficiency and high costs when used to discharge electricity back to the grid [65]. ETES builds a two-way link between the power and heat systems, as it stores electricity or heat as thermal energy, to use it at a later time as heat or as electricity (H₂P and/or P₂H). When used for power generation it has a low round-trip efficiency, nevertheless, it has commercial potential as thermal energy storage requires a significantly lower capital expenditure (CAPEX) than other electrical energy stores.

The storage technologies listed above are compared in Figure 2.4 according to their power rating and cost per kWh. The technologies in green colour are those that depend on the topography to keep their cost low, while the ones in grey are location-independent.

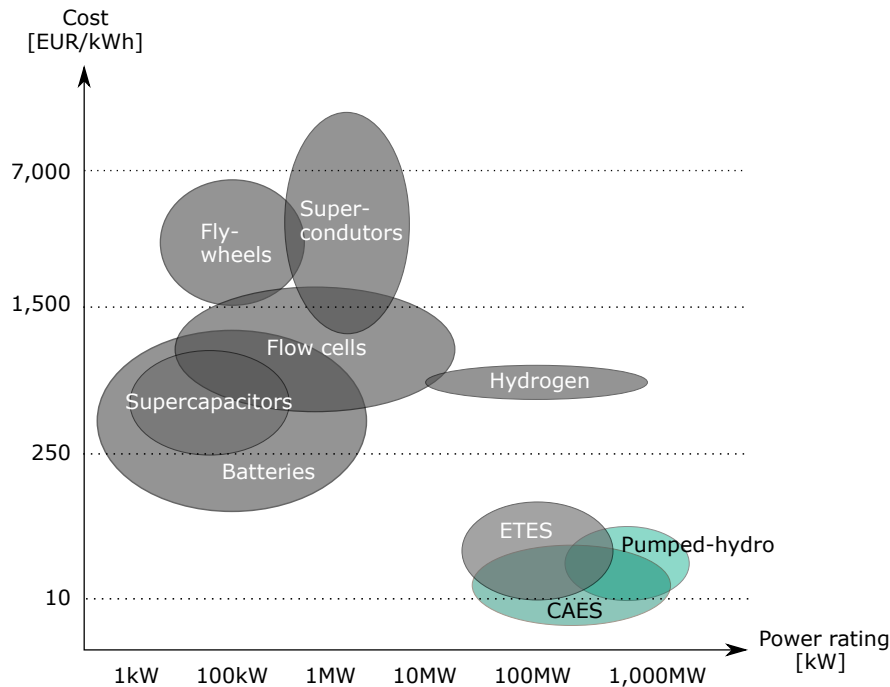


Figure 2.4: Electricity storage technologies displayed according to their power rating and cost per kWh. Based on [1]

From the perspective of the electricity storage market at the transmission level, the need for large-scale flexible storage like ETES will increase with the share of RES. This is due to the fact that with low RES penetration, other flexibility options can offer ancillary services in a more efficient way than ETES. The previously mentioned small power and capacity rating technologies have better capabilities to offer grid services like frequency regulation, due to for instance, their lack of inertia. However, this is not the main market for the ETES technology, which aims to offer security of supply to the system by accommodating large amounts of energy and increasing the flexibility of conventional plants.

Studies estimate that with a European renewable power share of 60% or higher, the need for large-scale and long-term electricity storage will increase dynamically [10]. This means that the technologies in the right-hand side of Figure 2.4 may experience a market expansion and will be less exposed to competition with other flexibility solutions. Lastly, it is also important to mention that, as shown in Figure 2.4, ETES is currently the only emerging affordable electricity storage technology for large-scale, location-independent systems.

3 | POTENTIAL APPLICATIONS

The versatility of the ETES technology allows for its use for different applications. This chapter introduces several use cases for ETES and their associated revenue streams. First of all, the benefits of integrating of ETES in renewable power plants are described. The impacts of a large share of renewables in the energy mix on the electricity market are then explained, together with the ways in which the storage technology can benefit from them. After the power generation applications have been covered, the chapter introduces the revenue streams from the sale of heat. Such 'heat applications' include the use of ETES by district heating networks and by heat-intensive industries. Lastly, the use of the storage asset as a means of increasing the flexibility of conventional power plants is explained.

3.1 INCREASED CONTROL OVER FLUCTUATING RENEWABLE POWER GENERATION

The power sector has already experienced an increasing trend of power generation from sources with low carbon emissions, with recent studies showing an 8.3% yearly growth in global RES capacity. The main drivers of this trend have been the extensive policy support schemes and a substantial cost reduction, mainly in solar PV and onshore wind [66]. The LCOE from RES is now competitive with that of fossil fuels, contributing to the phase-out of traditional high-carbon electricity generators and changing the plant portfolio of power systems. For instance, many European governments have announced their aim to cease coal use by 2030, putting 25% of Europe's currently operational coal fleet on a pathway to closure [67]. These changes pose significant challenges to the power sector, which needs to be transformed and increase its flexibility by sources like ETES.

RES have a different profile generation than fossil fuels, since they are intermittent and fluctuating in nature and therefore are not flexible on their own. The lower availability of traditional balancing power plants poses new challenges to the grid stability, where power generation should match consumption at all times and failure to do so may lead to blackouts and damage of the network. The mismatch between supply and demand can be seen as a twofold issue: a mismatch in space and a mismatch in time.

The mismatch in space occurs because the regions with the highest renewable power generation potential do not necessarily match the largest load regions. A good example of this is offshore wind, where the wind resource is at its highest

but distant from population and industry centres. A second issue is the concentration of wind power in a geographical area which is correlated up to an extension of about 500 km [68]. When the wind conditions are favourable, the regional wind turbines would tend to provide power simultaneously surpassing demand in a local space. A logical solution would be the transmission of the surplus generation to zones of lower generation, however, in some countries the regions of highest wind potential may coincide with the regions of highest grid congestion [69]. Consequently, congestion management caused by excess generation often involves renewable curtailment, which leads to high compensation losses and to the sub-optimal operation of the grid resources.

The mismatch in time is a result of wind and solar generation not being dispatchable, that is, they do not follow grid operators' requests but weather events that cannot be controlled. Solar peak production usually takes place at mid-day and wind peak production at night time [70], however, weather forecasts are not completely accurate so renewable generation cannot be unerringly predicted. Additionally, by its own nature regions high solar potential usually do not match regions of high wind potential, hence these power sources cannot be complemented to smoothen the renewable generation curve over time and meet the demand.

The issue of RES intermittency has led to the development of various solutions, among others, storage technologies, demand-side management, transmission grid reinforcement, and market mechanisms. Notwithstanding, with the exception of energy storage, these measures cannot provide time shift services from off-peak to peak periods. Export of electricity when there is over-generation or load curtailment only solves the spatial mismatch but cannot store the energy for future use, and may have negative effects on the market. Nonetheless, the future energy scenario is likely to include a combination of all the aforementioned solutions.

Based on the provided information, two revenue streams for renewable power plants can be identified:

Imbalance mitigation: the inaccuracy of renewable power generation forecasts cause imbalances between the market bid of renewable assets owners and real power production. Such imbalances are usually subject to economic penalties and therefore entail revenue losses. **Revenue stream:** in this case, ETES can be utilized to charge the surplus power, or to discharge energy when there is a shortage, to avoid imbalance penalties.

Curtailment mitigation: large shares of renewables in the energy mix increase the recurrence of periods with local power over-supply, due to their spatial correlation. When congestion-relief measures are not sufficient to ensure the stability of the grid, operators cut off renewable power production that could have been otherwise sold to the market. **Revenue stream:** ETES can be used to store surplus renewable power during times of grid congestion. This application is relevant in countries where curtailment compensation measures are not in place.

Additionally, a third application can be identified for grid operators. This utilization is currently not possible under many countries market regulation (e.g. Germany), but it might unfold in the future as the deployment of renewables reaches very high levels.

Grid upgrade deferral: the integration of large amounts of renewable energy in some grid nodes poses a threat to the stability of the system due to congestion. Large grid investments will be necessary mainly in regions with high renewable potential. **Revenue stream:** large scale storage like ETES can be a solution to avoid the large capital investments of grid upgrade. The storage can be used to take in power from the grid when there is excess generation, and return it to the grid when there is not enough supply.

3.2 ENERGY ARBITRAGE AND GRID SERVICES

The increased rigidity and uncertainty of the electricity system has impacted the wholesale electricity market, where generators, electricity suppliers, utilities, traders, and large industrial consumers trade the commodity and keep the grid balance. The wholesale market is disaggregated into different markets with different times between trading and delivery. The several electricity markets are depicted in Figure 3.1 and they include: the forwards, the day-ahead, the intra-day, and the energy balancing markets.



Figure 3.1: General timing of electricity markets

In the energy day-ahead (DA) market, sellers and buyers make their offers based on factors such as their marginal costs, forecasted renewable generation, demand, and so on. The generators are dispatched according to their merit order and the price of the generator that satisfies the marginal demand. Because renewable energy generation is fluctuating in nature, an increased penetration of RES increments the volatility of the prices and the market uncertainty. In order to reduce their exposure to unstable spot prices, market participants may choose to trade electricity in the forwards market. In such market, the trading parties agree on a fixed price through a bi-lateral contract (e.g. power purchase agreement (PPA)).

The intra-day and the energy balancing markets are those that take place closer to delivery, and they are designed to keep the power balance in the network. In

the intra-day scheme, the market participants can trade the difference between the electricity already sold/bought in the day-ahead and the intra-day forecasts. The energy balancing markets include processes from several hours before the delivery of electricity to real-time operation. Typical balancing markets include up to five processes to provide ancillary services to the system. The main processes are frequency containment reserves (FCR), frequency restoration reserves with automatic activation (aFRR), frequency restoration reserves with manual activation (mFRR), and replacement reserves (RR). These are explained in more detail in the following paragraphs.

Each balancing process has technical requirements that must be met by the generators, or in this case by the storage operator, in order to offer these services. The ensuing requirements correspond to the European normative [71].

Frequency Containment Reserves (FCR)

The FCR are in charge of stabilising the frequency at a steady-state value immediately after a disturbance occurs, and they are automatically activated. These reserves have a strict requirement of a maximum activation time of 30 seconds and in some countries the capable generators are obligated to reserve a certain amount of capacity to this end. The time response requirement makes the ETES technology unsuitable for this application under cold start conditions.

In most of Eastern-European countries and in several others like e.g. Spain, FCR can only be provided by generators, while currently pump storage and batteries are excluded from this market [72].

Frequency Restoration Reserves (aFRR and mFRR)

After 30 seconds the FCR are replaced by the aFRR, which are used to restore the frequency to its reference value (e.g. 50Hz). These reserves should have an activation time of approximately 5 minutes and provide the balancing energy between 30 seconds and 15 minutes. Both FCR and aFRR are also called spinning reserves as they have to be on-line but unloaded in order to react fast when a shortfall occurs. mFRR provides a similar service than aFRR and it can be spinning or non-spinning, if the technology is flexible enough. These reserves should be able to respond within 15 minutes and are activated manually or semi-automatically.

Similarly to the other balancing markets, the regulations vary across the different countries. For instance, in some countries grid users participate in a mandatory regime (e.g. Croatia, Hungary) for a fixed price or for free, while in others there is no obligation to offer reserve capacity (i.e. Germany). In most European countries there are also specific restrictions on the minimum bid size [72].

Replacement Reserves (RR)

Lastly, RR are used to provide reserve power in order to relieve the operating reserves and allow them to be restored and prepared to react if a new short-

fall occurs. The generators participating in this market should have a minimum start-up time of 15 minutes.

The evolution of the energy market and the rising of new market mechanisms such as the ones listed above are unfolding new revenue streams for storage assets. The most interesting applications to date in for ETES are summarized below:

Grid services: the intra-day and the energy balancing markets are becoming increasingly relevant due to the uncertainty and intermittency of renewable power generation. Energy storage can provide a wide range of energy services to the system in order to maintain the stability of the power grid and prices. **Revenue stream:** ETES can provide grid services while charging and discharging. More precisely, the possible applications depend on the operation, the design of the system, and the market design. In principle, ETES is suitable for providing aFRR, mFRR, and RR.

Energy arbitrage: electricity spot prices are not constant but dependent on many factors, such as adequacy between generation and demand, fuel costs, and so on. Additionally, the increase of renewables in the energy mix – which have a zero marginal cost and an intermittent nature – can increase the volatility of the energy prices. **Revenue stream:** ETES can be used in order to profit from such price variations in a direct way, buying electricity at low prices and discharging it at peak prices, and in an indirect way by not selling power when prices are low and storing it instead. The power generation efficiency plays an important role in this application due to the energy losses, which in turn result in revenue losses.

3.3 HEAT SUPPLY TO A NEARBY DISTRICT HEATING NETWORK

Despite being a fundamental component towards a low-carbon economy, the heating sector decarbonization has received little attention in the energy transition and in energy policy. In the European context, specific measures for increasing the share of renewable energy in this sector were provided for the first time in the revision of the Renewables Directive in 2018. Recent policy measures focus their efforts on the improvement of the heat use efficiency, promoting better building standards, insulation, and energy savings. As a result, direct renewable heat consumption has been deployed at a slower rate than renewable electricity consumption and its potential remains untapped.

The heat market is quite fragmented and composed of many different players, which also increases its complexity and delays its modernization. It closely interacts with other energy markets, especially the electricity and the fuel markets, but there are still uncertainties as regards the role that these links will play in the future energy system [73]. There is no equivalent to the electricity or gas spot markets, so most of the current supply is based on bilateral long-term contracts

between the heat producers and the heat suppliers. Despite its complexity, the industry is seeing some efforts to drive its decarbonization.

The emerging heating technologies that attempt to substitute traditional polluting technologies include non-electric, electric, and hydrogen technologies, hybrid systems, DHN, and surplus heat [74]. Together they currently provide 10.3% of the final heat consumption, of which 1.9% comes from electric technologies (i.e. electric heaters and electric heat pumps) [75]. The lack of local strategic planning for heating infrastructure, together with poor long-term political visibility, still present a significant barrier to the wide penetration and development of these technologies [76].

Among the large scale sustainable heating solutions, centralized DHNs are a more flexible and economically efficient approach than distributed heating systems. The effectiveness of centralized DHNs has been proven in some European countries like Denmark, where 60,000 km of district heating grid provide heating to 64% of all residential buildings [77]. Additionally, DHN have the potential to harvest the full benefits of wind power by reducing curtailment, due to the temporal correlation of wind availability and heat demand. Nevertheless, there are some challenges to the introduction of these systems such as institutional barriers, lack of space for new networks, and logistical challenges for plant siting [75]. Additionally, heating (and cooling) is consumed locally since its transportation on long distances is not economical and the thermal losses are large.

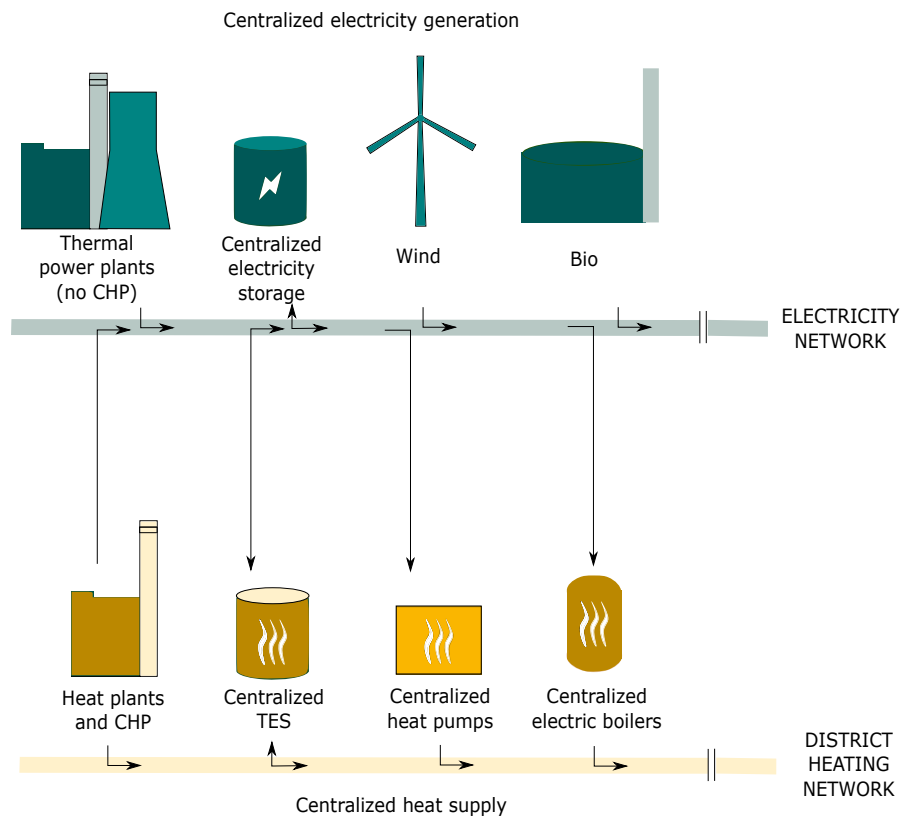


Figure 3.2: District heating and electricity network example. Adapted from [2]

The supply of heat through a DHN has different costs associated to it, including: capital costs of the piping, depreciation, operation and maintenance, administration costs, and purchasing costs of heat. The heat supplier is usually responsible for securing the heat, its transmission, and its distribution from the thermal source to the consumers. Among the previously mentioned costs, the purchase of heat typically accounts for the largest share of the bill, and it depends on the nature of the contract agreement between the contractual parties. Such price is usually dependent on [78]:

- The heat source and fuel costs: e.g. conventional power plant, biomass, heat pump, wind power, etc.,
- in cogeneration plants, the extent to which costs and revenues of the simultaneous generation of electricity and heat are allocated to heat,
- the extent to which the lost revenues from electricity generation are included in the heat purchase contract,
- the security of supply,
- the number and diversity of purchasing profiles (i.e. consumers),
- the pipe length per consumer, and the associated pipe losses.

Among all the aforesaid elements, the heat source is the most determining factor of the price at which a heat producer (e.g. ETES owner) can sell the good: the greener the source, the higher the price at which it is sold. This feature is beneficial for heat suppliers with renewable energy sources.

Lastly, it is important to mention the heat supply requirements and their impact to the ETES business case. The temperature of supply water is usually between 65-120°C, and the return water is usually in the range of 25-75°C. Because of this reason, low-temperature SHS systems such as water tanks present a more economical solution than high-temperature thermal storage like ETES. The installation of ETES in a DHN would only be justified by the cogeneration of heat and power, where the operation of the storage would follow the power demand and the sale of heat to a DHN would be an extra revenue stream. Because of this reason, the model of this thesis only considers the extraction of heat between the high-pressure and low-pressure turbines and not the extraction of high-temperature heat from the air cycle.

Sale of heat to a district heating network: the transition of the heating sector towards a decarbonized system passes by a greater integration of sustainable sources and by an increased efficiency. Consequently, solutions like centralized DHN are evolving and benefiting 'green-heat' suppliers. **Revenue stream:** ETES can be used to supply heat from renewable sources in a controllable way. Moreover, heat supply from sources with low emissions can be sold at a higher price than that from polluting plants. Because of the low temperatures of the district water flows and the availability of other cheaper storage technologies, the low-pressure steam from ETES would likely be a byproduct of electric power generation.

3.4 HEAT SUPPLY TO AN ENERGY-INTENSIVE INDUSTRY

Among all the end-use sectors, the industrial sector is the one that consumes the largest amount of delivered energy. Such energy is used for different applications comprising the already-mentioned heating and cooling, lighting, steam and cogeneration, process and assembly, and others [6]. Of the total energy, around 50% is delivered by natural gas, electricity, and renewables in OECD economies. The remaining energy sources are mostly comprised of coal and liquids (e.g. petroleum feedstocks). In non-OECD countries, the share of coal and oil products is larger.

The energy-intensive manufacturing industries are usually grouped into the seven categories presented in Table 3.1. The industries have been listed by decreasing order of expected energy consumption by the year 2040.

Table 3.1: Clustering of energy-intensive manufacturing industries, listed by expected decreasing energy consumption levels in 2040. Extracted from [6]

Industry clustering	Representative industries
Basic chemicals	Inorganic chemicals, organic chemicals (e.g., ethylene propylene), resins, and agricultural chemicals; includes chemical feedstocks
Iron and steel	Iron and steel manufacturing, including coke ovens
Refining	Petroleum refineries and coal products manufacturing, including coal and natural gas used as feedstocks
Nonmetallic minerals	Cement and other nonmetallic minerals, such as glass, lime, gypsum, and clay products
Food	Food, beverage, and tobacco product manufacturing
Pulp and paper	Paper manufacturing, printing and related support activities
Nonferrous metals	Aluminum and other nonferrous metals, such as copper, zinc, and tin

The largest potential for high-temperature storage rests in the industries where highly polluting energy carriers are burned to produce high-temperature heat. Because of this reason, among all the industries listed above, glass, ceramic, and metal manufacturing industries could be the most promising markets for the ETES concept. For instance, on the one hand steelmaking demands temperatures above 600°C, which is usually obtained from coal or natural gas. On the other hand, paper and pulp manufacturing only require temperatures up to 250°C [3], which can be supplied by more cost-effective solutions than ETES (e.g. biomass).

In order to provide a better understanding of the processes' requirements, the energy-intensive industries have been clustered by their heat temperature requisites in Figure 3.3.

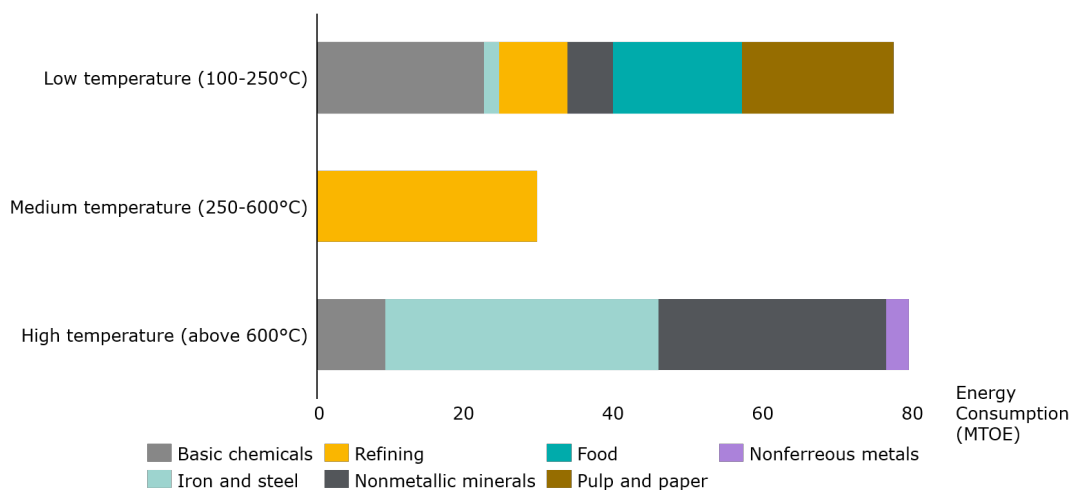


Figure 3.3: Energy industries by heat temperature requirements. Adapted from [3]

ETES can be integrated into energy-intensive industries with two main purposes: to store waste or by-product heat and/or to incorporate excess power from renewable energy sources. The need for thermal storage of waste heat originates when the by-product heat generation (from e.g. chemical reactions) and the demand of heat are not simultaneous. In this case, the heat needs to be stored to be used at a later moment in time. The reuse of released energy results in a more efficient usage of energy resources and in a lower fuel consumption, which lowers the operational costs of the plant. Additionally, thermal storage increases the end use alternatives of the waste heat, as it can be re-utilized in the same process in a closed loop, transferred to a different process in the manufacturing chain, or sold to an external heat demand like a DHN. As regards the integration of renewable power, the main goal in this case is the reduction of CO₂ emissions and their associated costs. The creation of a hybrid heat network (i.e. based on P₂H), also opens up the door to the participation on a demand response market, on mitigating the negative effects of renewable power curtailment, grid congestion, and mitigates investment risk by the diversification of energy sinks.

The potential of ETES in the industry has to be assessed against other competitor technologies. The most spread alternative to the burning of coal is the burning of natural gas, which can also deliver a high-temperature heat with a low carbon content. Therefore, in order to assess the business case for ETES in this market, the analysis results will be compared against the use of natural gas taking into account fuel costs, CO₂ price developments, etc.

Industrial waste heat recovery: multiple energy-intensive manufacturing processes release high-temperature heat that is not recovered and is therefore wasted. Such heat can be reused in a closed loop within the same process, or transferred to a different one. **Revenue stream:** ETES can provide time-shifting services to solve the temporal mismatch of heat demand and waste heat occurrence. The main benefits are a reduction of fuel consumption and CO₂ emissions, higher process efficiency, and additional revenues from external heat supply to e.g. a DHN.

Renewable energy sources integration by Power-to-Heat: the use of renewable electrical power is an upcoming strategy in order to decarbonize energy-intensive industries and use surplus power from renewables. The use excess of renewable power can also be beneficial to solve renewable curtailment and imbalance issues. **Revenue stream:** the main income for the industry would stem from the reduction of CO₂ emissions. Additionally, benefits can be derived from the diversification of revenues by the creation of hybrid heat networks and from 'P₂H arbitrage'.

3.5 FLEXIBILITY SOURCE FOR THERMAL POWER PLANTS

The envisaged increase of RES entails technical and economical challenges for traditional power plants, which were originally designed to provide baseload generation. This challenge is two-fold. Firstly, power plants need to flexibilize their operation to meet sudden demand peaks that cannot be supplied by renewables, as well as to respond to volatile price signals. Secondly, most power plants were developed to run on very polluting fuels that are increasingly penalized for their emissions. In some cases these penalties (e.g. CO₂ taxes) are so significant that plants have to be closed down because they are no longer profitable.

The system design of traditional power plants presents an important barrier for the increasingly required flexible operation. Table 3.2 gathers the technical characteristics of the most commonly used gas-fired and coal-fired power plants, as well as of the most advanced versions. As it can be observed, except for open cycle gas turbines (OCGT), fossil-fuelled power plants have very large start-up times that make them unsuitable to be online on time to meet demand peaks. Similarly, the ramping rates might sometimes not be enough even if they are already synchronized. The minimum load also presents a big restriction, since if power plants have great losses below these levels.

The introduction of thermal storage in these plants can increase their flexibility in different ways. For instance, regarding the minimum operational load, ETES can provide a heat sink to store the energy as an alternative to shutting down the plant. This way, the net generation and minimum load can be effectively reduced. The stored heat could later on be used for increasing the generation power without increasing the firing rate, thus decreasing fuel costs. Similarly, the stored power could be used to enhance the ramp rate and start-up capabilities, by means of providing feedwater preheating. Lastly, ETES can also increase the flexibility of CHP plants by decoupling the heat and power generation. If the generation follows the heat demand, the power can be stored and sold when it is more profitable in the electricity market. The opposite application would also be valid for and electric-demand following operation. An upside of using ETES

in existing power plants, is that some existing equipment can be integrated in the system to reduce the CAPEX.

As regards polluting power plants, they could be retrofitted to grid storage plants to provide grid support services. The investment of such plant update would strongly depend on the need to replace, partially or completely, the existing steam cycle assets.

Table 3.2: Technical characteristics of different gas-fired and coal-fired power generation technologies. Extracted from [7]

	Open cycle gas turbines (OCGT)	Combined cycle gas turbines (CCGT)	Hard coal-fired power plant	Lignite-fired power plant
Most commonly used power plants				
Minimum load	40-50%	40-50%	25-40%	50-60%
Ramp rate (per min)	8-12%	2-4%	1.5-4%	1-2%
Hot start-up time	5-11 min	60-90 min	2.5-3 h	4-6 h
Cold start-up time	5-11 min	3-4 h	5-10 h	8-10 h
State-of-the-art power plants				
Minimum load	20-50%	30-40%	25-40%	35-50%
Ramp rate (per min)	10-15%	4-8%	3-6%	2-6%
Hot start-up time	5-10 min	30-40 min	80 min - 2.5 h	1.25 - 4 h
Cold start-up time	5-10 min	2-3 h	3-6 h	5-8 h

The aforementioned advantages can be summarized into the following two applications.

Flexibility of power generation: the low flexibility of traditional power plants leads to high costs due to shut-downs and thermal fatigue of plant equipment. These issues are increasingly relevant as the penetration of RES in the system is increasing the volatility of the electricity markets. **Revenue stream:** by the integration of ETES in existing thermal power plants, the plants can improve their revenues by increasing their adaptability to electricity prices, by reducing shut-downs, and by expanding their equipment lifetime.

Retrofit of unprofitable polluting plants: power plants with high CO₂ emissions are seeing their business case fading out due to pollution penalizations. **Revenue stream:** these power plants can be retrofitted into storage plants with low GHG emissions, which can then yield revenues by doing electricity arbitrage, offering grid services, selling heat to a DHN, and so on.

4 | MODEL FORMULATION

This chapter aims at responding to the research sub-question 1. It presents the proposed model of the studied ETES technology and its integration with three main applications: the sale of heat to a heat-intensive industry, the sale of heat to a DHN, and the sale of electric power in the DA market. The set of constraints take into account the main technical limitations of the system, as well as the evolution of thermal energy stored over time. The search for the optimal boundary conditions is done by virtue of the model and by testing different input profiles that are further explained in Chapter 5.

The optimization has been carried out in Python using the solver 'Gurobi' and with a rolling horizon approach. The mentioned solver supports mixed-integer quadratically constrained programming (MIQCP), which is the type of problem herein formulated. An horizon of one week has been chosen on the grounds that it is a realistic time-frame for generation and demand forecasting, and in order to introduce some uncertainty to the optimization.

4.1 LAYOUT OF THE SYSTEM

The layout of the system and the main input and decision variables are shown in Figure 4.1. Such variables are explained in the following section.

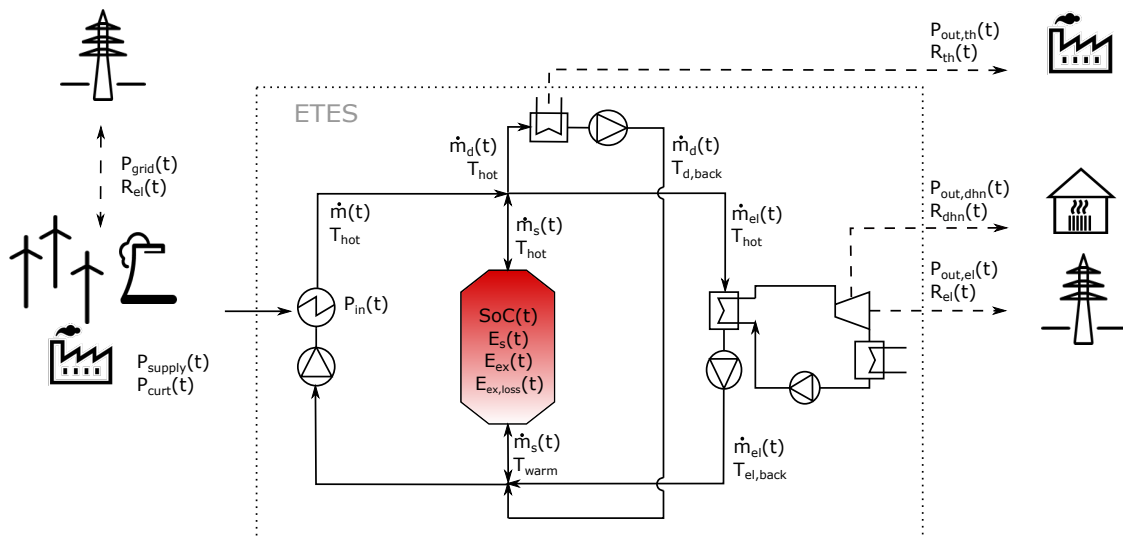


Figure 4.1: Layout of the system with thermal demand, power generation, and access to a DHN

4.2 NOMENCLATURE

The charging or discharging processes herein mentioned do not allude to the input or output of energy to or from the rock bed. They instead refer to the introduction of power into the overall ETES system through the resistive heater or heat exchanger, and to the output of power to the different demands. Whenever they refer to the packed bed, this will be clearly indicated.

Input variables

The input variables can be adapted to the specific case study by setting the unnecessary demands to zero.

$D_{\text{dhn}}(t)$	District heating network demand [kW]
$D_{\text{th}}(t)$	High-temperature heat demand [kW]
$P_{\text{supply}}(t)$	Electric or thermal power supply [kW]
$R_{\text{dhn}}(t)$	District heating network heat price [€/kWh]
$R_{\text{el}}(t)$	Day-Ahead market price [€/kWh]
$R_{\text{th}}(t)$	High-temperature heat price [€/kWh]

Storage's parameters and costs

β	Power loss coefficient when there is steam extraction [-]
$C_{\text{opex,el}}$	Variable costs per unit of electric power discharged [€/kWh]
$C_{\text{opex,th}}$	Variable costs per unit of thermal power discharged [€/kWh]
$C_{\text{SU,el}}$	Start-up costs of Rankine cycle [€]
$C_{\text{SU,in}}$	Start-up costs of the resistive heater [€]
E_{etes}	Thermal capacity rating [kWh]
L_{ex}	Loss in exergy inside storage due to conduction and natural convection per time step [kWh/t]
L_{self}	Self-discharge of the storage bed to ambient per time interval [-]
η_{dhn}	Efficiency of the thermal discharging process to a DHN [-]
η_{el}	Efficiency of the Rankine Cycle [-]
η_{heater}	Efficiency of the resistive heater [-]
η_{th}	Efficiency of the thermal discharging cycle [-]
$\bar{P}_{\text{etes,in}}$	Maximum thermal power input (i.e. input power rating) [kW]
$\underline{P}_{\text{etes,in}}$	Minimum thermal power input [kW]
$\bar{P}_{\text{etes,out,el}}$	Maximum electric power output (i.e. electric power rating) [kW]
$\underline{P}_{\text{etes,out,el}}$	Minimum electric power output [kW]
$\bar{P}_{\text{etes,out,th}}$	Maximum thermal power output (i.e. thermal power rating) [kW]

$P_{etes,out,th}$	Minimum thermal power output [kW]
$RD_{out,el}$	Ramp-down limit of the steam turbine [kW]
$RU_{out,el}$	Ramp-up limit of the steam turbine [kW]
$SD_{loss,el}$	Shut-down energy loss of the Rankine cycle [-]
$SD_{out,el}$	Shut-down ramping limit of the steam turbine [-]
SOC_o	Initial state of charge of the storage bed [-]
SOC_{max}	Maximum state of charge of the storage bed [-]
SOC_{min}	Minimum state of charge of the storage bed [-]
$SU_{loss,el}$	Start-up energy loss of the Rankine cycle [-]
$SU_{out,el}$	Start-up ramping limit of the steam turbine [-]
TD_{in}	Minimum down-time for charging [intervals of t]
$TD_{out,el}$	Minimum down-time for the Rankine cycle [intervals of t]
$TD_{out,th}$	Minimum down-time for thermal discharging [intervals of t]
TU_{in}	Minimum up-time for charging [intervals of t]
$TU_{out,el}$	Minimum up-time for the Rankine cycle [intervals of t]
$TU_{out,th}$	Minimum up-time for thermal discharging [intervals of t]

Air flow parameters

$C_{p,d,back}$	Specific heat capacity of air at $T_{d,back}$ [kJ/(kgK)]
$C_{p,el,back}$	Specific heat capacity of air at $T_{el,back}$ [kJ/(kgK)]
$C_{p,hot}$	Specific heat capacity of air at T_{hot} [kJ/(kgK)]
$C_{p,warm}$	Specific heat capacity of air at T_{warm} [kJ/(kgK)]
$T_{d,back}$	Temperature of the air flow returning to the system [K]
$T_{el,back}$	Temperature of the air flow returning from the Rankine cycle [K]
T_{hot}	Temperature of the air flow at the hot side [K]
T_{warm}	Temperature of the air flow at the warm side of the storage [K]

Decision variables

$E_s(t)$	Total thermal energy inside the storage bed [kWh]
$E_{ex}(t)$	Total exergy inside the storage bed [kWh]
$E_{ex,loss}(t)$	Total loss of exergy inside the storage bed [kWh]
$\dot{m}(t)$	Total air mass flow rate [kg/s]
$\dot{m}_d(t)$	Air mass flow rate to thermal demand [kg/s]
$\dot{m}_{el}(t)$	Air mass flow rate to Rankine cycle [kg/s]

$\dot{m}_s(t)$	Air mass flow rate to charge the storage bed (positive if charging, negative if discharging) [kg/s]
$P_{\text{curt}}(t)$	Power supply that is shut-down [kW]
$P_{\text{grid}}(t)$	Electric power sold to the grid (positive if selling power, negative if buying power) [kW]
$P_{\text{in}}(t)$	Thermal power input above minimum [kW]
$\hat{P}_{\text{in}}(t)$	Total thermal power input [kW]
$P_{\text{out,dhn}}(t)$	Thermal power sold to the district heating network [kW]
$P_{\text{out,el}}(t)$	Electric power output above minimum [kW]
$\hat{P}_{\text{out,el}}(t)$	Total electric power output [kW]
$P_{\text{out,th}}(t)$	Thermal power output above minimum [kW]
$\hat{P}_{\text{out,th}}(t)$	Total thermal power output [kW]
$u_{\text{in}}(t)$	State variable (1 if there is input power, 0 otherwise)
$u_{\text{out,el}}(t)$	State variable (1 if there is electric output power, 0 otherwise)
$u_{\text{out,th}}(t)$	State variable (1 if there is thermal output power, 0 otherwise)
$u_{\text{soc}}(t)$	State variable (1 if the storage is fully charged, 0 otherwise)
$u_{\text{soc,ex}}(t)$	State variable (1 if there is exergy, 0 otherwise)
$v_{\text{in}}(t)$	Start up variable (1 if charging starts up at t, 0 otherwise)
$v_{\text{out,el}}(t)$	Start up variable (1 if the Rankine cycle starts up at t, 0 otherwise)
$v_{\text{out,th}}(t)$	Start up variable (1 if discharging thermal power starts up at t, 0 otherwise)
$z_{\text{in}}(t)$	Shut down variable (1 if charging turns off at t, 0 otherwise)
$z_{\text{out,el}}(t)$	Shut down variable (1 if the Rankine cycle turns off at t, 0 otherwise)
$z_{\text{out,th}}(t)$	Shut down variable (1 if discharging thermal power turns off at t, 0 otherwise)

4.3 OBJECTIVE FUNCTION: MAXIMIZING THE REVENUE

In order to assess the economic performance of ETES under different conditions, the optimization is designed to maximize the annual net revenue (ANR), which is defined as:

$$\max ANR = \sum_{t=1}^n [R(t) - C(t)] \quad (4.1)$$

ANR Annual net revenue [€/year]

$R(t)$ Aggregated revenues in the time interval t [€]

$C(t)$	Aggregated costs in time interval t [€]
t	Index for the time intervals during the optimization
n	Chosen number of time intervals t per year

The aggregated revenue is made up from multiple revenue streams and depends on the considered application. The revenues are shown in Equation 4.2 in the following order: sale of thermal power to a heat intensive industry, sale of electric power to the DA market, and sale of heat to a DHN.

$$\begin{aligned}
 R(t) = & \hat{P}_{out,th}(t)R_{th}(t) \Delta t \\
 & + \hat{P}_{out,el}(t)[1 - SU_{loss,el} v_{out,el}(t)][1 - SD_{loss,el} z_{out,el}(t+1)] R_{el}(t) \Delta t \\
 & + P_{out,dhn}(t)R_{dhn}(t) \Delta t, \quad \forall t
 \end{aligned} \tag{4.2}$$

Additionally, if the power supply is electric and the system has a grid connection, the supply can bypass the storage and be directly sold to the market. In that case, the following element should be added to Equation 4.2:

$$P_{grid}(t) R_{el}(t) \Delta t, \quad \forall t \tag{4.3}$$

Note that the electric power in Equation 4.2 has some fixed start-up and shut-down energy losses, which should not be considered in the revenues. These losses represent the start-up and shut-down trajectories that depend on the technology, on the size of the turbine, and on the start-up conditions (i.e. cold, warm, or hot start-up). In this thesis they are approximated by a constant 50% start-up and shut-down energy loss, as shown in Figure 4.2, which means that the system needs one hour to ramp-up from zero to the minimum output power, and vice-versa. The online ramp-up and ramp-down losses are not considered in order to simplify the formulation. This assumption implies that the ramp capabilities are large enough to achieve the maximum power output in a negligible timescale compared to the time interval Δt .

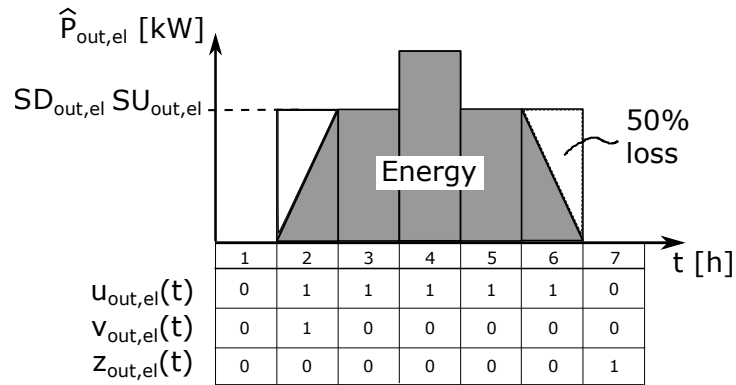


Figure 4.2: Start-up and shut-down energy losses of the Rankine cycle

The costs are determined by Equation 4.4. They include the operational expenditures of the storage, which are expressed as a cost per unit of electric energy or thermal energy discharged. The electricity consumption of the blower is also

taken into consideration. In theory such consumption depends on the SoC of the storage (the higher the SoC, the higher the work needed), however, in order to linearize the optimization, the consumption was approximated as 5% of the total (thermal) power discharged. The aforementioned consumption was obtained from empirical results from the pilot plant. In some applications, the power supply has a cost associated with it (C_{supply}), e.g. supply of electricity to the storage under a PPA, which should be also taken into account. Nevertheless, in most use cases this cost is set to zero, e.g. power supply from a wind farm. Lastly, the start-up cost of the Rankine cycle and of the charging system are considered. The former is simplified as a constant amount and approximated by using gas turbines' start-up costs given in [79], and the start-up ramping capability of the system. The latter is approximated by dividing the capital cost of the electric heater by the maximum number of cycles per lifetime, and should be only taken into account if the input power is electric.

$$\begin{aligned}
C(t) = & + \hat{P}_{out,el}(t) C_{opex,el} \Delta t \\
& + [\hat{P}_{out,th}(t) + P_{dhn}(t)] C_{opex,th} \Delta t \\
& + 0.05 \left[\frac{\hat{P}_{out,th}(t)}{\eta_{out,th}} + \frac{\hat{P}_{out,el}(t)}{\eta_{out,el}} \right] R_{el}(t) \Delta t \\
& + C_{supply} P_{in} \Delta t \\
& + C_{SU,el} v_{out,el}(t) + C_{SU,in} v_{in}(t), \quad \forall t
\end{aligned} \tag{4.4}$$

4.4 CONSTRAINTS

The model constraints have been clustered into: system wide constraints, demand constraints, and technical and operational constraints. The first include the constraints referring to the storage bed and the power supply. The second include the discharging limits and the demand levels. Lastly, the third includes the unit commitment equations, the operational limits imposed on the system, and the ramping capabilities of the steam turbine.

4.4.1 System constraints

Firstly, the total energy stored in ETES at the beginning of the time interval is defined as follows:

$$E_s(t) = \begin{cases} SOC_0 E_{etes}, & \text{if } t = 0 \\ E_s(t-1)[1 - L_{self}] + [C_{p,hot} T_{hot} - C_{p,warm} T_{warm}] \dot{m}_s(t-1) \Delta t, & \text{if } t > 0 \end{cases} \tag{4.5}$$

The first term in 4.5 represents the energy that remains inside the storage after the losses to the ambient temperature (L_{self}) are considered. As explained in Section 2.2.3, these losses are minimized by the container insulation. They are almost negligible for short time intervals, notwithstanding, they gain relevance for longer time horizons and prevent the technology from being used as seasonal storage. The second term embodies the energy charged or discharged to the storage bed, as a function of the difference in energy content between the inlet and the outlet air flows.

The usable energy inside the storage bed differs from the total energy and varies with time. Such loss in usable energy (or exergy) occurs due to natural convection and conduction between the hot and warm sides of the storage. The exergy loss process was explained in Section 2.2.3, and it can be understood as a lower temperature gradient between the inlet and outlet of the storage. Empirical results show that the loss in exergy is almost linear with respect to time, and that it takes place whenever the storage does partial cycling, that is, whenever it has not been fully charged. In this thesis, the exergy and the lost exergy are modelled by Equations 4.6 and 4.7, which have been obtained empirically. The value of exergy loss per time step (L_{ex}) depends on the design of the system and on the size of the storage tank, and therefore it should be tailored to each case study.

$$E_{ex}(t) = E_s(t) - E_{ex,loss}(t), \quad \forall t \quad (4.6)$$

$$E_{ex,loss}(t) = \begin{cases} 0, & \text{if } t = 0 \\ [E_{ex,loss}(t-1)[1 - L_{self}] + L_{ex} u_{soc,ex}(t)] [1 - u_{soc}(t)] \Delta t, & \text{if } t > 0 \end{cases} \quad (4.7)$$

The first element of the addition in Equation 4.7 represents the losses to the ambient, similarly to the formulation of the total energy in the storage container in Equation 4.5. The second element represents the loss in exergy per unit of time, which is approximately linear. The loss per time interval (L_{ex}) is multiplied by the state variable $u_{soc,ex}(t)$, and all the elements in the equation are multiplied by $[1 - u_{soc}(t)]$. The purpose of the first is to ensure that the exergy loss stops increasing when the exergy content is zero (i.e. the temperature gradient is already flat and no more natural convection and conduction occurs inside the rock bed). The second term resets the lost exergy to zero whenever the storage is fully charged and, consequently, the temperature transition region is restored and the exergy content is maximized. The aforementioned binary variables are formulated as follows:

$$u_{soc,ex}(t) \geq \frac{E_{ex}(t)}{SOC_{max} E_{etes}}, \quad \forall t \quad (4.8)$$

$$u_{soc}(t) \leq \frac{E_s(t)}{SOC_{max} E_{etes}}, \quad \forall t \quad (4.9)$$

In the optimization problem, $u_{\text{soc,ex}}(t)$ will always tend to be zero to minimize the exergy loss from Equation 4.7, and the opposite occurs with $u_{\text{soc}}(t)$, which tends to be one. Therefore, if there isn't any exergy left inside the storage, the first binary will be zero, and if the storage is fully charged, the second binary will be one. By modelling the state variables as shown above, it is likewise ensured that they will only take these values when all the exergy has been discharged, and when the storage is full, respectively. A graphic example of the energy, exergy, and exergy loss is shown in Figure 4.3. This example has been extracted from the simulations and the time and energy scales have been removed for confidentiality reasons.

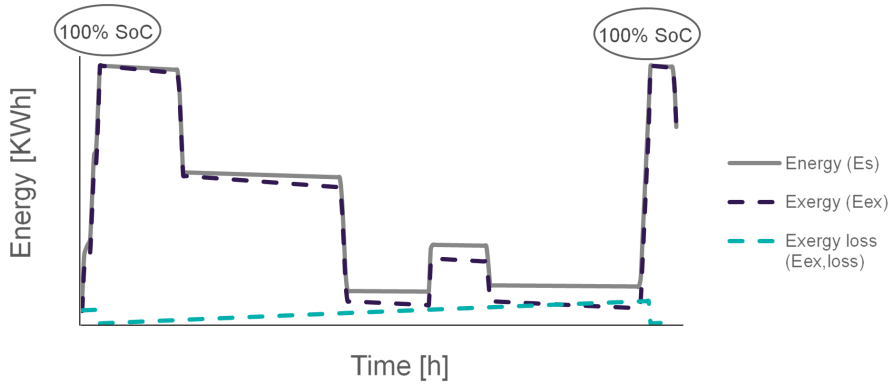


Figure 4.3: Example of the energy, exergy, and exergy loss curves

The balance between the supply power, the curtailed power, the input power, and the power sold or bought from the grid, depends on whether the input power is electric and has a grid connection,

$$P_{\text{supply}}(t) = P_{\text{curt}}(t) + \frac{\hat{P}_{\text{in}}(t)}{\eta_{\text{heater}}} + P_{\text{grid}}(t), \quad \forall t \quad (4.10)$$

or is thermal:

$$P_{\text{supply}}(t) = P_{\text{curt}}(t) + \frac{\hat{P}_{\text{in}}(t)}{\eta_{\text{heater}}}, \quad \forall t \quad (4.11)$$

The curtailed power variable refers to the power that has to be shut-down when, for instance, the electricity prices are negatives and the maximum charging power of the storage has already been reached. In any case the supplied power always has to be larger than the curtailed power:

$$P_{\text{supply}}(t) \geq P_{\text{curt}}(t), \quad \forall t \quad (4.12)$$

The input power to the system, $\hat{P}_{\text{in}}(t)$, is thermal and it is calculated by means of the energy balance in the electric heater or heat exchanger. The constraints below should be adapted depending to the application, that is, looking upon whether the $\dot{m}_{\text{el}}(t)$ or $\dot{m}_{\text{th}}(t)$ terms should be included.

$$\begin{aligned} \hat{P}_{in}(t) = & \dot{m}(t)C_{p,hot}T_{hot} - \dot{m}_s(t)C_{p,warm}T_{warm} \\ & - \dot{m}_d(t)C_{p,d,back}T_{d,back} - \dot{m}_{el}(t)C_{p,el,back}T_{el,back}, \quad \forall t \end{aligned} \quad (4.13)$$

The conservation of the air mass flows through the pipes is taken into consideration by the Equation 4.14.

$$\dot{m}(t) = \dot{m}_s(t) + \dot{m}_d(t) + \dot{m}_{el}(t), \quad \forall t \quad (4.14)$$

In the cases when the electricity prices are negative, the optimization may lead to the simultaneous charging and generation of electric power. This can happen due to the difference between the charging process and the Rankine cycle efficiencies (almost 100% vs. 30-45%) that result in profit generation. However, in reality such operation is forbidden in many countries (e.g. Germany). Therefore, to prevent the simultaneous input and output of electric power when the electricity prices are below zero, the following constraint has been added:

$$u_{in}(t) + u_{out,el}(t) \leq 1, \quad \forall t \quad (4.15)$$

4.4.2 Demand constraints

The thermal demand requirements are satisfied by the two expressions below, which represent the thermal output power after the losses and the maximum output power, respectively.

$$\hat{P}_{out,th}(t) = \eta_{th} \dot{m}_d(t) [C_{p,hot}T_{hot} - C_{p,d,back}T_{d,back}], \quad \forall t \quad (4.16)$$

$$\hat{P}_{out,th}(t) \leq D_{th}(t), \quad \forall t \quad (4.17)$$

Regarding the electricity generation, the overall output efficiency depends on that of the Rankine cycle and on whether there is steam extraction to supply heat to a DHN or not. The former varies with the output power of the turbine. Nevertheless, since the largest losses happen under partial loading and a minimum output power has been imposed to the system (explained later in Equations 4.34 and 4.35), the efficiency has been simplified as a constant value (η_{el}). The latter is due to the fact that high-quality heat would be extracted between the high pressure and low pressure turbines and, therefore, the overall electric power generation would be further reduced. This effect is taken into account in the model by means of the *power loss factor*, β . For more information about the efficiency of the Rankine cycle and β , please refer to Section 2.2.3.

$$\begin{aligned} \hat{P}_{out,el}(t) = & \eta_{el} \dot{m}_{el}(t)[C_{p,hot}T_{hot} - C_{p,el,back}T_{el,back}] \\ & - \beta \frac{P_{out,dhn}(t)}{\eta_{dhn}}, \quad \forall t \end{aligned} \quad (4.18)$$

The output power to the DHN is limited by several elements: by an own efficiency factor that represents the efficiency of the heat exchanger between the turbine and the district water cycle (η_{dhn}); by the Rankine cycle as the system can only discharge heat from the turbine if the turbines are running and generating power ($1 - \eta_{el}$); and by the maximum DHN demand. These efficiency coefficients are depicted in Figure 4.4.

$$P_{out,dhn}(t) \leq [1 - \eta_{el}] \eta_{dhn} \dot{m}_{el}(t) [C_{p,hot} T_{hot} - C_{p,el,back} T_{el,back}], \quad \forall t \quad (4.19)$$

$$P_{out,dhn}(t) \leq D_{dhn}(t), \quad \forall t \quad (4.20)$$

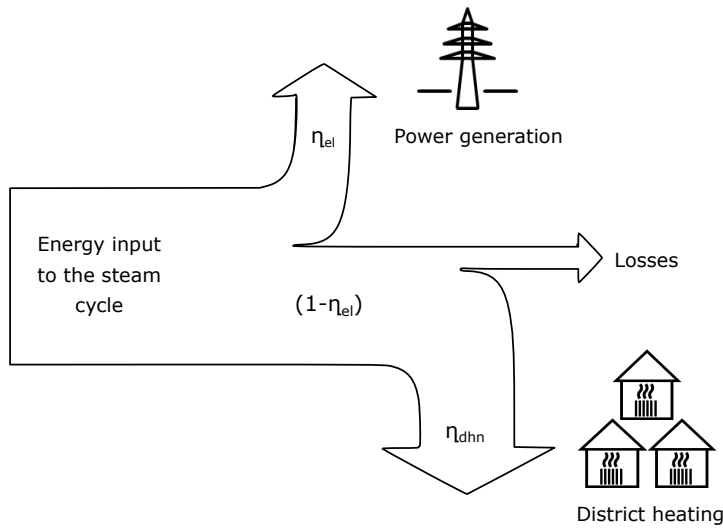


Figure 4.4: Power and thermal losses of the Rankine cycle with steam extraction

4.4.3 Technical and operational constraints

Lastly, the technical and operational constraints of the charging cycle, and of the electric and thermal discharging cycles are presented. The unit commitment, the minimum up-times and down-times, and the output power equations herein presented have been adapted from the unit commitment formulation from [80].

The unit commitment constraints of the charging and discharging equipment are the following:

$$u_{in}(t) - u_{in}(t-1) = v_{in}(t) - z_{in}(t), \quad \forall t \quad (4.21)$$

$$u_{out,th}(t) - u_{out,th}(t-1) = v_{out,th}(t) - z_{out,th}(t), \quad \forall t \quad (4.22)$$

$$u_{out,el}(t) - u_{out,el}(t-1) = v_{out,el}(t) - z_{out,el}(t), \quad \forall t \quad (4.23)$$

The minimum up-times for the heater, the heat exchanger, and the Rankine cycle are expressed in the three following equations.

$$\sum_{i=t-TU_{in}+1}^t v_{in}(i) \leq u_{in}(t), \quad \forall t \in [TU_{in}, T] \quad (4.24)$$

$$\sum_{i=t-TU_{out,th}+1}^t v_{out,th}(i) \leq u_{out,th}(t), \quad \forall t \in [TU_{out,th}, T] \quad (4.25)$$

$$\sum_{i=t-TU_{out,el}+1}^t v_{out,el}(i) \leq u_{out,el}(t), \quad \forall t \in [TU_{out,el}, T] \quad (4.26)$$

Likewise, the minimum down-times are modelled by means of the state variables as per below.

$$\sum_{i=t-TD_{in}+1}^t z_{in}(i) \leq 1 - u_{in}(t), \quad \forall t \in [TD_{in}, T] \quad (4.27)$$

$$\sum_{i=t-TD_{out,th}+1}^t z_{out,th}(i) \leq 1 - u_{out,th}(t), \quad \forall t \in [TD_{out,th}, T] \quad (4.28)$$

$$\sum_{i=t-TD_{out,el}+1}^t z_{out,el}(i) \leq 1 - u_{out,el}(t), \quad \forall t \in [TD_{out,el}, T] \quad (4.29)$$

The input and output powers can take values within a certain range between a minimum and a maximum, or zero. This entails that the electric heater, the heat exchanger, and the Rankine cycle only start working after a certain power threshold has been reached, and operate up to their maximum capacity. If there is not enough supply or demand, the devices are shut down. The variables therefore have a so-called semi-continuous nature. Because semi-continuous variables are not supported by the chosen solver, the input and output power are modelled by means of auxiliary and binary variables as proceeds:

$$P_{in}(t) \leq \eta_{heater} [\bar{P}_{etes,in} - \underline{P}_{etes,in}] u_{in}(t), \quad \forall t \quad (4.30)$$

$$\hat{P}_{in}(t) = \eta_{heater} \underline{P}_{etes,in} u_{in}(t) + P_{in}(t), \quad \forall t \quad (4.31)$$

The same formulation is used for the thermal output power,;

$$P_{out,th}(t) \leq [\bar{P}_{etes,out,th} - \underline{P}_{etes,out,th}] u_{out,th}(t), \quad \forall t \quad (4.32)$$

$$\hat{P}_{out,th}(t) = \underline{P}_{etes,out,th} u_{out,th}(t) + P_{out,th}(t), \quad \forall t \quad (4.33)$$

and the electric output power:

$$P_{out,el}(t) \leq [\bar{P}_{etes,out,el} - \underline{P}_{etes,out,el}] u_{out,el}(t), \quad \forall t \quad (4.34)$$

$$\hat{P}_{out,el}(t) = \underline{P}_{etes,out,el} u_{out,el}(t) + P_{out,el}(t), \quad \forall t \quad (4.35)$$

Because heat extraction to a DHN only happens when the turbines are generating power, the limits for $P_{out,dhn}(t)$ are implicitly included in Equations 4.34 and 4.35 and they do not require extra constraints.

The speed at which the steam turbine can increase or reduce the load is taken into consideration by virtue of the ramping capability limits of the steam turbine. The start-up or shut-down capabilities are also included:

$$P_{out,el}(t) - P_{out,el}(t-1) \leq RU_{out,el} - [RU_{out,el} - SU_{out,el}]v_{out,el}(t), \forall t \quad (4.36)$$

$$P_{out,el}(t-1) - P_{out,el}(t) \leq RD_{out,el} - [RD_{out,el} - SD_{out,el}]z_{out,el}(t), \forall t \quad (4.37)$$

Equations 4.36 and 4.37 were constructed in such a way that when the system is starting-up or shutting-down, they are reduced to the following two (respectively):

$$P_{out,el}(t) - 0 \leq SU_{out,el}, \quad \forall t \quad (4.38)$$

$$0 - P_{out,el}(t-1) \leq SD_{out,el}, \quad \forall t \quad (4.39)$$

Additionally, attention was paid to the magnitude of the start-up and shut-down ramping capabilities to ensure that they are larger or equal to the minimum power output $\underline{P}_{etes,out,el}$, in order to avoid discrepancies among the constraints and ensure the proper functioning of the model.

4.5 ROLLING HORIZON FRAMEWORK

The objective function and constraints presented above have been used within a rolling horizon framework. The rolling horizon methodology consists in solving the optimization in several sub-problems where only the input values of the prediction horizon are known. In this study, the optimization of the yearly operation of the storage has been divided into the optimization of weeks, which obtain the initial state of the system from the last optimization results. In this way, uncertainty and forecasts limitations are included in the solution.

The algorithm for the rolling horizon approach is presented in Figure 4.5.

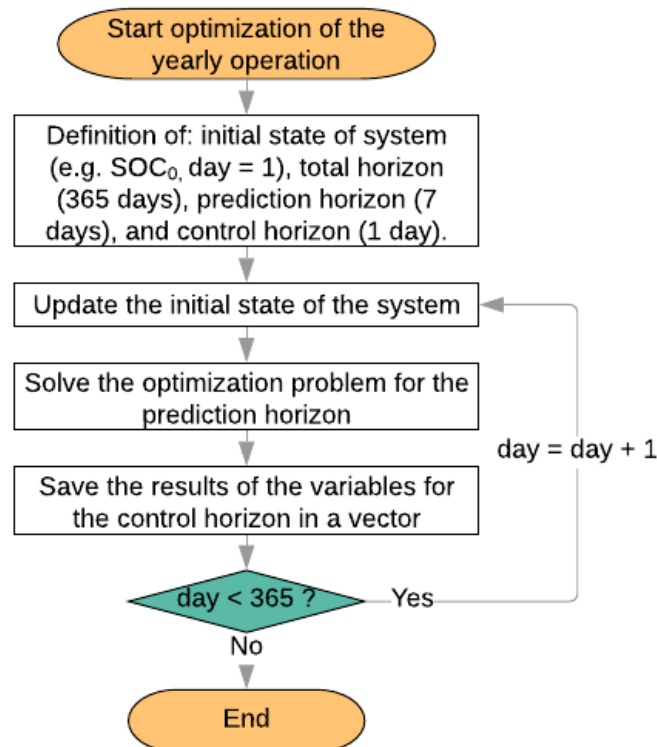


Figure 4.5: Rolling horizon scheme

4.6 MODEL VERIFICATION

The verification of the model has been performed by tracing the variables' results and by checking the final outputs, using diverse input combinations. After each simulation, a dynamic plot containing all variables results has been examined to identify potential errors in the formulation. For example, the start-up capabilities ($SU_{out,el}$ and $SD_{out,el}$) and the minimum discharging power ($P_{etes,out,el}$) of the Rankine cycle have been tested in the following way. If the value of the first parameters were smaller than the second one, the system never discharged electricity because it could not start-up or shut-down the steam cycle. Another example is the length of the minimum up-times of the charging and discharging components. When extreme values were tested, the revenues dramatically de-

creased due to the large constraints imposed to the operation of the system. The efficiency of the heat extraction from the turbine was also tested. If the power loss factor β was increased to very large values (e.g. above 2), the system did not discharge power to the DHN because of the large losses. Lastly, regarding the verification of the operational costs, this has been done examining their impact on the storage usage. For instance, without start-up charging costs ($C_{SU,in}$) the system underwent many and very short charging cycles. On the contrary, as the costs were increased, the system charged at minimum power between bigger cycles, as long as this was more profitable than stopping and re-starting the charging process.

In order to provide insight into the model's variables, a 24-hours extraction of a simulation is shown in Figure 4.6. The case study included a 70 MW high-temperature heat demand and a 78 MW DHN demand. The storage power rating was 139 MW, and the storage capacity 834 MWh.

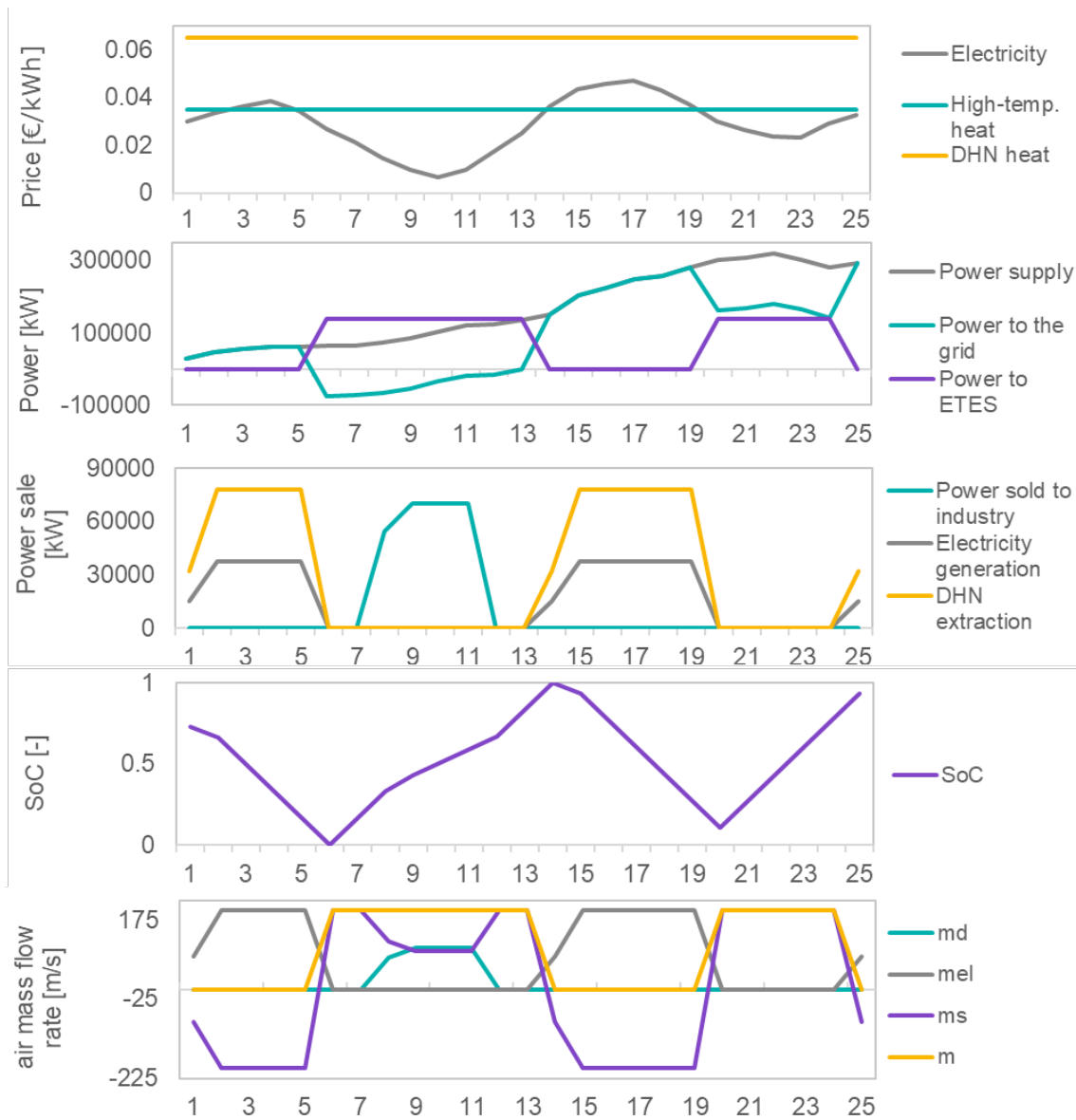


Figure 4.6: Simulation results of different variables

The first sub-plot shows the prices of the three available revenue streams. Because the electricity price oscillates, also the use of the storage varies pursuing the largest revenues. For instance, in the second sub-plot it can be observed that the power supply by-passes the storage and is injected into the grid whenever the electricity price is higher than the heat price. On the contrary, when the heat price is higher, all the power supply is introduced into the system and, because the power supply is below the maximum charging rating, the remaining power is bought from the grid (hence it takes negative values). The third sub-plot shows the power sales which confirm the aforementioned maximization of revenues. It is also confirmed that the maximum generation limits are respected and that, when the system is generating electricity, no power is simultaneously being bought from the grid. Lastly, the last two sub-plots show the SoC and the air mass flow rates. It is clearly seen how 'm' is the addition of all mass flow rates, and that the only variable that takes negative values is 'm_s' when the rock bed is being discharged for the generation of electric power.

4.7 FINANCIAL EVALUATION

The economic viability of the implementation of ETES under different boundary conditions was assessed by means of the NPV. The NPV was chosen among other financial indicators because it takes into account the time value of money, as compared to other indicators such as the payback period or the internal rate of return. By obtaining this value for different use cases, the main research question can be answered.

The NPV function is shown in Equation 4.40. As it can be seen, this indicator accounts for the net cash flows (i.e. objective function of the optimization problem; ANR), the initial investment (CAPEX), the lifetime of the project (N), and the discount rate (r). The simulations considered a lifetime of 30 years and a discount rate of 3.4%. Additionally, in order to carry out the analysis in a more conservative way, it was considered that the projects do not yield revenues during the first three years during which the investment is made. As pointed out by the Literature, sensitivity analyses have to be performed in order to mitigate the risks of the assumptions on the inputs to the model.

$$NPV = - CAPEX + \sum_{n=0}^N \frac{ANR}{(1+r)^n} \quad (4.40)$$

The decision whether to invest or not, was made by comparing the potential revenues with storage to the revenues earned in a *reference case* without storage. For instance, it can be the case that the NPV of a project with ETES is positive, but smaller than the NPV prompted without ETES. This would mean that the extra revenues yielded from storing power are not large enough to justify the

investment. Because of this reason, all the NPV results given in Chapter 6 (*Results and Discussion*) are relative values calculated as shown in Equation 4.41.

$$NPV = \frac{NPV_{ETES} - NPV_{ref.case}}{NPV_{ref.case}} 100\% \quad (4.41)$$

The calculation of $NPV_{ref.case}$ was carried out for every case study as explained below. A summary of the equations is shown in Table A.1 in Appendix A. Such calculation was similarly performed from a conservative perspective, where no extra operational and capital costs were taken into account. The rationale behind the calculations was the following:

1. Firstly, the nature of the supply power has to be determined (i.e. heat or electricity). This distinction is crucial for determining the discharging efficiency to the different applications. If the supply power is heat, in order to participate in the electricity market it should be transformed into electricity and incur into Rankine cycle losses. On the contrary, if it is electric, the energy losses do not need to be considered. This point goes hand in hand with the next one.
2. Secondly, just like Point 1, the energy type of the energy sinks has to be identified. The options have been classified into: heat only (i.e. energy-intensive industry), electricity only (i.e. day-ahead market), or heat and electricity combined (i.e. all possible applications). Similarly to Point 1, the main consequence of this step is the determination of the discharging efficiencies.
3. Thirdly, the boundary conditions (i.e. prices and demand) have to be analysed to calculate the optimal revenue stream. Firstly, it has to be checked whether it is more profitable to sell power or heat, whenever both options are available. Once this is determined, the amount of power supply has to be compared to the thermal demand (if there is one). As long as the power supply is larger than the demand, all the demand can be delivered. If on the contrary the demand is larger than the available power, then only this power can be supplied.
4. The resulting revenues have been calculated for each hour of the year, and later on aggregated to determine the total annual revenue for the *reference case*. This value was then introduced in Equation 4.40 (with no CAPEX) to calculate the $NPV_{ref.case}$ value.

A flow chart of the process explained above has also been included in Appendix A.

5 | ANALYSIS APPROACH

The search for the optimal market and demand conditions should be conducted in a way that generalized answers can be given to the research questions. With this aim, the analysis has been based on the use of artificial input signals constructed from real data. This approach allowed to evaluate and isolate the impact of key factors (e.g. average, price volatility, etc.) of each input curve (i.e. power supply, demand curves, and price curves) on the results. By doing so, the study of a very complex and uncertain field as it is the energy system, is narrowed down to the independent evaluation of its constituent elements.

The generation of the artificial signals was done via the fast Fourier transform (FFT) algorithm, herein explained. After a brief introduction to the methodology, the resulting curves that have been used in the analysis are presented. The chapter ends by giving an overview of the considered applications, prior to the discussion of results in Chapter 6.

5.1 SIGNAL PROCESSING IN THE FREQUENCY DOMAIN

Signal processing consists of the manipulation of real data with the aim to display it in a way that its information is easier to process. Among the different types of signals, some present time-varying oscillations that enable to express them in the frequency domain. In order to find the dominant frequencies of such fluctuations, a spectral analysis on actual data is usually performed to uncover hidden periodicities.

The spectral analysis can be carried out by means of the FFT algorithm, which is an efficient tool for computing the discrete Fourier transform (DFT). In few words, the Fourier Transform is a mathematical tool that returns the strength $Y(f)$ of a continuous function $y(t)$ at a certain frequency f :

$$Y(f) = \int_{-\infty}^{\infty} y(t) e^{-2\pi i f t} dt \quad (5.1)$$

The DFT is the equivalent of the continuous Fourier Transform expressed above, but for a finite sequence of data with N sample values. Because continuous-time signals cannot be processed by digital computers, the original signal is discretized and the DFT is used instead. The FFT is a very computationally-efficient algorithm of the DFT, which consists of dividing the discrete sample of data into

two sequences of length $N/2$ (because of this reason, the sample data has to be a power of two). Once the dominant frequencies have been obtained with the FFT, they can be used to decompose the time-series into a weighted sum of sine functions of the form:

$$F(t) = A_0 + \sum_{i=1}^N A_i \sin(2\pi f_i (t - \phi_i)) \quad (5.2)$$

where A_0 denotes the average, A_i the amplitude, f_i the frequency, and ϕ_i the phase-shift.

This periodic behaviour can be found in multiple real-life phenomenons. Of all the pertinent signals of this study, the ones that have a clear periodic nature are: the district heating demand, the high-temperature heat demand, and the DA market prices. The periodicity of these signals is analyzed in depth in the following section. The spectral analysis was carried out by means of the FFT built-in function of Matlab.

5.2 INPUT SIGNALS MODELLING

Among the different input signals of the model, the following three were considered to have an oscillating nature and have been subject to a FFT analysis:

- District heating demand (D_{dhn})
- Energy-intensive industry heat demand (D_{th})
- Day-Ahead electricity prices (R_{el})

The spectral analysis of the aforementioned variables is presented in the next sections. As regards the remaining input curves, namely, the power supply, the DHN market price, and the high-temperature heat price, they were left out of the frequency domain analysis for the following reasons:

- Power supply (P_{supply}): depending on the nature of the power supply, the input signal could have a periodical nature (e.g. power from a solar plant). Nevertheless, in order to introduce some stochasticity, which is the origin of most issues concerning renewables, an unaltered wind power curve was used in the simulations. Because the losses in the electric heater are nearly zero, the results also apply to a thermal input power (instead of electric).
- DHN market price (R_{dhn}): the price of heat supply to DHN is usually fixed in bi-lateral contracts between the heat producer and the supplier. Additionally, the transparency of district heating prices is very limited because this sector is excluded from the *European Energy Price Transparency Directive* and historical prices are not accessible [81]. For these reasons it was decided to fix R_{dhn} to a constant value.

- High-temperature heat price (R_{th}): similarly to most natural gas supply contracts, this price is usually agreed on a long-term supply agreement between the heat producer and the consumer. Consequently R_{th} was also modelled as a constant value.

5.2.1 District heating demand (D_{dhn})

The search of aggregated information about district heating demand and prices is a challenging task. Neither international scientific energy journal articles, nor energy agencies such as the IEA, Eurostat, or the European Commission, provide databases or detailed reports about this market. Consequently, the district heating load profile has been obtained from an alternative study that estimates the demand by means of meteorological conditions and temperatures [82]. The study gathers data from a weather station in Hamburg in the year 2012, and it follows a methodology provided by the *German Association of Energy and Water Industries* to generate the demand time series. It takes into consideration different types of buildings and demand (e.g. commercial buildings, residential buildings, agriculture, etc.), and scales up the profile to match the total annual heat consumption of the city, which is known.

Once the DHN demand was obtained, its spectral density was extracted by means of the FFT. The results are depicted in Figure 5.1, where the dominant frequencies have been highlighted. The coefficients (or amplitudes) and frequencies that were used in the sinusoidal curves are summarized in Table 5.1. Regarding the frequencies, they have been classified into low spectrum (frequencies larger than a week) and high spectrum (frequencies equal or smaller than a week). As regards the amplitudes, they are presented as a fraction of the average annual demand.

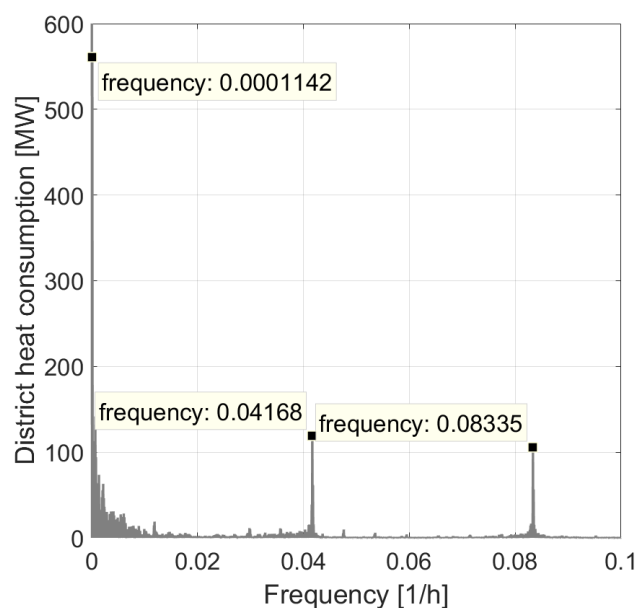


Figure 5.1: Spectral density of the hourly district heating demand of Hamburg

Table 5.1: Results from the spectral density analysis of the 2012 district heating demand of Hamburg

	f [1/h]	T [day]	Amplitude [% of the average demand]
Low spectrum	0.0001142	364.8	88.5 %
High spectrum	0.04168	1	18.8 %
	0.08335	0.5	16.7 %

The amplitudes and frequencies are caused by seasonal and societal recurrences. On the one hand, the lowest frequency (i.e. 365 days) is a logical outcome of the variation of meteorological conditions throughout the year. The ambient temperature is the main driver of heating demand and it has an annual fluctuation in most inhabited regions of the world. On the other hand, the higher frequencies (i.e. 1 and 0.5 days) are rooted in social habits and lifestyle of the population, such as holidays, weekdays, and weekends. For instance, the daily peaks mostly occur at 6 a.m. and 7 p.m., which are the times when the citizens wake up and when they come back from work. Lastly, regarding the magnitude of the demand, it is mainly driven by the number and type of consumers.

Information about the phase shifts is not given by the spectral study, thus the phase values were introduced to align the demand spikes with the actual demand. A phase of minus 7,000 hours (i.e. approximately 10 months) was added to the low frequency element to place the higher demands on the first and last months of the year. A phase of minus 4 hours was added to the higher frequencies in order to place the demand peaks in the morning and in the evening.

The resulting district heating demand signal is shown in Equation 5.3:

$$\begin{aligned}
D_{dhn}(t) &= \overline{D_{dhn}} + \sum_{i=1}^N D_{dhn,i} \sin(2\pi f_i (t - \phi_i)) \\
&= \overline{D_{dhn}} \left[1 + \frac{88.5}{100} \sin(2\pi \cdot 0.0001142 (t - 7000)) \right. \\
&\quad + \frac{18.8}{100} \sin(2\pi \cdot 0.04168 (t - 4)) \\
&\quad \left. + \frac{16.7}{100} \sin(2\pi \cdot 0.08335 (t - 4)) \right], \forall t
\end{aligned} \tag{5.3}$$

Where $\overline{D_{dhn}}$ is the average district heating demand, which will be varied in the analysis. The resulting sinusoidal curve is plotted in Figure 5.2 together with the actual demand.

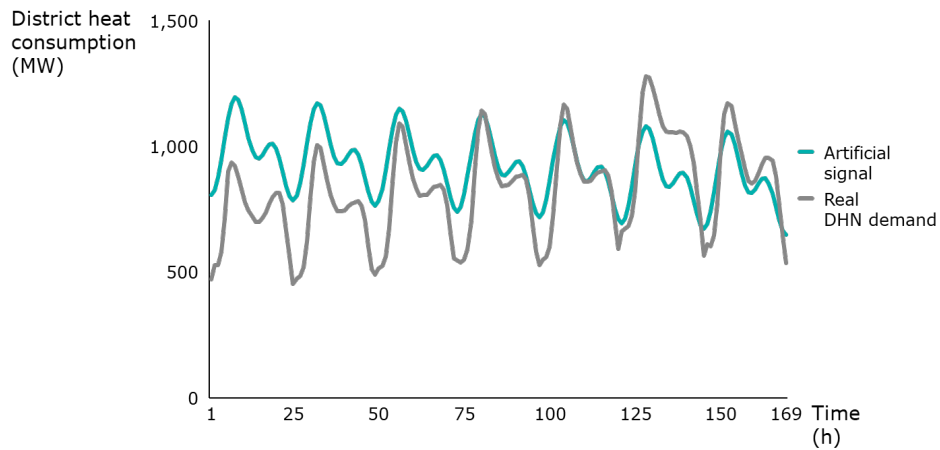


Figure 5.2: Real district heating demand and its equivalent artificial signal consisting of the sum of three sines (with periods of a year, a day, and half a day)

The analysis was also carried out for a constant district heating demand, which could be agreed, for instance, in a bi-lateral contract. In order to test such signal, the sinusoidal coefficients of Equation 5.3 were set to zero.

5.2.2 High-temperature heat demand (D_{th})

The high-temperature heat demand sinusoidal curve was developed using data from a real manufacturing plant. The selected plant operates continuously and therefore has a continuous steam demand that varies following the thermal load schedules. The spectral results are depicted in Figure 5.3 and summarized in Table 5.2. As the actual time series consisted of daily averages, the frequencies are given in a larger scale than the DHN data.

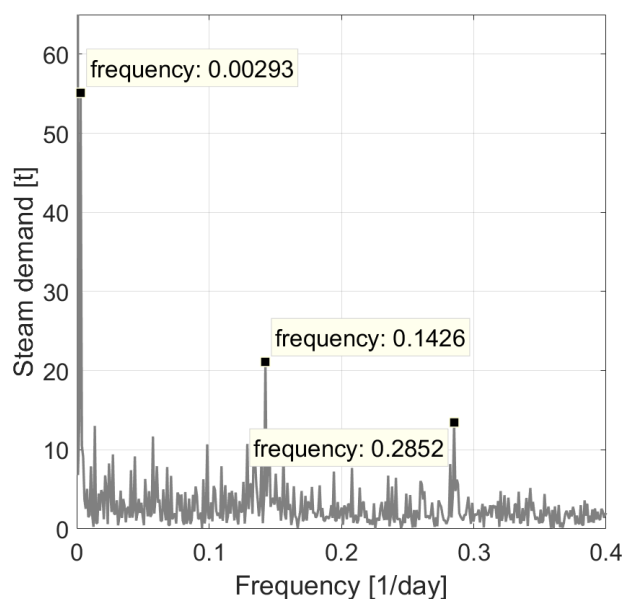
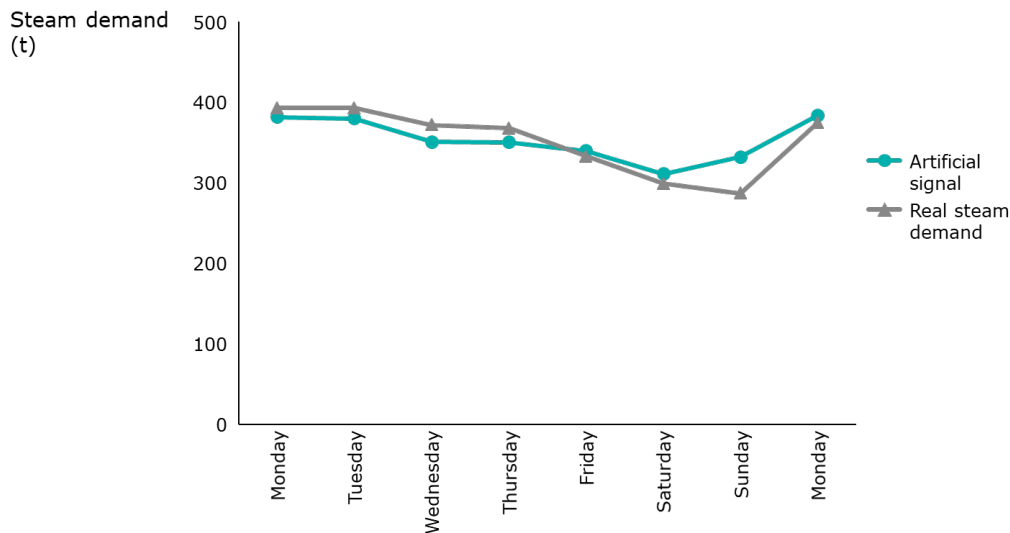


Figure 5.3: Spectral density of the steam daily demand of an industry

Table 5.2: Results from the spectral density analysis of the steam demand of an industry

	$f[1/\text{day}]$	$f[1/\text{h}]$	$T[\text{day}]$	Amplitude [% of the average demand]
Low spectrum	0.00293	0.000122	341.3	13.9 %
High spectrum	0.1426	0.000594	7	7.2 %
	0.2852	0.011883	3.5	4.4 %

The intermittency or load schedules of industrial processes can be explained by production requirements and by societal factors. For instance, the lowest frequency (i.e. 341 days) is a byproduct of the summer season, which depending on the industry may result in a lower production. In some cases, such frequency can be also be linked to the seasonality of some industries like e.g. construction or agriculture sectors. The remaining frequencies (i.e. 7 and 3.5 days) add up to increase the demand profile during the week-days and decrease it during the weekends. Such effect is clearly shown in Figure 5.4. As regards the magnitude of the fluctuations, these values are case-specific and therefore they have been subject to a sensitivity analysis.

**Figure 5.4:** Real steam demand and its equivalent artificial signal for a random week

Similarly to the district heating demand curve, the phase for each element was found by aligning the peaks to those of the real demand. A phase of minus 250 days (i.e. 6,000 hours) was added to the low frequency component to shift the absolute minimum to the summer period, and a phase of minus 6 days (i.e. 144 hours) was added to the higher frequencies to increase the demand in the working days and decrease it in the weekends. Because of the non-homogeneity of the actual demand, white noise (E) was also included to increase the unpredictability of the load throughout the week.

These elements build up the demand curve presented in Equation 5.4.

$$\begin{aligned}
 D_{th}(t) &= \overline{D_{th}} + \sum_{i=1}^N D_{th,i} \sin(2\pi f_i (t - \phi_i)) \\
 &= \overline{D_{th}} \left[1 + \frac{13.9}{100} \sin(2\pi 0.000122 (t - 6000)) \right. \\
 &\quad + \frac{7.2}{100} \sin(2\pi 0.0005942 (t - 144)) \\
 &\quad \left. + \frac{4.4}{100} \sin(2\pi 0.011883 (t - 144)) \right] + E, \forall t
 \end{aligned} \tag{5.4}$$

Figure 5.5 shows the full year profile of the actual and sinusoidal demand signals. The four outliers of the real demand coincide with regional holidays.

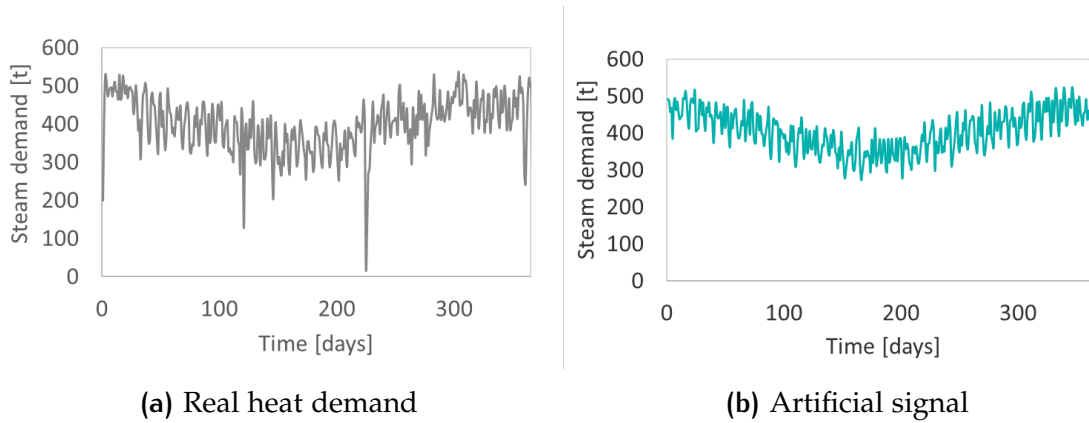


Figure 5.5: (a) Real annual heat demand data and (b) its equivalent artificial signal consisting of the sum of three sines (with periods of a year, a week and half a week) and white noise

In order to evaluate the application of ETES in industries with a continuous and constant demand level, simulations with constant demand curves were also analyzed. These simulations would apply to any industry where the demand does not change significantly over the time horizon of the simulation.

5.2.3 Day-ahead market price (R_{el})

The DA market price signals were constructed using data from two different European markets: the German and the Spanish markets. They were chosen among other European markets because these countries count with the largest renewable capacity installed. Most of the simulations were carried out with the German price characteristics, as this market is more attractive for storage due to its higher volatility. Nevertheless, the FFT was performed for both countries to spot potential country-specific features. The results of such analysis are shown in Figure 5.6 and the most relevant findings are shown in Table 5.3.

In order to find the spectral densities of lower frequencies, the hourly data of DA prices for the years 2014-2018 was also analyzed (see Appendix B). Additionally, the price coefficients of Germany were adapted so the price curve had the

same price spread as the actual one. This is an important modification, as it will be explained in the next chapter.

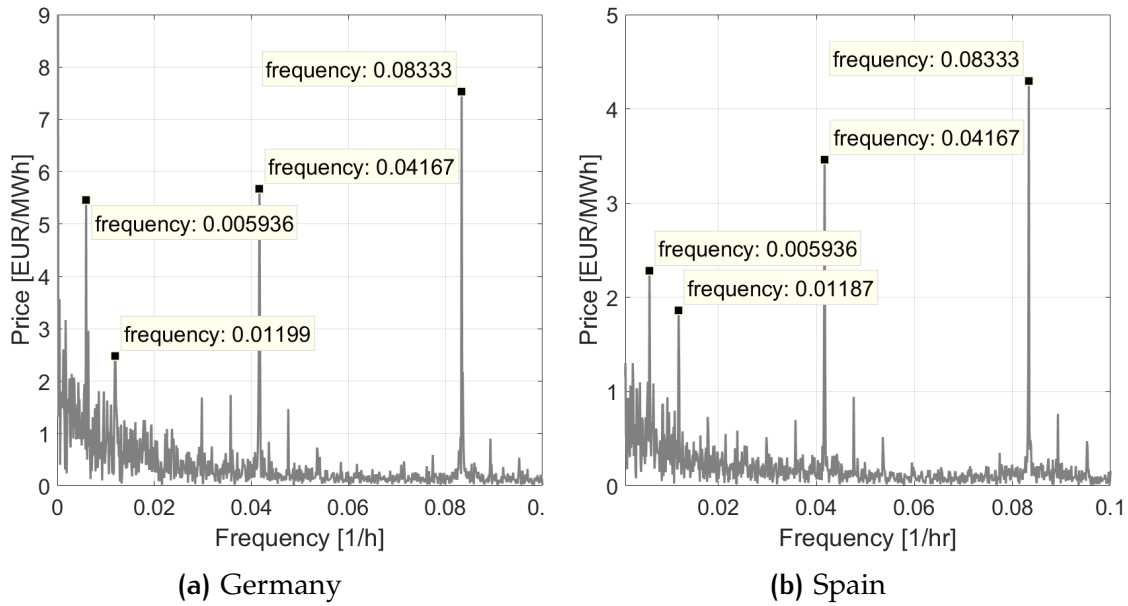


Figure 5.6: Spectral density of the 2018 day ahead markets prices of (a) Germany and (b) Spain

Table 5.3: Results from the spectral density analysis of the DA market prices of Germany and Spain

	f [1/h]	T [day]	Amplitude [EUR/MWh]		Average (\bar{R}_{el}) [EUR/MWh]	
			Germany	Spain	Germany	Spain
Low spectrum	0.0001141	365.2	10.57	9.37	45.52	57.24
	0.0002282	182.6	4.27	3.90		
High spectrum	0.005936	7	13.70	2.28		
	0.01187	3.5	8.51	1.86		
	0.04167	1	7.43	3.46		
	0.08333	0.5	13.70	4.29		

The electricity price formation is a result of many influencing factors, ranging from fuel prices to economic activity, and more recently to renewable sources availability. Regarding the low frequencies (i.e. 365 and 183 days), they add up to increase the prices in the first months of the year, and to create a large spike in September. Such spike was presumably caused by an increase in the natural gas commodity and CO₂ prices, which raised the wholesale rates in Europe (see Figure 5.7). As regards the frequencies in the high spectrum, they are an outcome of societal factors. The living schedules raise the demand during the week with respect to the weekends (i.e. 7 and 3.5 days), and build up two daily peaks in

the morning and in the evening (i.e. 1 and 0.5 days). The characteristics of the traditional generation fleet align the demand peaks with price peaks, however, the introduction of large shares of renewables may alter this relationship in the near future.

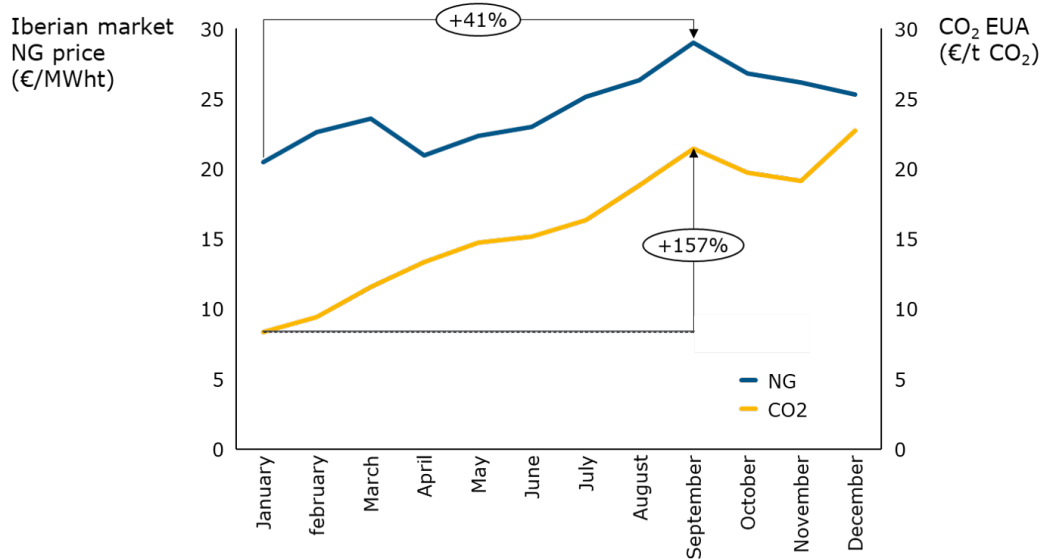


Figure 5.7: Evolution of the natural gas and CO₂ prices in the Iberian peninsula in 2018

In order to align the price peaks with the actual ones, a phase of minus 5,040 hours (i.e. 7 months) was added to the low frequencies (i.e. 365 and 183 days) components of both, the German and Spanish prices. The phase shifts of the higher frequencies (i.e. 7, 3.5, 1, and 0.5 days) differ for each country due to the different life schedules. In the case of Germany the phase shift was found to be minus 3 hours, whereas in the Spain data the phase corresponds to minus 5 hours. White noise was also added to include some uncertainty and variability to the signal. The German price, which is the one used in the simulations, is displayed in Equation 5.5:

$$\begin{aligned}
 R_{el}(t) &= \overline{R_{el}} + \sum_{i=1}^N R_{el,i} \sin(2\pi f_i (t - \phi_i)) \\
 &= \overline{R_{el}} + 10.57 \sin(2\pi 0.0001141 (t - 5040)) \\
 &\quad + 4.27 \sin(2\pi 0.0002282 (t - 5040)) \\
 &\quad + 13.70 \sin(2\pi 0.005936 (t - 3)) \\
 &\quad + 8.51 \sin(2\pi 0.01187 (t - 3)) \\
 &\quad + 7.43 \sin(2\pi 0.04167 (t - 3)) \\
 &\quad + 13.70 \sin(2\pi 0.08333 (t - 3)) + E, \forall t
 \end{aligned} \tag{5.5}$$

And the sinusoidal curve equivalent to the Spanish electricity price is:

$$\begin{aligned}
R_{el}(t) &= \overline{R_{el}} + \sum_{i=1}^N R_{el,i} \sin(2\pi f_i (t - \phi_i)) \\
&= \overline{R_{el}} + 9.37 \sin(2\pi 0.0001141 (t - 5040)) \\
&\quad + 3.90 \sin(2\pi 0.0002282 (t - 5040)) \\
&\quad + 2.28 \sin(2\pi 0.005936 (t - 5)) \\
&\quad + 1.86 \sin(2\pi 0.01187 (t - 5)) \\
&\quad + 3.46 \sin(2\pi 0.04167 (t - 5)) \\
&\quad + 4.29 \sin(2\pi 0.08333 (t - 5)) + E, \forall t
\end{aligned} \tag{5.6}$$

Figures 5.8 and 5.9 plot a week of the actual and sinusoidal profiles of Germany and Spain, respectively. It can be observed that the volatility of the German market is larger.

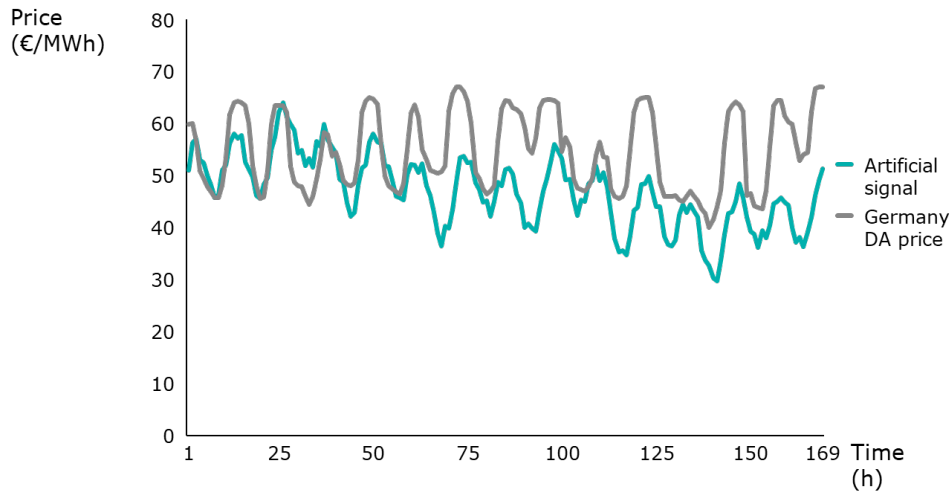


Figure 5.8: Real weekly electricity price of Germany and its equivalent artificial signal

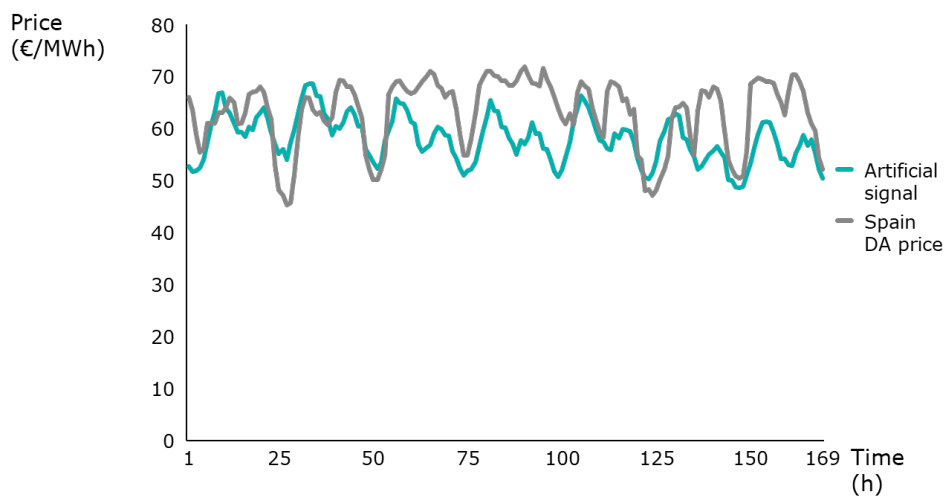


Figure 5.9: Real weekly electricity price of Spain and its equivalent artificial signal

The analysis aimed at finding the minimum requirements for the electricity prices and the most influential conditions for the business case (i.e. research sub-question 3). To this end, the following variables have been assessed:

- Rankine cycle efficiency: the Rankine cycle efficiency leads to important energy losses that limit the total amount of energy that can be sold back to the market. Thus, the system has been evaluated for larger efficiencies in order to assess their impact on the business case, and to determine whether it could be worth investing in improving this feature. The assessment also evaluates the trade-off between an increased efficiency and an increased CAPEX, to find out if under current conditions there is a market for any storage technology based on arbitrage only.
- Volatility of electricity prices: a business case based on energy arbitrage only is strongly dependent on the fluctuation of prices. Because of this reason, different electricity price profiles with varying volatilities have been tested.

5.3.2 Case 2: Power-to-Power and district heating

This case study builds upon Case 1 by adding an extra revenue stream from heat sales to a DHN. The main aim is to evaluate how much the revenues increase with respect to energy arbitrage only. The layout of the system is presented in Figure 5.11.

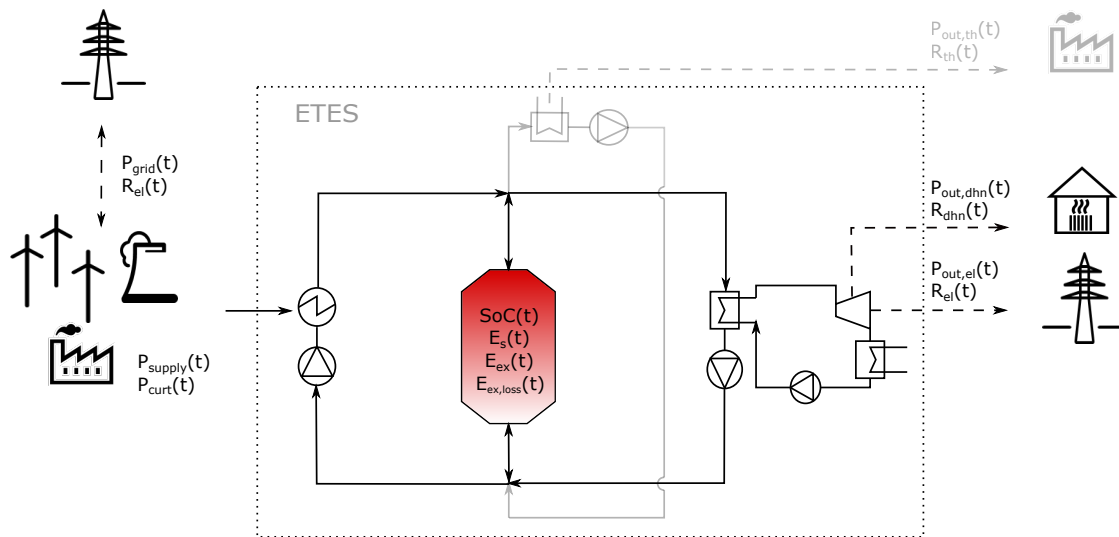


Figure 5.11: Layout of the system for a Power to Power and district heating application

Similarly to the previous Power-to-Power study, the analysis aimed at identifying the answers to the research sub-question 3, namely the most relevant boundary conditions for the business case. The analysis focused on:

- District heating price: the set of both, electricity and district heating prices, determine the operation of the storage. Several DHN price levels have been

modelled to observe the change in revenues with respect to changes in this variable, as well as to find the break-even price.

- District heating demand profile: the fluctuation of the district heating demand throughout the year was varied in order to examine its impact on the business case. A constant demand profile was also tested and compared to the oscillating demand.
- Rankine cycle efficiency: as in Case 1, the Rankine cycle efficiency was analyzed due to its relevance in the generation of power. Therefore, this parameter was also varied in the same way as in Case 1.
- Volatility of electricity prices: as energy arbitrage is one of the two revenue streams of this case, the volatility of prices was studied similarly to Case 1 and the results were compared against each other.

5.3.3 Case 3: Power-to-Heat

The Power-to-Heat application refers to the use of renewable power to generate high-temperature heat for an industry. The goal of this case was to study the potential of ETES in hybrid heat networks. The CAPEX considered in this configuration does not include the steam cycle, thus its lower than the one used in Cases 1 and 2. The layout of this case study is shown in Figure 5.12.

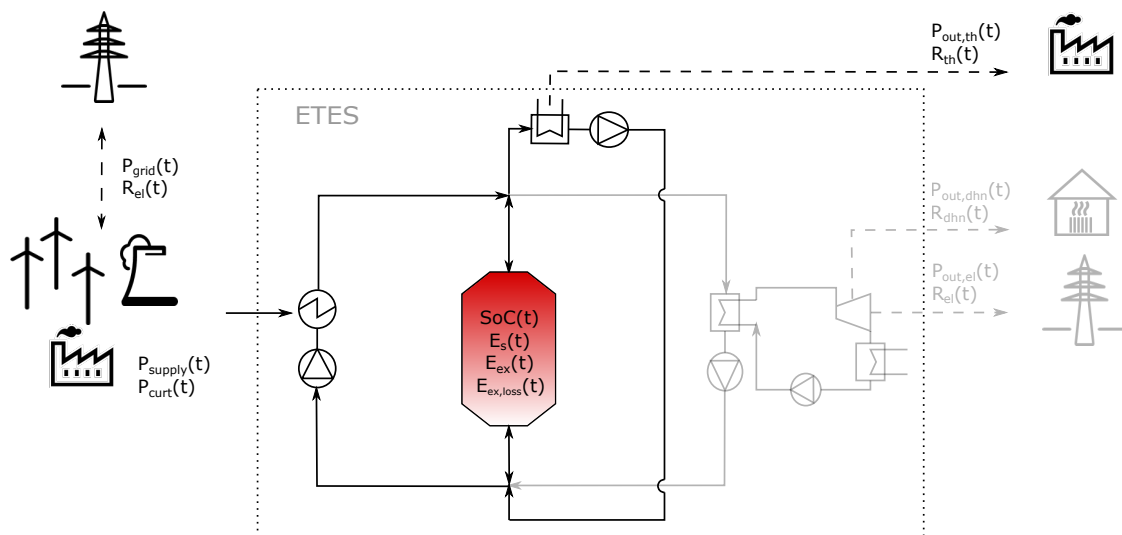


Figure 5.12: Layout of the system for a Power to Heat application

The obtained results can be compared to those of the previous ones to find which sector (i.e. heat or power) currently has the largest potential. This analysis corresponds to the research sub-question 2. In that regard, the study has focused on the following variables:

- High-temperature heat price: as previously mentioned, the heat price can have a big impact in the business case. Thus, several price levels have been tested and the break-even prices for Germany and Spain have been found.
- High-temperature heat demand profile: the fluctuation of thermal loads requires energy storage for time-shifting. The impact of such fluctuation profile on the operation of the storage has been analyzed by varying the corresponding input signal.
- Volatility of electricity prices: the electricity prices' impact on the business case was also studied for this application. The main difference with respect to the previous cases consists of the possibility of doing arbitrage by either selling electricity to the DA market, or by selling heat to the thermal load. This application therefore leverages from the difference between electricity and heat prices.

5.3.4 Case 4: Power-to-Heat-and-Power

Lastly, all revenue streams were merged in the same configuration in order to determine how the economics improved with revenue stacking. The modelled configuration is depicted in Figure 5.13.

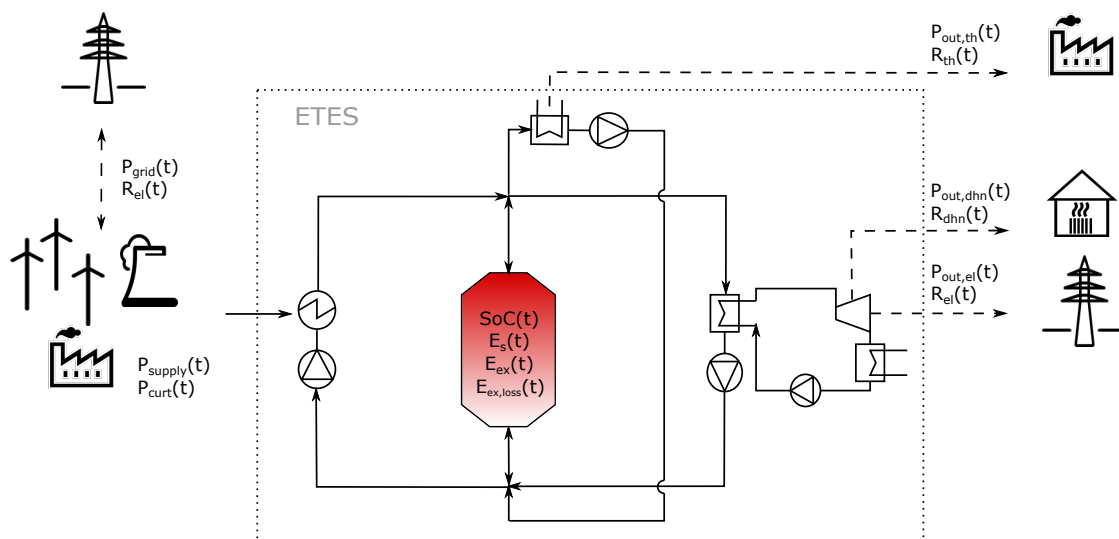


Figure 5.13: Layout of the system with the three applications

The variables under study are all the previous ones combined:

- District heating and high-temperature heat demand levels: different constant heat demand levels were tested to compare the sensitivity of the results to changes in demand, against changes in the prices.
- Rankine cycle efficiency: larger efficiencies were simulated with the aim to observe the changes in the operation of the storage. The analysis was done by using the break-even prices obtained from the preceding cases.

- Volatility of electricity prices: the profitability of ETES can be optimized by the diversification of energy sinks (i.e. electricity market, district heating, and industrial heat). The impact of the volatility in the individual applications was the same as with revenue stacking.

5.3.5 Summary of cases

The variables analyzed in each case study are summarized and compared in Figure 5.14.

	Case 1	Case 2	Case 3	Case 4
Electricity prices	✓	✓	✓	✓
Rankine cycle efficiency	✓	✓	-	✓
District heating price	-	✓	-	✓
District heating demand profile	-	✓	-	✓
High-temperature heat price	-	-	✓	✓
High-temperature heat demand profile	-	-	✓	✓

Figure 5.14: Summary of the case studies and their pertinent variables.

6

RESULTS AND DISCUSSION

The main findings and results to provide fundamental answers to the research questions are presented in this chapter. The analysis has been structured into four main applications or case studies: Power-to-Power (P2P), Power-to-Power and district heating (P2P and DHN), Power-to-Heat (P2H), and Power-to-Heat-and-Power (P2H&P). The first one aims to assess the profitability of ETES for electricity arbitrage only. The second case constructs on the previous one by adding an extra revenue stream from the sale of heat to a district heat network. The third case consists of the sale of high-temperature heat to a nearby industry, and the last case brings together all the previous ones. The sensitivity of the results to changes in several inputs has also been studied.

6.1 CASE 1: POWER-TO-POWER

The first case study is the analysis of ETES for only one application: energy arbitrage. The study concludes by assessing whether the necessary market conditions for achieving a positive business case are already in place.

All simulations were carried out with the price signal as expressed in Equation 5.5. This signal comprehends the DA market features of Germany in 2018, where the average price is around 45 €/MWh and the price spread is around 17 €/MWh. The price spread is similar to the standard deviation (σ), which measures the dispersion of the set of prices from the mean (μ). In a normal distribution, a standard deviation covers 68.2% of the values. In this case, it would mean 68.2% of the prices are within the range of 17 €/MWh above or below 45 €/MWh (i.e. between 28 €/MWh and 62 €/MWh), which shows a high volatility.

The simulations were also carried out with the real price data in order to validate the sinusoidal signals. The obtained errors were within an acceptable range of 3.8% and 0.05%.

6.1.1 Rankine cycle efficiency

The NPV results for Case 1 are depicted in Figure 6.1. The main findings are summarized below:

1. The relative NPV of ETES for energy arbitrage resulted in negative values of around -10% for the two storage capacities. These results indicate that it is

very unlikely that under current market conditions the business model of ETES could be based exclusively on electricity arbitrage. Notwithstanding, the simulations did not take into account possible upside conditions, such as high power curtailment or grid connection taxes, which could significantly improve the business case.

2. The sensitivity analysis on the Rankine cycle efficiency revealed that the impact of this parameter is only relevant for values above 45%, however, these efficiencies are barely achievable due to Carnot limits. This result is explained by the calculation below, which entails that in order to have a positive revenue, the buying price has to be lower than the selling price after the power losses.

$$\text{Buying price} < \text{Selling price} \times \eta_{el} ; 28 \frac{\text{EUR}}{\text{MWh}} < 62 \frac{\text{EUR}}{\text{MWh}} \times \eta_{el} ; \eta_{el} > 45.1\% \quad (6.1)$$

Consequently, it can be concluded that the worthiness of the investing in an efficiency improvement is directly linked to the volatility of electricity prices. Such dependency has been approximated by the Equation 6.2. If the minimum obtained η_{el} is within reach, then the efficiency improvement should be further investigated.

$$\eta_{el} > \frac{\mu - \sigma}{\mu + \sigma} \quad (6.2)$$

3. Lastly, it is observed that regardless of the efficiency, the small scale storage (i.e. 6h) does not reach a positive NPV. This indicates that a large energy capacity is more profitable for electricity arbitrage because more energy can be traded.

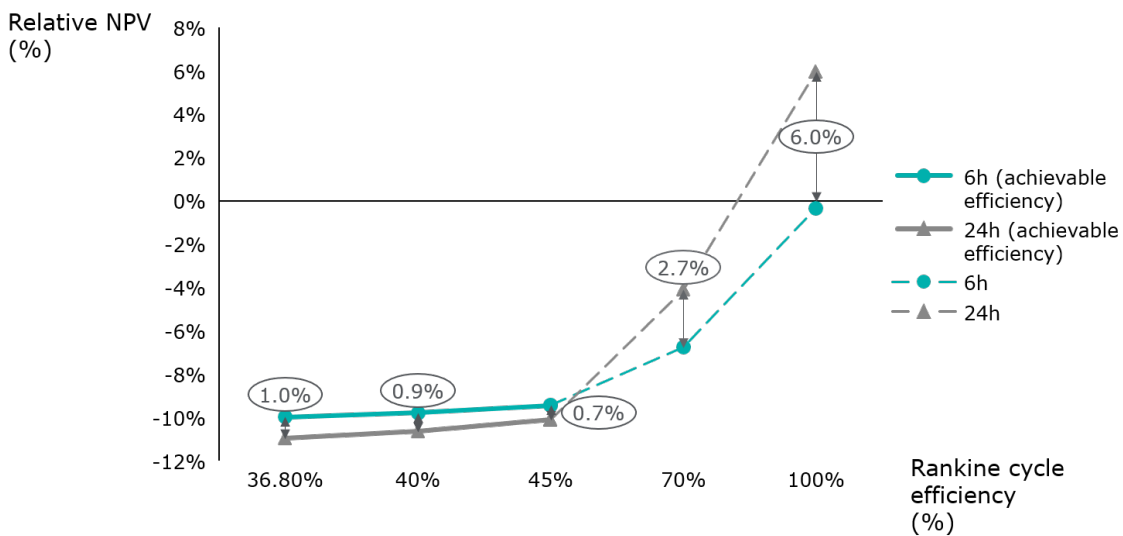


Figure 6.1: P2P: sensitivity of the NPV to changes in the Rankine cycle efficiency, for two different storage capacities

In order to obtain a more cohesive picture of the overall current market for energy storage technologies and electricity arbitrage, the following analysis was performed. The NPV was calculated for technologies with efficiencies close to 100% (e.g. batteries), using their corresponding CAPEX. The CAPEX values were estimated for storage capacities of 0.8 GWh and 3.3 GWh, equivalent to the ETES systems of 6h and 24h respectively. The NPV results are compared to those of ETES with a 100% efficiency in Figure 6.2. The main findings are:

1. The revenues obtained from doing electricity arbitrage with the most efficient storage technologies are not large enough to cover their investment. This means that, as of today, no energy storage technology can base its business model solely on electricity arbitrage.
2. The relative NPV of the larger 3.3 GWh capacity decreases in a stronger way (i.e. from 6% to -126%) than the smaller 0.8 GWh capacity (i.e. from 0% to -30%). This results show that the scalability of very efficient storage technologies entails larger costs than the scalability of ETES.

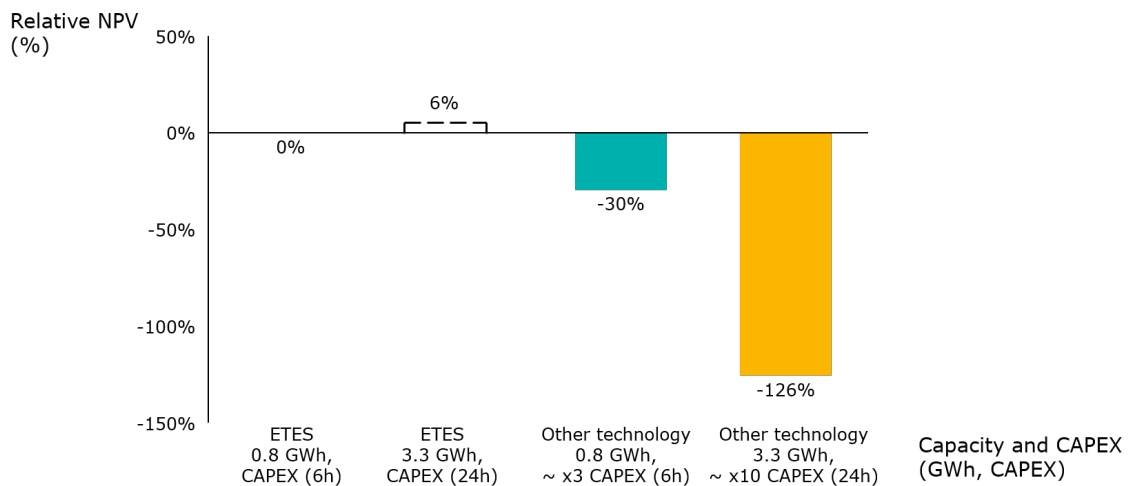


Figure 6.2: P2P: comparison of the NPV of ETES to other storage technologies with higher efficiencies, for two different storage capacities

6.1.2 Electricity prices

To find out the impact of the price coefficients on the revenues, a sensitivity analysis was carried out by changing each price coefficient independently and comparing the results to the base case. In order to avoid the potential distortion of results due to the different coefficients' magnitude, a new artificial price signal was developed as shown in Equation 6.3. This new signal has the same price spread as the German price curve of 2018 (i.e. 17 €/MWh), the same average

price, the same fundamental frequencies, and the same phase-shifts. The only difference lies in the coefficients (A_i), which all equal 10 €/MWh.

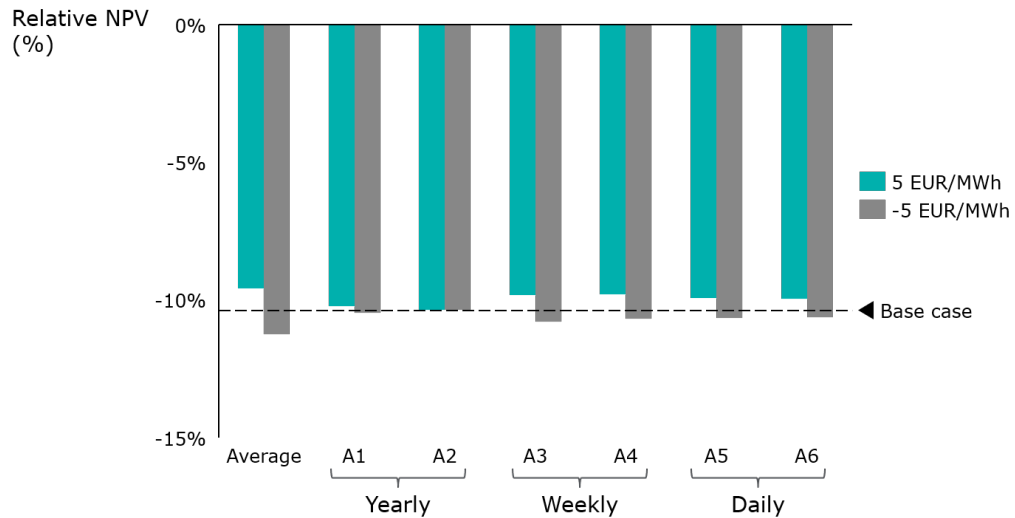
$$R_{el}(t) = \overline{R_{el}} + \sum_{i=1}^N 10 \sin(2\pi f_i (t - \phi_i)), \forall t \quad (6.3)$$

For the sensitivity analysis the coefficients A_i were increased and decreased by 5 €/MWh, that is, from 10 to 15 and 5 €/MWh. The average price was also increased and decreased by the same amount, to 50 and 40 €/MWh. The coefficients have been classified in line with their corresponding frequencies into:

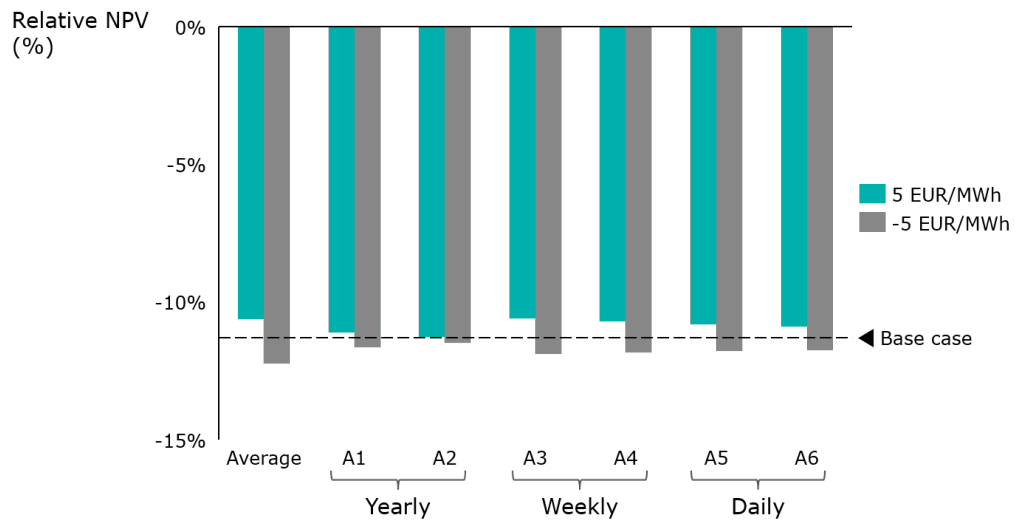
- Yearly: frequencies of 365 and 183 days, A_1 and A_2 respectively
- Weekly: frequencies of 7 and 3.5 days, A_3 and A_4 respectively
- Daily: frequencies of 1 and 0.5 days, A_5 and A_6 respectively

The results are shown in Figure 6.3. The base case refers to the simulation in which all price coefficients equal 10 €/MWh. The results obtained with this new price signal are nearly the same as those obtained with the German curve shown in Figure 6.1. Because the results from the Rankine efficiency analysis showed that very high efficiencies are needed to impact the NPV, all the simulations were carried out with a steam cycle efficiency of 37%. The following observations were derived from the analysis:

1. An increase or decrease of 50% in the price coefficients does not cause any significant change on the NPV. The main reason is that the resulting volatility of electricity prices and the Rankine efficiency are not enough to cause a significant change in the operation of the storage. For instance, if the new price spreads are introduced in Equation 6.2, the minimum efficiencies required are 40.6% and 47.0%, compared to the 37% used.
2. The NPV is mostly sensitive to the average electricity price. The higher the average electricity price, the larger the revenues and viceversa. Additionally, from the results it is confirmed that larger volatilities (i.e. results for +5 €/MWh) are beneficial for doing electricity arbitrage. Consequently, it can be concluded that the optimal markets for electricity arbitrage are those that present a combination of high prices and high volatility.
3. The NPV is less sensitive to yearly fluctuations in the electricity price. Because the time horizon of the simulation is only a week, the model doesn't perceive variations in longer timescales. As ETES is not meant to be a seasonal storage, this modelling framework does not impact the conclusions.
4. The sensitivity analysis results for the small scale storage are very similar to the large scale storage. This involves that the business case under these conditions is more dependent on the electricity prices than on the storage capacity.



(a) 6h storage



(b) 24h storage

Figure 6.3: P2P: sensitivity of the NPV to changes in the electricity price coefficients

Discussion

From Case 1 it can be concluded that, under current market conditions, a business model based exclusively on electricity arbitrage is not possible. Neither for ETES nor for any other storage technology. This is due to the fact that the difference between the buying and selling prices is not enough to cover the investment. In order to consider such application, new market developments should generate other incentives such as e.g. grid congestion, curtailment, grid instability, and so on. These results coincide with the findings of previous studies, which determine that electricity arbitrage only is not enough to recover the investment. Additionally, an equation was developed for estimating the minimum steam cycle efficiency required for observing changes in the NPV.

6.2 CASE 2: POWER-TO-POWER AND DISTRICT HEATING

In the previous case it was concluded that electricity arbitrage as the only revenue stream is not economically viable for storage. Because of this reason, the economics of ETES with a new revenue stream linked to power generation is evaluated in this case study. Such income source consists of the heat sale to a nearby district heating network. Given that the heat is obtained from an intermediate step between the high-pressure and low-pressure turbines, the reward for doing electricity arbitrage is now two-fold.

6.2.1 District heating price

The first milestone was to determine whether there are any DHN price conditions under which the business case is positive. To this end, a constant district heating demand equal to the maximum rating (i.e. 78 MW) was used. The resulting NPV obtained for different constant district heating prices are shown in Figure 6.4. The conclusions of the analysis are:

1. The NPV shows a large improvement with respect to Case 1, where there were no district heating revenues. Such improvement is more accentuated for district heating prices above 45 €/MWh, for which the NPV increases from -10% to at least -4%.
2. The break-even prices are: 52 €/MWh for a large energy capacity (i.e. 24h) and 57 €/MWh for a small energy capacity storage (i.e. 6h). The reason behind the price difference is that a large capacity is more adequate for this market, as more electricity arbitrage can be done and therefore more heat can be sold to the DHN.
3. Lastly, it is necessary to compare the obtained break-even prices against the market prices of other competitor energy sources. Among the most established energy sources for district heating, natural gas is the less polluting fossil fuel source and therefore was used as the benchmark. The price of this commodity has been below 27 €/MWh [83] for the last two years in the Dutch Title Transfer Facility (TTF), which is the reference European gas market. Consequently, if ETES needs to compete against this commodity, there should be incentive schemes in place that reward other positive side-effects such as: absence of emissions of the heat source, integration of RES in the heating sector, security of supply, and so on.

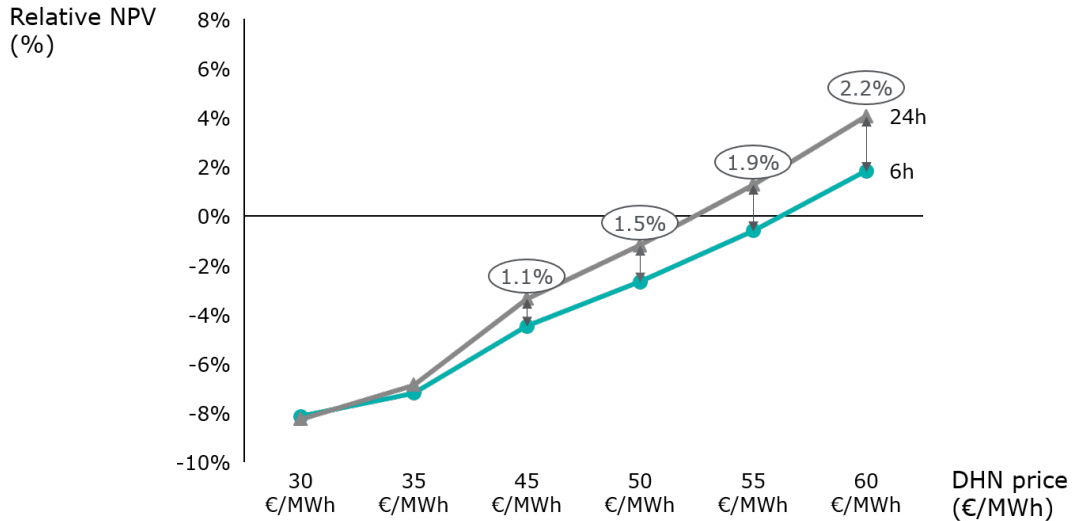


Figure 6.4: P2P and DHN: Sensitivity of the NPV to changes in the district heating price, for two different storage capacities

6.2.2 District heating demand profile

As previously mentioned, the demand curve used in the previous section was fixed to a constant value. Nonetheless, in many countries the district heating demand varies with the seasons and within the same day, as demonstrated in Chapter 5. On those grounds, the second milestone was to evaluate how the revenues change with a demand of these characteristics. The results of both demand profiles are compared in Figure 6.5. The Figure only compiles the results for the 24h storage, as this capacity entails larger revenues, and the three larger district heating prices. The main findings are:

1. The NPV of ETES with a variable district heating demand is lower than with a constant load. This result is counter-intuitive as one would expect an increased use of the storage capacity with larger demand fluctuations (e.g. charging the storage when the demand is very low, and discharging it when the demand increases). After a closer analysis of the results, it was found out that the main cause of the revenue decrease is the yearly fluctuation of the variable demand. In other words, the variable demand is nearly zero in the summer months, and for this reason the total annual demand and revenues are lower.
2. The sensitivity of the NPV to changes in the district heating prices is lower for a variable demand than for a constant one. Similarly to the previous point, this effect is a consequence of the overall lower annual demand.

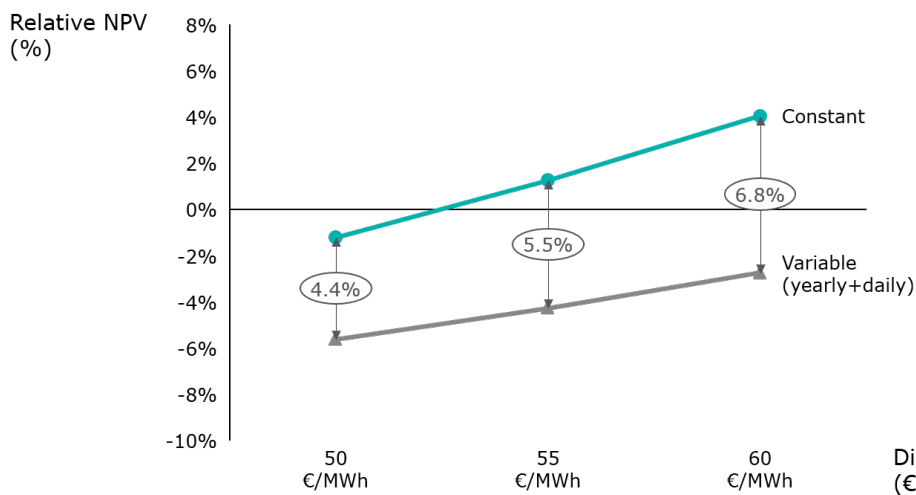


Figure 6.5: P2P and DHN: sensitivity of the NPV to changes in the district heating price, for a 24h storage and two different demand profiles

In order to separate the effect of the yearly periodicity from the assessment of the variability of the demand, two extra simulations were carried out. In the first simulation the daily fluctuations of the demand were doubled (i.e. by doubling the demand coefficient of the pertinent frequencies), and in the second one the coefficients were halved. A close-up of the effect of the higher and lower daily fluctuations is shown in Figure 6.7, and the NPV results for these curves are shown in Figure 6.6. From these results it can be concluded that, on the contrary as it was shown in Figure 6.5, a larger district heating demand fluctuation is beneficial for the business case. Notwithstanding, it does not payoff the low demand in the summer.

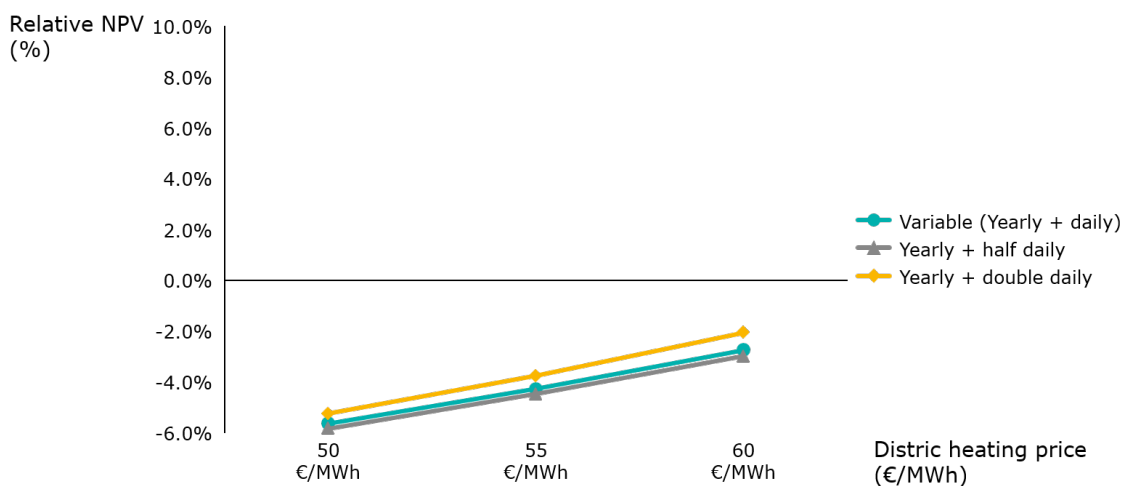


Figure 6.6: P2P and DHN: sensitivity of NPV to changes in the daily district heating demand fluctuations for a 24h storage

The results above are a consequence of the correlation between the district heating demand and the DA market prices. A larger district heating fluctuation increases the district heating demand in the mornings and decreases it at night,

likewise to the electricity prices. This is favourable for the economics because, firstly, the storage can charge at night when the electricity prices and the heating demand are at their lowest, and secondly, it can sell more heat when the electricity prices are at their highest. Consequently, the overall revenues are larger.

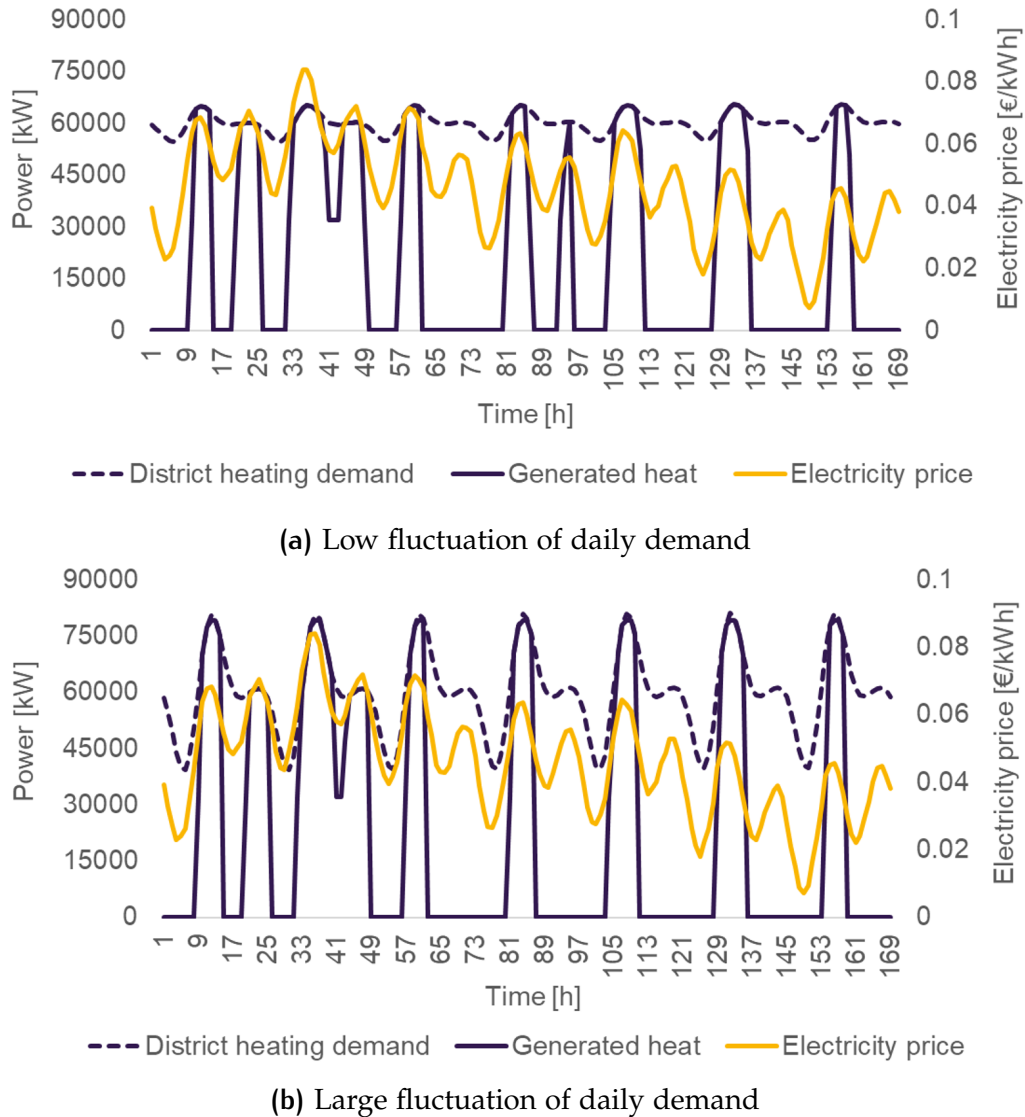


Figure 6.7: P2P and DHN: one week simulation of the electricity prices, district heating demand, and district heating sales, for two different demand spreads

6.2.3 Rankine cycle efficiency

Similarly to the case without district heating, the sensitivity of the NPV to changes in the Rankine efficiency was evaluated. The analysis was carried out for a 24h storage, a constant district heating demand of 78 MW, and two different district heating prices (see Figure 6.8). If the results are compared to the first ones obtained for a 37% efficiency (Fig. 6.4), it can be concluded that there are no significant changes in the results. For example, the break-even price only decreases from 52€/MWh to 50€/MWh for an efficiency increase of 8.2%. In order to

decrease the break-even price even further to 45€/MWh, an efficiency increase of almost 20% would be required. This could be due to the fact that, in this case, a higher Rankine efficiency means lower heat available for DHN.

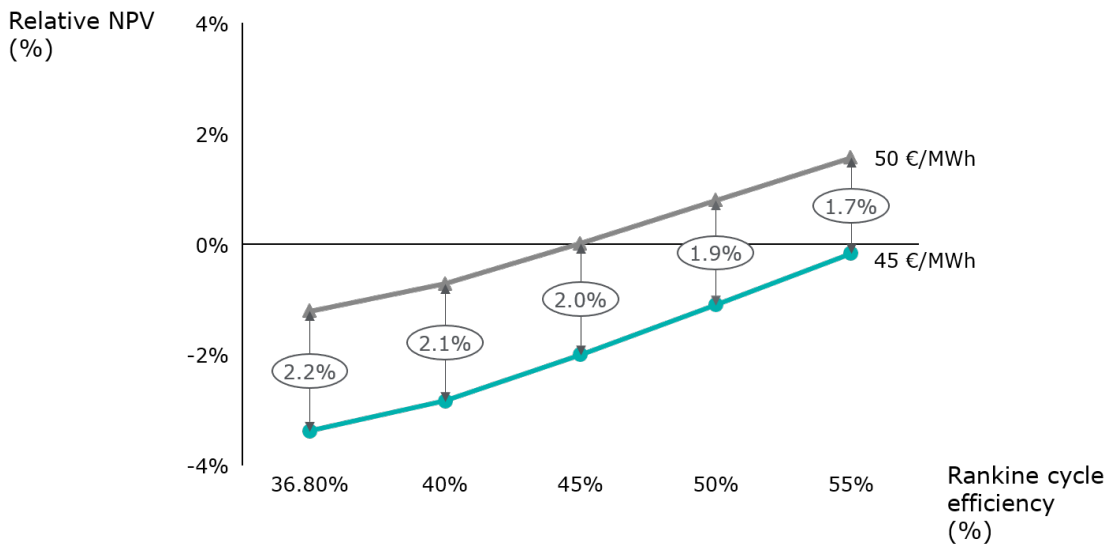


Figure 6.8: P2P and DHN: sensitivity of the NPV to changes in the Rankine cycle efficiency for two different district heating prices

6.2.4 Electricity prices

The sensitivity of the NPV to variations in the electricity price components was performed in a similar way to Case 1, that is, using the *base case* curve from Equation 6.3. Additionally, in order to give a high-level view on how the operation of the storage is affected by the electricity prices, the heat sales and the number of storage cycles were also evaluated. All simulations were carried out for a 24h storage and a DHN price of 50 €/MWh. The main findings of the sensitivity analysis of the NPV are listed below, and the results are shown in Figure 6.9:

1. The average electricity price is the variable with the largest impact on the revenues. The obtained results are inverse to those of the electricity arbitrage: the higher the average price, the lower the NPV. The explanation for this outcome lies in the improvement of the *reference case* without storage, i.e. the $NPV_{ref.case}$. If the electricity prices increase for a fixed DHN price, the relative revenues obtained from heat sales decrease, hence the profitability of ETES also decreases.
2. Among all the price coefficients, the NPV is more sensitive to changes in the price coefficients with higher frequencies (i.e. A4, A5, A6), and among them, to A5 (i.e. 24h period). This effect is explained by the fact that the periodicity of the price element has the same length as the discharging time of ETES. Consequently, the price cycles fit better to the storage cycles.

3. Lastly, and along the same lines of the electricity arbitrage results, higher price volatilities result in higher revenues.

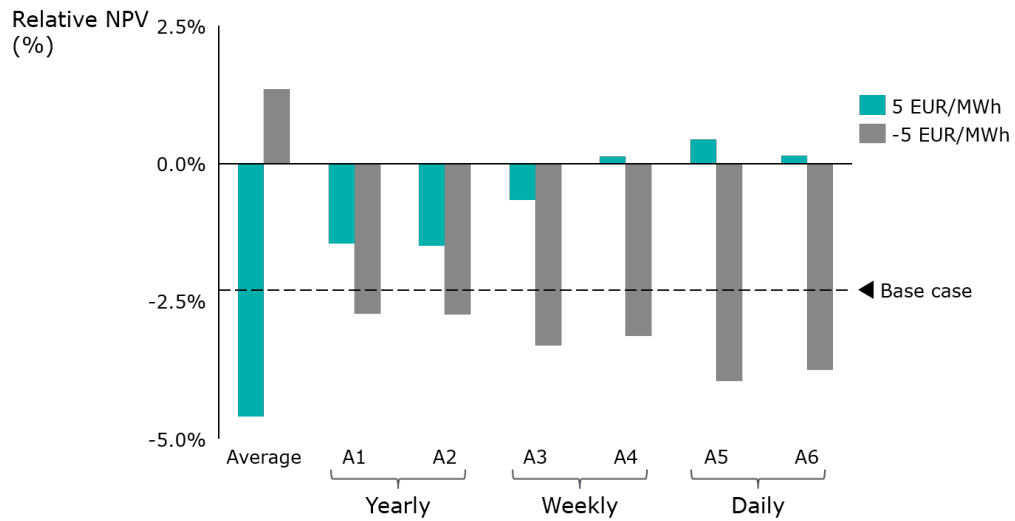


Figure 6.9: P2P and DHN: sensitivity of the NPV to changes in the electricity price coefficients, for a 24h storage

The changes in the district heating sales are shown in Figure 6.10, as total energy sold per total energy demand in a year. From the graph it is observed:

1. The district heating sales increase with a lower average electricity price. Similarly to the NPV, this result should be evaluated in comparison to the *reference case*. With lower electricity prices, the relative revenues from the DHN become more relevant for the business.
2. Larger daily price variations lead to more district heating sales. This is an effect of the correlation between the electricity prices and the demand fluctuations, previously explained in Section 6.2.2.

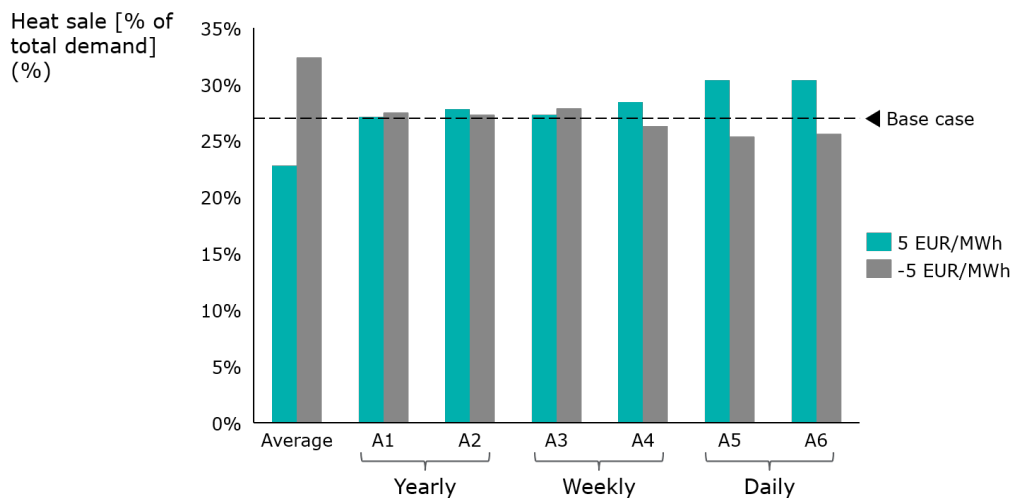


Figure 6.10: P2P and DHN: sensitivity of the heat sales to changes in the electricity price coefficients, for a 24h storage

Lastly, the changes in the total number of storage cycles per year are depicted in Figure 6.11. It is observed that:

1. The most relevant coefficient is the smaller period of 12h (A6): if this coefficient is increased, the price fluctuates more frequently and therefore the storage carries out more and shorter cycles. The opposite effect occurs if A6 is decreased. This information should be mainly taken into account for the storage wear and the lifetime of the charging and discharging equipment.
2. The second most relevant parameter is the average electricity price. As previously mentioned, if the electricity prices are low and the DHN price remains high, selling heat to the DHN can improve the business case. Thus, more electricity arbitrage is done and the storage is charged and discharged more times.

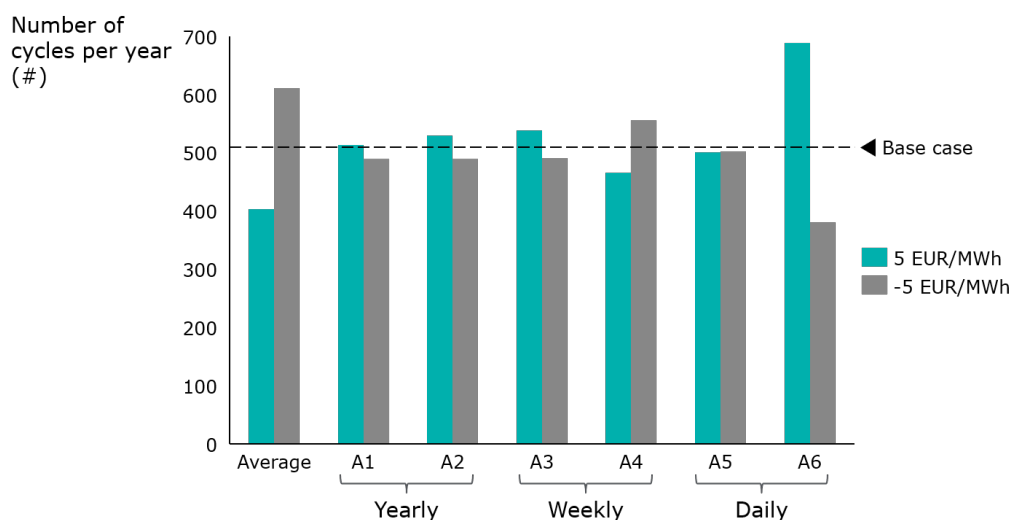


Figure 6.11: P2P and DHN: sensitivity of the storage cycles to changes in the electricity price coefficients, for a 24h storage

Discussion

With Case 2 it has been shown that the business model for electricity arbitrage significantly improves if a second revenue stream is attached to it. Additionally, the minimum selling prices for heat have been found. These prices could be realised only under an incentive scheme for low-emissions technologies, as natural gas prices are still too competitive. The analysis included an assessment on whether an improvement in the steam cycle efficiency would significantly decrease the DHN break-even prices, which was not the case.

As regards the optimal demand profile, it has been determined that a variable demand improves the business case when the district heating demand peaks are simultaneous to the electricity price peaks. This takes place due to the simultaneity between the power generation and the heat withdrawal of the system. Since heating demand spikes occur in the morning and in the evening, revenues could increase in a market with large shares of solar power. Because the sunlight is directly related to the ambient temperature, low district heating

demand times would coincide with low electricity prices (i.e. at mid-day). Notwithstanding, closer attention should be paid to the overall annual demand as it has a larger impact on the NPV.

Similarly to Case 1, the analysis did not include other possible conditions such as high wind curtailment or grid congestion, which would improve the results. Lastly, it is important to mention that instead of a DHN, the extra revenue stream could consist of a steam demand from industry. The analysis of such demand would differ in the study of the specific load schedules and the steam requirements.

6.3 CASE 3: POWER-TO-HEAT

The Power-to-Heat case study covers the sale of high-temperature heat to a thermal sink. The energy can come directly from the wind farm or it can be bought from the grid when the difference between the heat and electricity prices is large enough. The business case therefore depends on a sole application, which has been analyzed in depth in this section.

6.3.1 High-temperature heat price

The analysis started with the search for the break-even price to reach a positive NPV. Such study was carried out with a constant heat demand of 133 MW, which is the maximum the system can output considering the transmission losses. Because the results were positive for relative low heat prices, the business case under the Spanish electricity price conditions was also tested. The results are shown in Figure 6.12. The main observations are the following:

1. The break-even prices obtained with the German prices are around 33 €/MWh for the small storage capacity, and around 35 €/MWh for the large storage capacity. These results show that, as opposed to the electricity arbitrage application, a large storage capacity might not be optimal. Additionally, they indicate that ETES could already be competitive with natural gas, which in the last two years has reached prices up to 27 €/MWh.
2. The break-even prices obtained with the Spanish prices are around 57 €/MWh for the small storage capacity, and around 60 €/MWh for the large storage capacity. These results are worse for the business case than the ones for Germany, since the selling price would be less competitive.
3. The difference in break-even prices between Germany and Spain is linked to the different electricity prices. Firstly, the average electricity price of Germany is 45 €/MWh, whereas the average electricity price in Spain is above 57 €/MWh. Because of this reason, the sale of electric power to the DA market yields more revenues than the sale of heat in Spain and,

therefore, the *reference case* is better. Secondly, the volatility of the German market is larger, which means that the prices below the mean price are lower in average. Due to this difference, it is cheaper to buy electricity in Germany. This is proved by the following facts which were obtained from the simulations:

- Germany: the average of the prices below the mean (i.e. 45€/MWh) is 31€/MWh. Of all the hours in the year when the prices are below the mean price, in 74% the system buys electricity from the market.
- Spain: the average of the prices below the mean (i.e. 57€/MWh) is 49€/MWh. Of all the hours in the year when the prices are below the mean, in only 56% the system buys electricity from the market (and at a higher cost than in Germany).

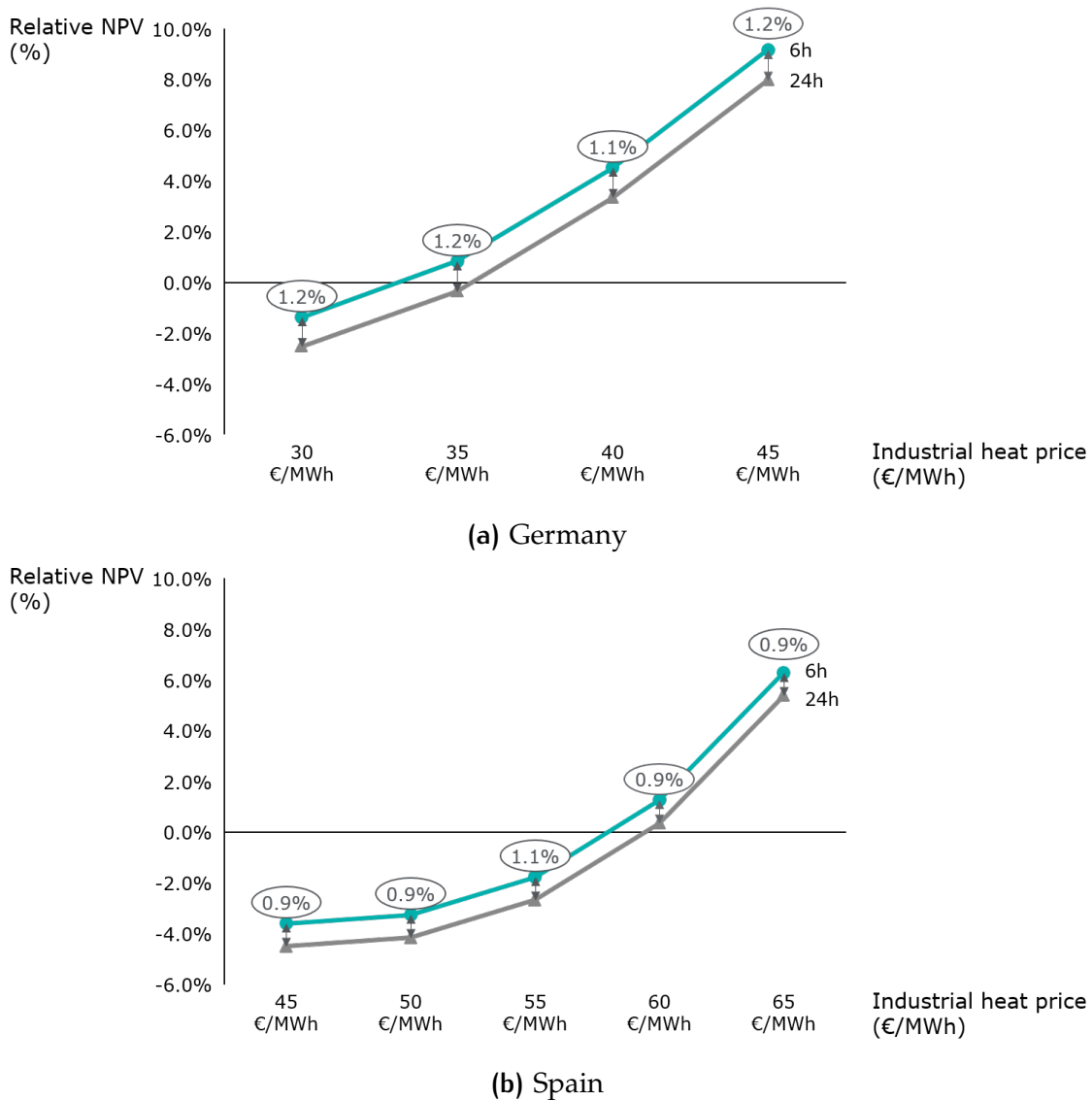


Figure 6.12: P2H: sensitivity of the NPV to changes in the heat price, for two different storage capacities

Consequently, it can be concluded that – similarly to Case 2 – markets with low average electricity prices and high price volatilities are advantageous for the business case.

6.3.2 High-temperature demand profile

After the break-even heat price has been found, the next step is the analysis of the energy-intensive industry demand. The study has been divided into two: first, the analysis of a constant heat demand level, and second, the analysis of a variable demand with different standard deviations. All the simulations were carried out with the German electricity prices and with the break-even heat price of 35 €/MWh.

Constant heat demand profiles

The constant heat demand profiles were obtained by setting all the sinusoidal coefficients from Equation 5.4 to zero. The main aim was to determine how dependent the NPV is on the average demand. Because the business case in this application is directly related to the heat sales, the latter have also been evaluated. The NPV results are plotted in Figure 6.13, and the plots of the heat sales and the storage cycles are included in Appendix C.

The main finding of the analysis is that the revenues do not increase linearly with the demand, because the heat sales also do not increase linearly with it. For instance, for a 50 MW load, it is found that the system meets the 42% of the annual demand. However, when the load is increased to 133 MW, the sales decrease to 21% of the total demand. Due to the fact that the selling price is the same and the total heat sold is very similar in both cases¹, the NPV results are also similar.

This result is an outcome of the power difference between the charging rating (i.e. 139 MW) and the demand. With a constant and continuous demand of 133 MW, hardly any power is left to be stored and used at a later time. This does not happen when the demand is decreased to 50 MW, thus the system can charge enough power to serve the load and heat up the storage bed simultaneously.

The difference between the thermal demand and the charging power also explains why the economics of the larger storage (i.e. 24h) are worse than the smaller one. As the demand level decreases, more extra power can be stored in the larger capacity and eventually the difference in NPV decreases. Lastly, if the heat price was even higher, the heat sales and the NPV would increase as shown in the heat price analysis in Section 6.3.1.

¹ 50 MW x 0.42 = 21 MW; 133 MW x 0.21 = 28 MW

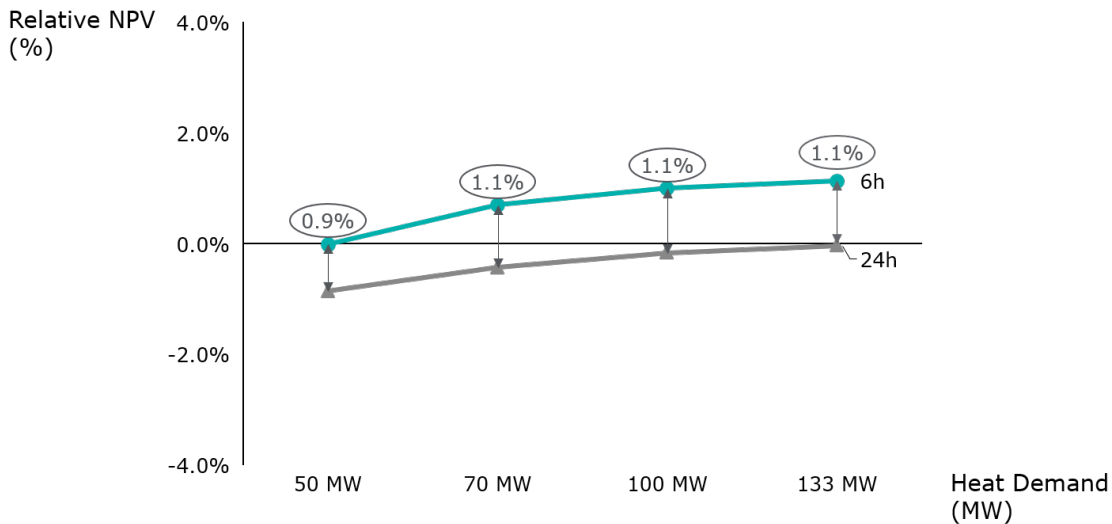


Figure 6.13: P2H: sensitivity analysis of the NPV to changes in the constant heat demand level, for two different storage capacities

In view of the results, the business case for industries with constant heat demand profiles would probably improve with batch (i.e. intermittent) processes instead of continuous. This analysis is out of the scope of the research and has been included in the recommendations for future work.

Variable heat demand profiles

Once the operation of the storage under different constant heat demand levels has been understood, the second analysis focuses on the evaluation of different fluctuating demands. To this end, the heat demand from Equation 5.4 was modelled with an average of 70 MW and two different standard deviations, namely, 9.5 MW and 25 MW. The standard deviations were obtained by multiplying each curve coefficient by a factor of 0.5 and 3 respectively. The results are compared against those of the fully constant curve of 70 MW in Figure 6.14, for a heat price of 35 €/MWh, and a 6h storage. The main results are the following:

1. A higher fluctuation of the demand results in lower NPV. This result is counter-intuitive, especially after the previous section where it was demonstrated that a larger difference between the demand and the charging power rating is advantageous. Nevertheless, it is explained by the concurrence in time of low electricity prices and low industrial demand. This is clearly shown in Figure 6.15, where the moving averages of the electricity prices and the heat demand have been plotted for a whole year simulation. The simultaneity of low electricity prices with low thermal demand is not beneficial, as the revenues from arbitrage are minimized (i.e. when the electricity prices are low and the system buys power, the demand is also low and for that reason also the revenues). This conclusion is contrary to Case 2 where such condition is favourable, but this is due to the synchronism between the power generation and the steam generation.

2. The concurrence of the high electricity prices with high heat demand levels also impact the heat sales, which decrease, and the total number of storage cycles per year, which also decrease. The heat sales and the storage cycles of the three curves are compared in Figures C.3 and C.4 in Appendix C.

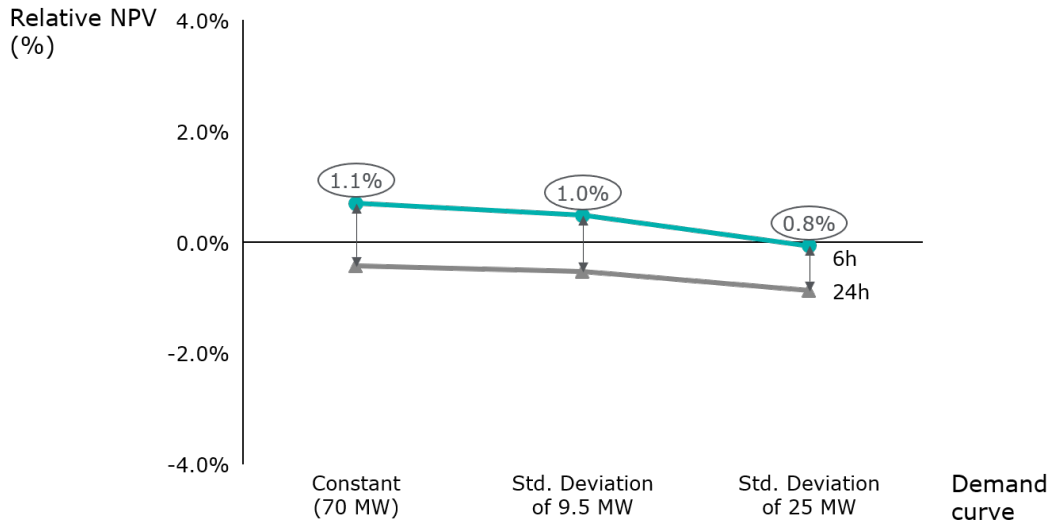


Figure 6.14: P2H: sensitivity of the NPV to changes in the variability of the heat demand, for two different storage capacities

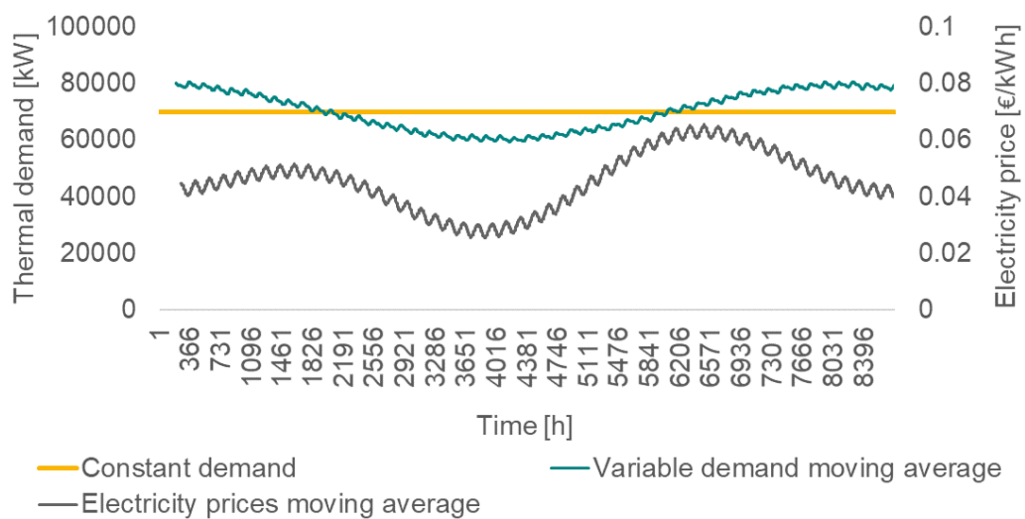


Figure 6.15: Yearly plot of the demand moving average, the electricity prices moving average, and a constant demand of 70 MW

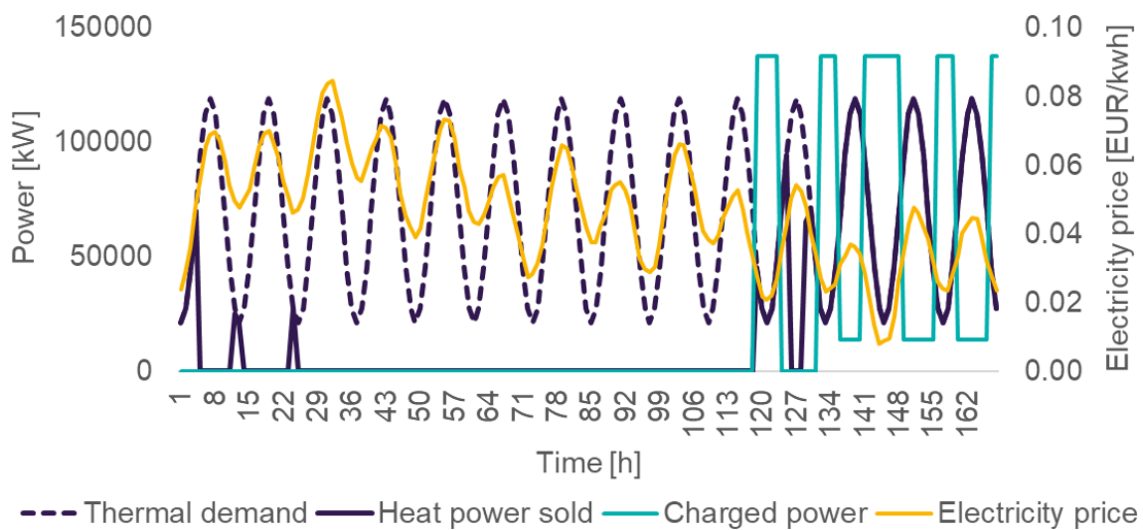
Phase difference between the heat demand and the electricity price

The previous analysis on the variable heat demands naturally raises the question about how the difference in phase between the demand and the electricity price impacts the results. This subsection aims at providing some insight in this regard.

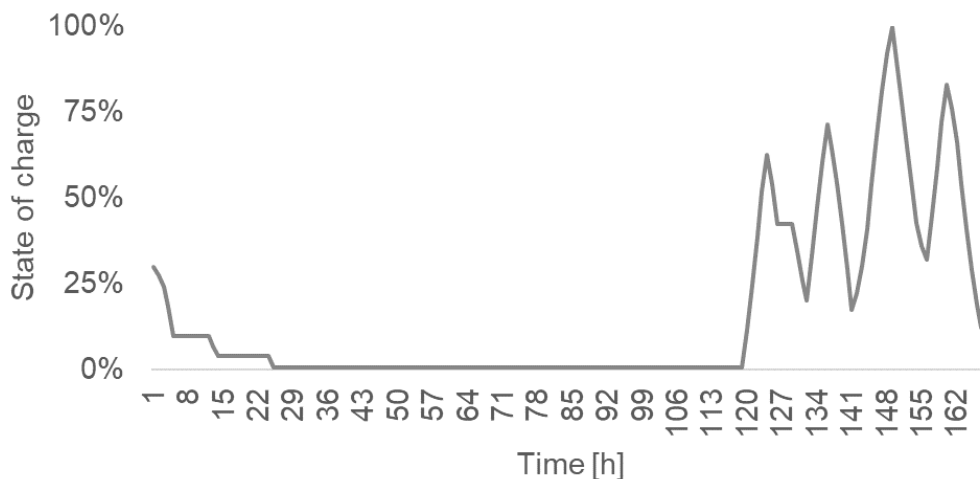
With that aim, the demand curve was modified to have the 12h period only, and the same average value as before (i.e. 70 MW). A 12h period was chosen

because the electricity price also has a 12h component, and because the changes in the storage cycles are easier to observe in smaller scales. The signal was then tested with two different phase shifts: one in phase with the 12h component of the electricity price, and another one with a 6h phase difference.

A close-up of the simulation with the heat demand and the electricity prices with a 0h phase difference is shown in Figure 6.16. Additionally, the state of charge for the same week is included. The plot clearly shows how the demand peaks coincide with the price peaks. The resulting 'heat power sold' and 'charged power' curves reveal that the system only charges power when the electricity prices are low enough to earn profit by selling heat.



(a) Weekly plot of the power curves and the electricity price

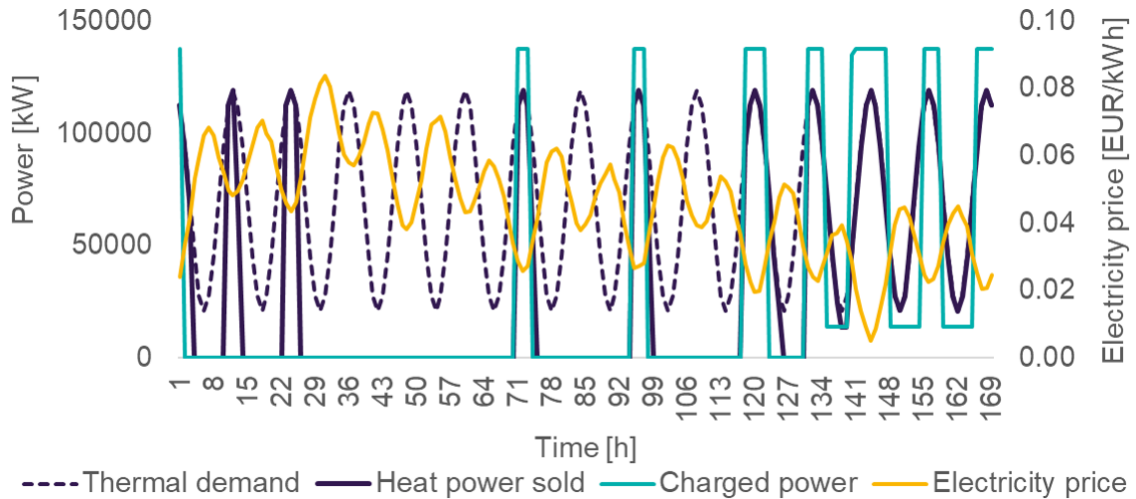


(b) Corresponding State of Charge

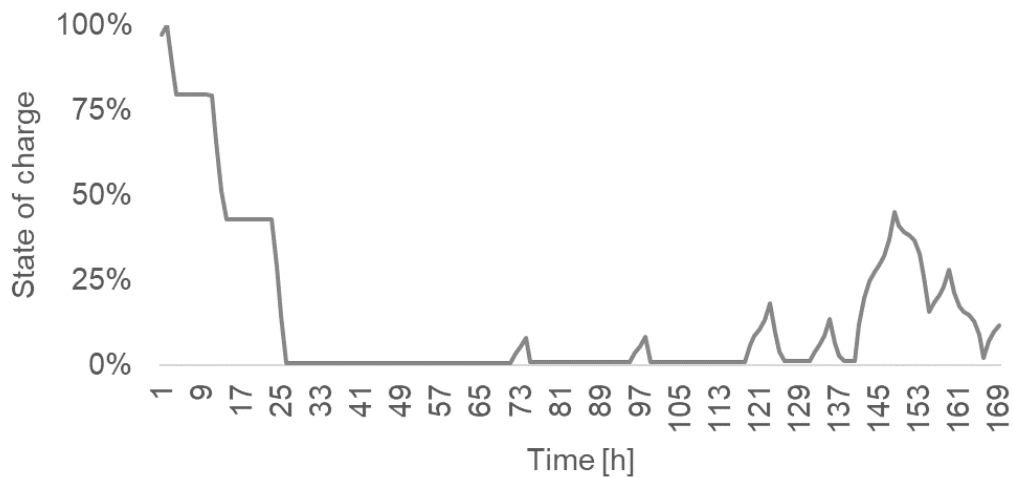
Figure 6.16: P2H: weekly plot of the heat demand, heat sold, charged power and electricity prices, and the corresponding state of charge of the storage, for 0h phase difference between the demand and the electricity prices

A similar close-up for the simulation with a 6h phase difference is shown in Figure 6.17. This time it can be observed how the times of maximum prices

coincide with the times of lowest demand and viceversa. The main difference with respect to the previous case, is that in this one, the system can sell more heat power. For instance, it charges during the last hours of the week (just as the oh difference case), but it also charges and sells heat in the middle of the week. This improves the revenues with respect to the *reference case*.



(a) Weekly plot of the power curves and the electricity price



(b) Corresponding State of Charge

Figure 6.17: P2H: weekly plot of the heat demand, heat sold, charged power and electricity prices, and the corresponding state of charge of the storage, for 6h phase difference between the demand and the electricity prices

Lastly, it is observed that with a 6h phase difference there is less power left for charging the storage. This trade-off should be kept in mind for the analysis of different demand profiles.

The aggregation of the total additional power sales led to a NPV difference of about 0.26%. In addition, an improvement of 0.04% was achieved with respect to the fully constant signal. These results are shown in Figure 6.18.

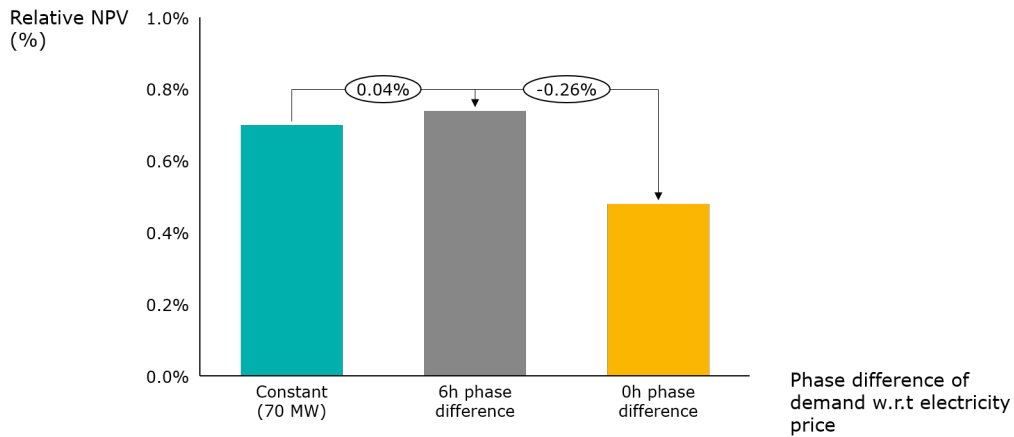


Figure 6.18: P2H: sensitivity of the NPV to the phase shift between the heat demand and the electricity price, for a 6h storage

6.3.3 Electricity prices

Lastly, the sensitivity of the NPV to variations in the electricity price components was assessed in the same way as in Cases 1 and 2 (see Figure 6.19). All simulations were carried out for a 6h storage and a constant heat price of 35 €/MWh. The results resemble the results of Case 2:

1. The average electricity price is the variable with the largest impact on the revenue. Because the NPV of the *reference case* without storage improves with larger electricity prices, a high average price negatively impacts the NPV of ETES.
2. The NPV increases with the volatility, and its sensitivity to changes in the coefficients grows with higher frequencies. Nevertheless, the growth is not significant.

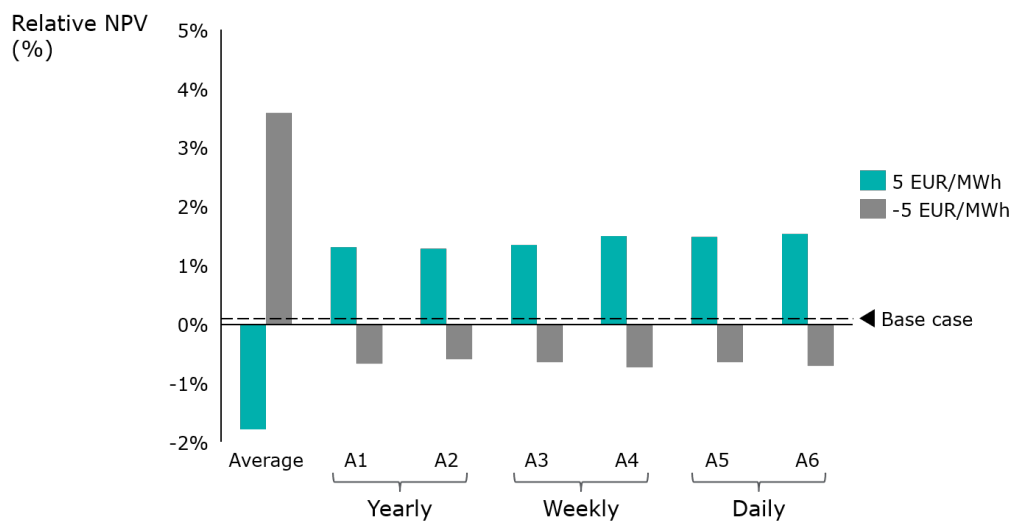


Figure 6.19: P2H: sensitivity of the NPV to changes in the electricity price coefficients, for a 6h storage

The changes in the high-temperature heat sales are shown in Figure 6.20 and are equivalent to the aforementioned changes in the NPV:

1. The heat sales are mostly sensitive to the average electricity prices. The lower the electricity price, the larger the revenues obtained from P2H arbitrage.
2. Larger price volatilities also lead to larger sales. The explanation is the same as above: with higher volatilities there are periods of lower electricity prices that, in turn, foster the heat sales.

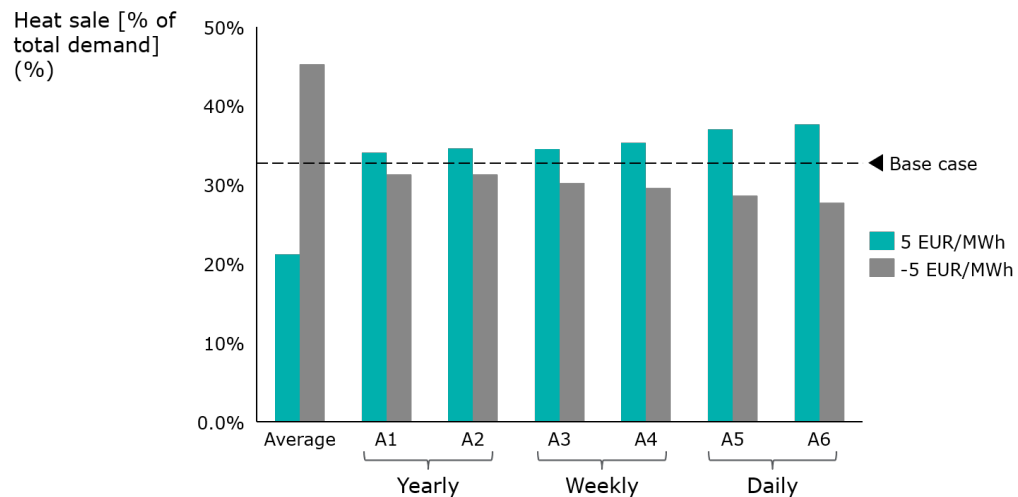


Figure 6.20: P2H: sensitivity of the heat sales to changes in the electricity price coefficients, for a 6h storage

The analysis concluded by evaluating the changes in the total number of storage cycles per year. These are shown in Figure 6.21. The results are exactly the same as in Case 2.

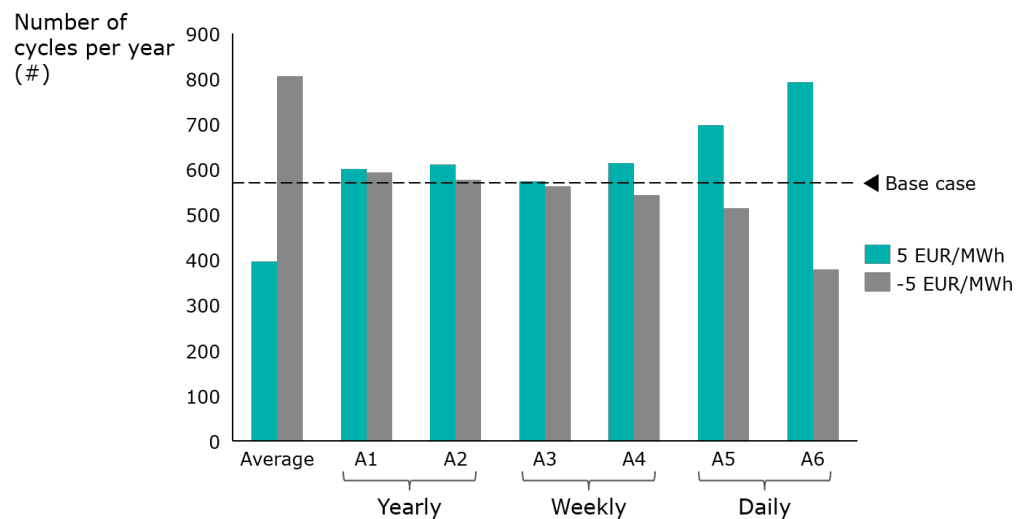


Figure 6.21: P2H: sensitivity of the number of cycles to changes in the electricity price coefficients, for a 6h storage

Discussion

The comparison of results of Cases 1 and 2 with Case 3 points to the conclusion that, under current market conditions, ETES has a larger potential in P₂H than in P₂P. Such conclusion is derived from the fact that the obtained break-even heat price is nearly competitive with natural gas. A low selling price could be achieved by virtue of the relatively low average and high volatility of the German DA price, which provides an opportunity for buying cheap electricity for 'P₂H arbitrage'. Additionally, the business case is also enhanced by the lower CAPEX, which does not include the steam cycle. Thus, taking into account that a larger penetration of RES is expected to accentuate these market conditions, and that higher CO₂ taxes might further increase the costs of natural gas, this business case will likely improve further.

Other conditions that were found to have a relevant impact on the business case were: the demand level and the phase difference between the demand schedules and the DA market prices. The former is strongly dependent on the design of the power ratings of the storage, which is out of the scope of this research. The latter is relevant for optimizing the energy arbitrage: if the low prices coincide with demand peaks, the revenues are maximized. A real market example of this condition would also be a market with a large share of solar power. The industries' demand are usually higher during the day than during the night-shifts, and higher in the winter than in the summer (only if they do not manufacture seasonal products). These demand schedules match the solar PV generation, which lowers the electricity prices when it is introduced in large amounts.

Lastly and in the same way as in the other case studies, it is important to remind that not all the potential applications were included. 'P₂H arbitrage' could also be done in order to provide e.g. grid services. Additionally, the business case could be improved by additional external factors such as the costs of CO₂ avoidance or the re-use of industrial waste heat. These additional revenues would depend on the specifications of each application or industry, and should be looked more into detail.

6.4 CASE 4: POWER-TO-HEAT-AND-POWER

The final case encompasses all the previous applications, with a view of observing how they interact among each other under different conditions.

For the sensitivity analysis, a heat price of 50 €/MWh and 35 €/MWh were used for the DHN and the industry respectively, since these were the break-even values found in the previous analysis. Furthermore, constant demand levels were used instead of variable signals, in order to avoid distortions in the results. More specifically, a district heating demand of 78 MW and a high-temperature heat demand of 133 MW were used. Similarly to the previous case studies, the heat sales have been expressed as a fraction of the total demand. As regards

the electric power generation, it is expressed as a fraction of the total possible generation (i.e. electric generation power rating times the total number of hours in a year).

6.4.1 District heating price

Firstly, the NPV and the power and heat sales for different levels of district heating prices were obtained. The main objective of this analysis is to learn about how the NPV increases with revenue stacking, and how these revenues are re-structured when the DHN price is increased. The results are shown in Figures 6.22 and 6.23, and the major findings are summarized below:

1. The break-even DHN prices do not significantly change with respect to Case 2. They remain 52 €/MWh for the 24h case, and they slightly decrease from 57 to 55 €/MWh for the 6h. This is due to the fact that the industrial heat sales barely contribute to the NPV. They decrease from 21% of the total demand in Case 3, to 9%² in the smaller scale storage, and to 3%³ in the larger scale storage (for the initial district heating price of 50 €/MWh). From the aforementioned results, it can be concluded that under the considered price conditions, it is more profitable to generate electricity and steam than heat for an industry.
2. The extra CAPEX belonging to the steam cycle has a very relevant impact on the business case. Under the same high-temperature heat conditions in Case 3, the NPV was around 1%, whereas in this case is negative.
3. Similarly to the 'electricity arbitrage' in Cases 1 and 2, a large scale energy storage is more advantageous.

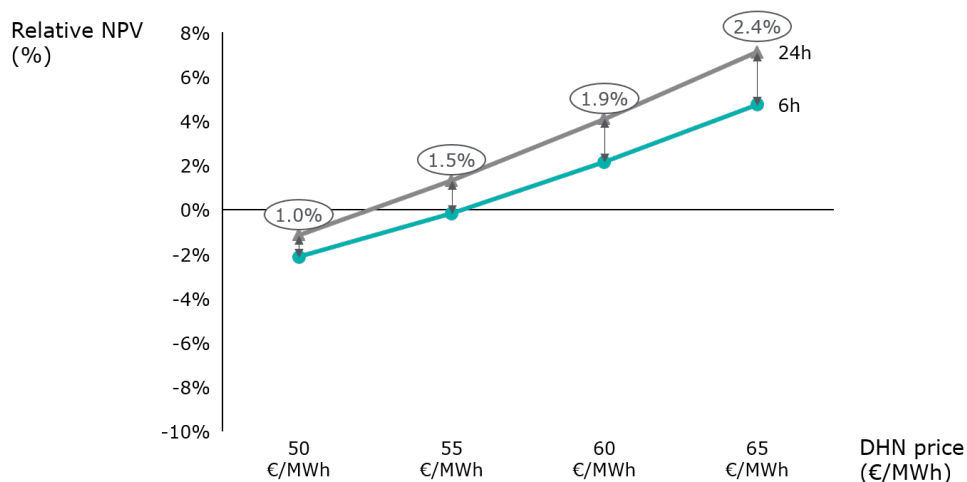


Figure 6.22: P2H&P: sensitivity analysis of the NPV to changes in the DHN price, for two different storage capacities

² 133 MW x 0.09 = 12 MW

³ 133 MW x 0.03 = 4 MW

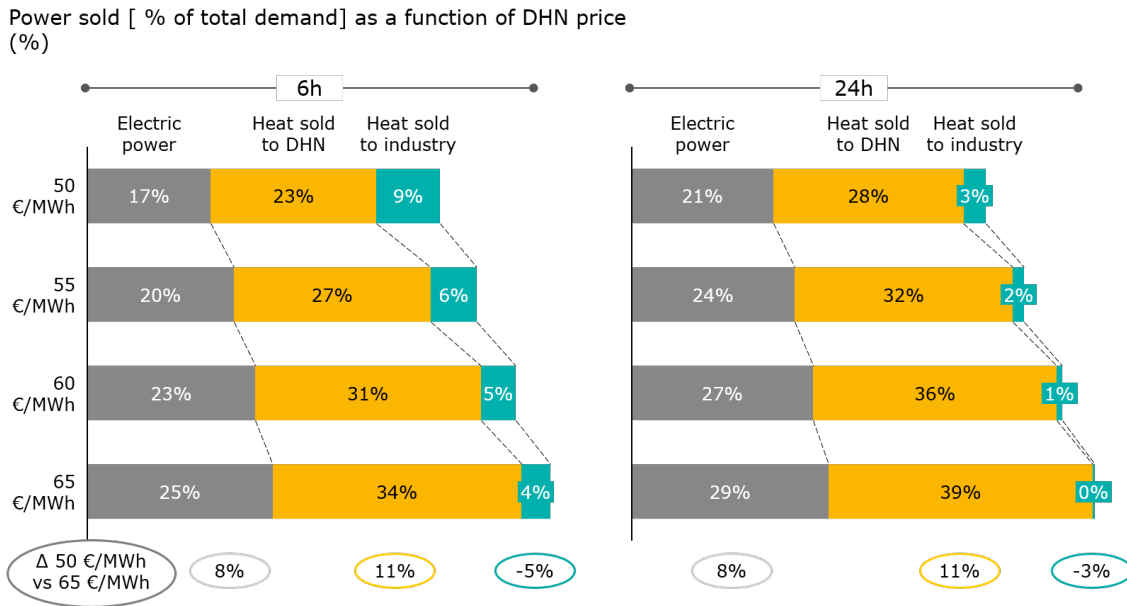


Figure 6.23: P2H&P: sensitivity analysis of the electric and thermal discharged powers to changes in the DHN price

6.4.2 District heating demand

After the district heating prices have been investigated, the constant district heating demand level has been varied to determine whether the results are more sensitive to changes in this variable, or to changes in the prices. The NPV results are depicted in Figure 6.24, and the power sales are shown in Figure 6.25.

By observing the plots it can be concluded that the NPV is more sensitive to changes in the prices than to changes in the DHN demand. This is due to the fact that the DHN sales do not increase linearly with the demand. For instance, when the demand is on the lower end, i.e. 30 MW, 30% of this value is served⁴. Conversely, when the demand is the maximum possible, i.e. 78 MW, the power sold decreases to 23% of the total demand⁵. On a final note, it is also noticed that as the demand level decreases, also does the difference between the NPV of the 6h and the 24h storage systems. For low demand levels, on the range of 30 MW, the NPV of both storage capacities is very similar. This is a result of larger high-temperature heat sales in the 6h storage (i.e. 19%), which compensate the lower revenues from the sale of electricity and heat to the DHN.

⁴ 30 MW x 0.30 = 9 MW
⁵ 78 MW x 0.23 = 18 MW

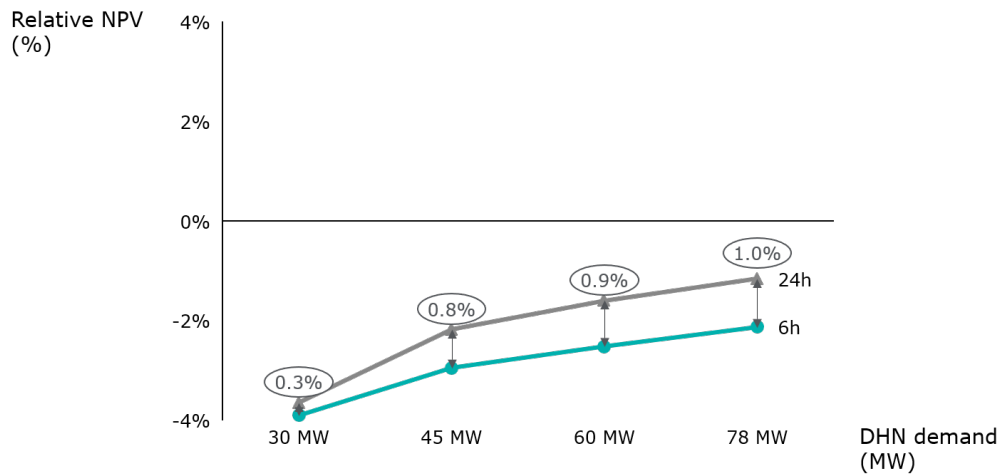


Figure 6.24: P2H&P: sensitivity analysis of the NPV to changes in the DHN demand, for two different storage capacities

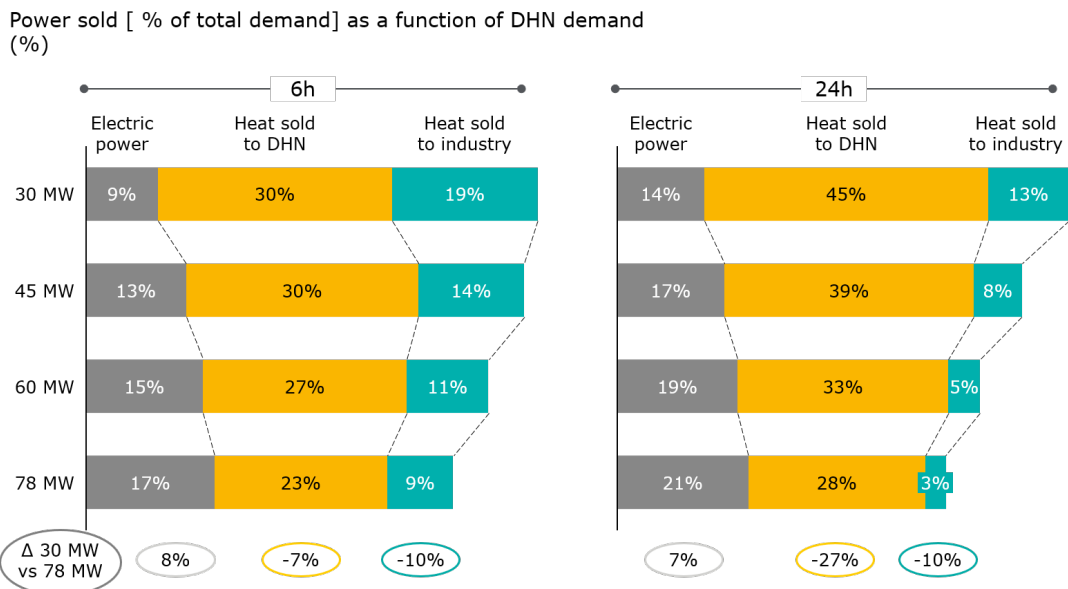


Figure 6.25: P2H&P: sensitivity analysis of the electric and thermal discharged powers to changes in the DHN demand

6.4.3 High-temperature heat price

After the two defining variables for the DHN application have been studied, namely the price and the demand, the same analysis is performed in this section for the high-temperature heat sales. The main goal is to determine the minimum price under which the industrial sales are balanced with the power and steam ones. The main findings are the following (observed from Figures 6.26 and 6.27):

1. The break-even prices increase from 33 and 35 €/MWh in Case 3, to around 41 and 42 €/MWh for the 6h and 24h storage sized respectively. The main reason is the increase in CAPEX caused by the steam cycle, which in Case 3

was not included. Because the increase in CAPEX is relatively larger for the small storage (increase in storage capacity vs. increase in cost), the impact in the break-even price is larger. Thus, the NPV of the 24h storage improves and steps closer to the 6h.

2. The gradual increase in the heat price clearly results in an increase of heat sales to the demand. In the 6h storage example, the industrial heat sales surpass the DHN under a 40€/MWh price. This means that for a selling price of 40€/MWh or above, the industrial heat sales become the first income source. In the 24h example, this development takes place for heat prices of 45 €/MWh or higher.

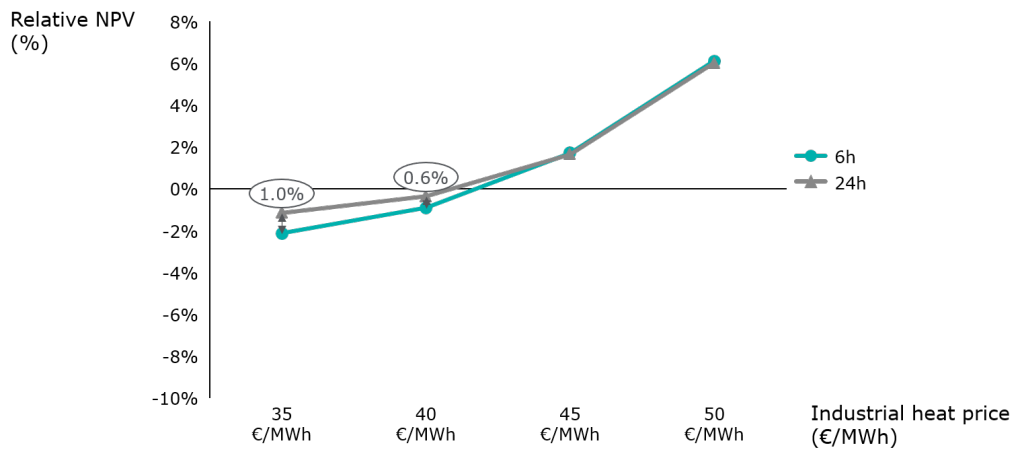


Figure 6.26: P2H&P: sensitivity analysis of the NPV to changes in the high-temperature heat price, for two different storage capacities

Heat sold [% of total demand] as a function of industrial heat price (%)

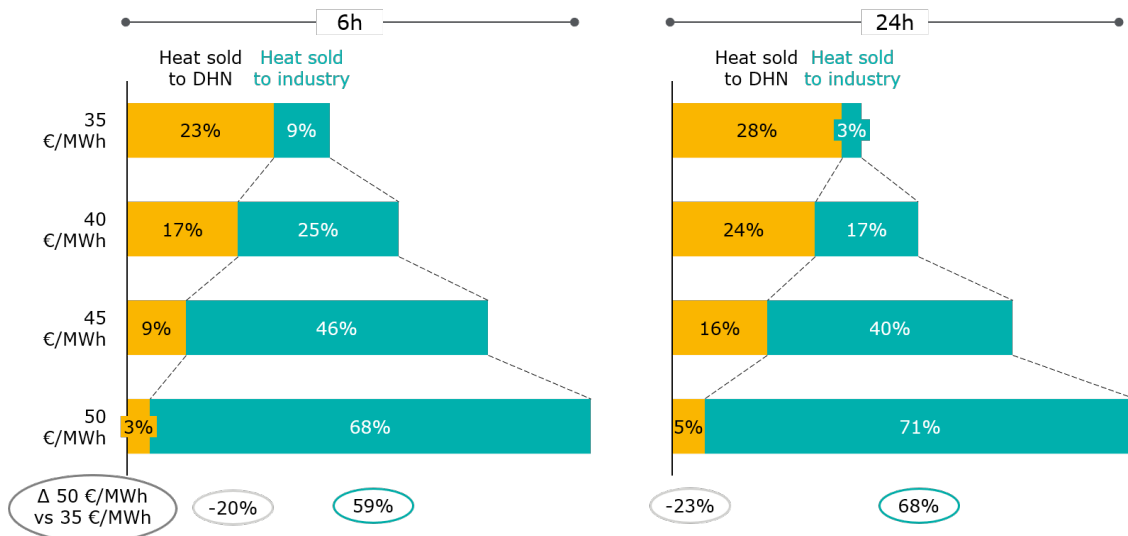


Figure 6.27: P2H&P: sensitivity analysis of the electric and thermal discharged powers to changes in the high-temperature heat price

6.4.4 High-temperature demand profile

The sensitivity of the NPV shown in the previous section, are now compared to the sensitivity of revenues to changes in the high-temperature heat demand. The analysis of the impact of different constant demand levels between 50 MW and 133 MW, is shown in Figures 6.28 and 6.29. The results show that the variation of the heat demand from industry, barely affects the NPV. This result is an outcome of the total heat sales remaining approximately constant after each demand variation. The reason for this was explained in Case 3, Section 6.3.2. Additionally, the used heat price (i.e. 35 €/MWh), is below the new break-even price (i.e. 41 €/MWh) and therefore the sale of heat to the DHN remained the most profitable revenue stream. Since the heat sales remained nearly constant, also did the DHN heat sales.

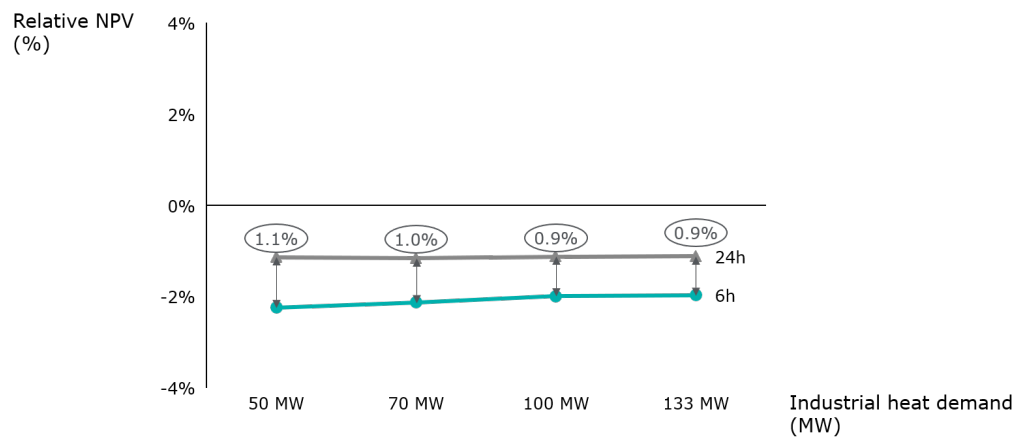


Figure 6.28: P2H&P: sensitivity analysis of the NPV to changes in the high-temperature heat demand, for two different storage capacities

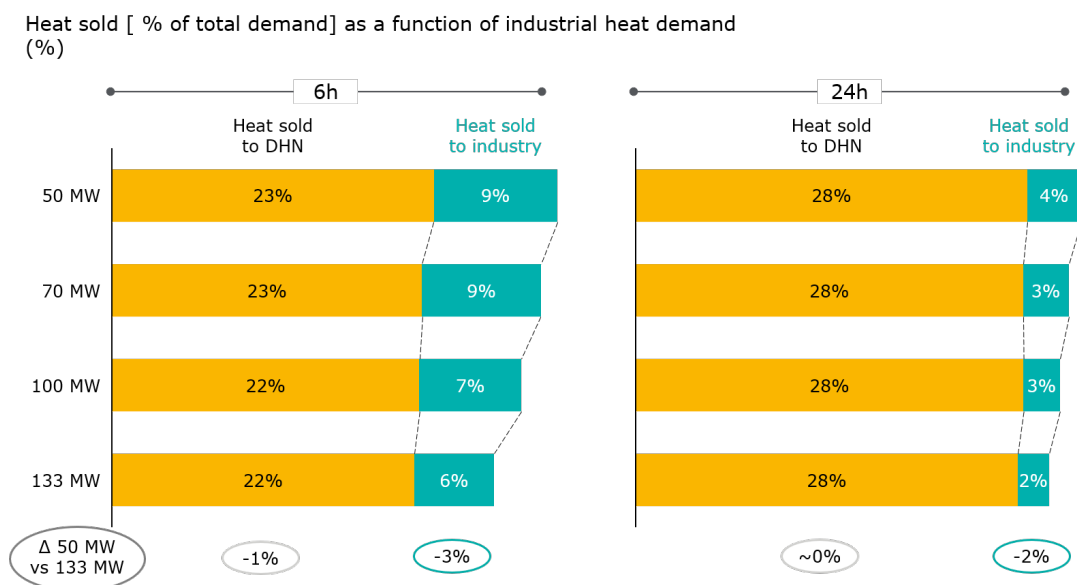


Figure 6.29: P2H&P: sensitivity analysis of the electric and thermal discharged powers to changes in the high-temperature heat demand

6.4.5 Rankine cycle efficiency

Lastly, the impact of the steam cycle efficiency on the NPV has also been evaluated as in the previous Cases 1 and 2 (Figure 6.30). This time, a detailed examination of the implication of this parameter on the heat and power sales has also been included (Figure 6.31).

The inquiry was conducted with the reference prices of 50 €/MWh and 35 €/MWh, for the district heating and high-temperature heat respectively. From the curves the following is observed:

1. The 'break-even' efficiency improves slightly with respect to the value obtained for Case 2. This is a result of the extra revenues from industry, which increase the overall NPV. In accordance to what was already concluded, the increase in efficiency does not lead to positive NPV results with small storage capacities.
2. In absolute terms, a 15% increase in efficiency results in around a 2% increase in the NPV. Because of the relatively low increase in revenues, the cost of such efficiency enhancement should be evaluated in comparison with the extra NPV obtained.
3. Regarding the changes in power sales, an increased efficiency leads to larger electric power sales and lower DHN sales. More concretely, the electric power sold increases by 11% (i.e. for the 6h storage) and 13% (i.e. for the 24h storage) for a total increase in efficiency of around 15%. Due to the higher efficiency of the turbine or steam cycle, less heat can be extracted for the district heating, hence the DHN sales decrease. Lastly, also an increase in industrial heat sales is observed, due to the larger availability of power. Notwithstanding, this increase is almost negligible.

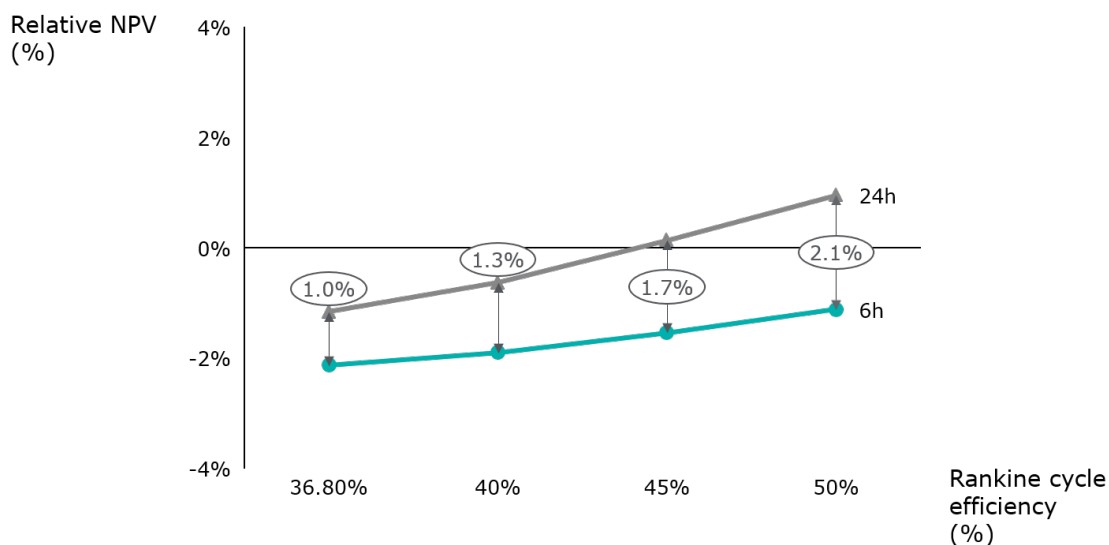


Figure 6.30: P2H&P: sensitivity analysis of the NPV to changes in the Rankine cycle efficiency, for two different storage capacities

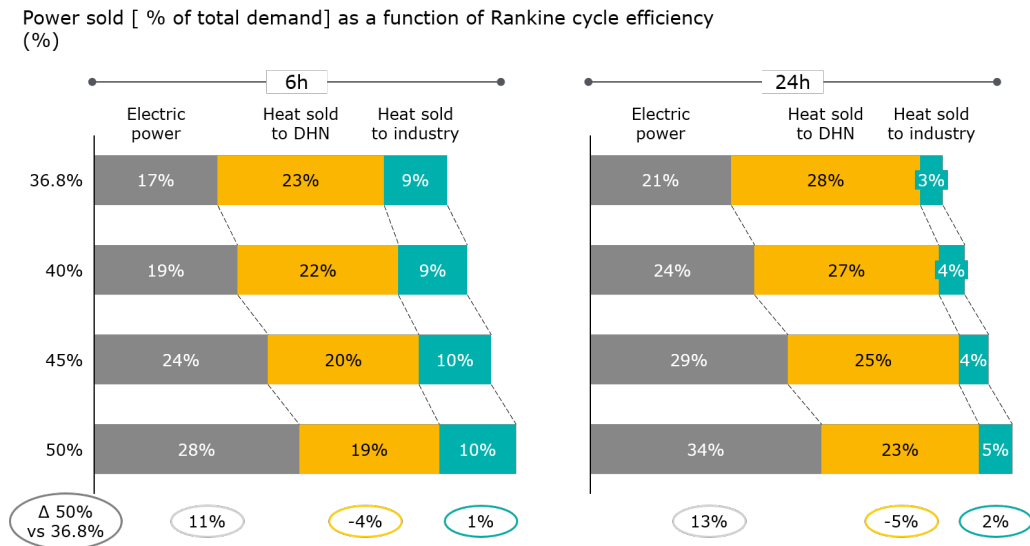


Figure 6.31: P2H&P: sensitivity analysis of the electric and thermal discharged powers to changes in the Rankine cycle efficiency

The same analysis was performed for a DHN price of 55 €/MWh, and a high-temperature heat price of 40€/MWh. The obtained results are given in Appendix C, in order to expand the understanding on the impacts of these prices.

6.4.6 Competitiveness of ETES with natural gas

Lastly, in view of the previous findings, a closer study of the selling heat price has been performed to compare it with natural gas in Figure 6.32.

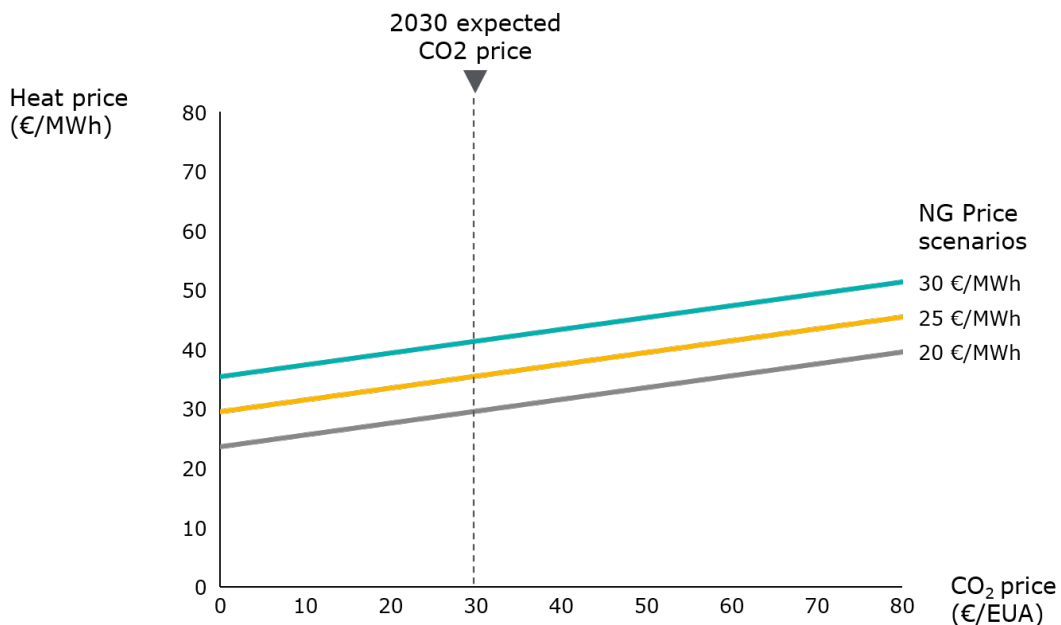


Figure 6.32: Maximum heat price to be competitive with natural gas considering CO₂ prices, for three different natural gas scenarios

Figure 6.32 shows three possible scenarios for the price of this commodity in 2030, namely, 20, 25, and 30 €/MWh. Because the burning of natural gas involves CO₂ emissions [84], the CO₂ taxes will rise the cost of using this commodity. Many price forecasts predict a maximum CO₂ price of 30€/EUA (i.e. 30€/t) in 2030 [85]. Thus, the maximum selling heat price can be obtained as the price paid to obtain the same amount of energy by burning natural gas, in addition to the CO₂ price attached to it. The figures have been developed considering a boiler efficiency of 80%.

As shown in the figure above, the increase of CO₂ prices will improve the business case for ETES. Additionally, it can be seen that even for very low CO₂ prices, ETES could be competitive in the high-temperature heat market (i.e. Case 3) without the need for further developments. In the case of heat sales to a DHN, high CO₂ price will be required to be competitive with natural gas, or alternatively other incentives for low-carbon heat.

Discussion

The main aim of Case 4 was the evaluation of the storage performance and the revenue forming, when the three available applications are combined: electric power sale to the DA market, heat sale to a DHN, and heat sale to an industry. The main intake from the results is that the relevance of each application strongly depends on the selling price. The selling price of each market actively influences the revenue stacking structure and the distribution of energy resources, and particularly more if compared with the analysis of the demand level. For example, due to the combination of revenue sources, the break-even price for the DHN heat is slightly improved. However, the high-temperature break-even price is increased due to the increased CAPEX, which in this case includes the steam cycle. Keeping this in mind, it is concluded that whenever there is the possibility for revenue stacking, the sizing of each discharging equipment should be tailored to optimize the revenues of each stream according to its potential and to minimize the investment costs. This requires a dedicated assessment of the individual contractual conditions of each specific case.

7 | CONCLUSIONS

The conclusions of the conducted study as well as some recommendations for future work are herein provided. The conclusions are presented by responding to the three sub-questions that have structured this project. The answers have been deduced from the results of the research and from the sensitivity analysis performed on the most relevant variables. Detailed information about the model has been presented in Chapter 4, and the outcomes of the study have been given in Chapter 6. The thesis concludes by identifying the missing elements that should be object of future investigations.

7.1 RESEARCH FINDINGS

The main goal of this thesis was to assess which market conditions are optimal for the commercial implementation of ETES, by means of the development of a detailed model of the technology. The most relevant research findings are listed below.

1. How should a programming-based model be formulated to evaluate the thermodynamic performance of ETES and its implementation for different applications?

The novelty of the Electric Thermal Energy Storage and its limited integration in the energy system has resulted in few academic studies about this technology. As pointed out in the Literature review, the few works that include electrothermal storage make use of greatly simplified approaches or focus on niche applications. Consequently, the first aim of this thesis has been to create a model of the technology from the start, covering its most important components and describing its operation in detail.

Firstly, in order to assess the business potential of ETES, the model has been constructed based on an optimization approach following a revenue maximization goal. The maximization of revenues has been selected as the objective function since this approach enables to assess the commercial implementation of the technology. Once the maximum revenues under certain conditions had been obtained, the net present value (NPV) of the technology has been compared to a reference case without storage in order to determine its commercial viability. Such exercise has shown that, even though the economics are positive for some

applications (i.e. positive NPV), the need for storage is not enough to justify the investment (i.e. negative relative NPV).

Secondly, the constraints have been modelled with a great level of detail in order to include important efficiency parameters and mechanical restrictions that influence the operation of the system. The energy content of the storage has been formulated in thermodynamic terms as a means to gain a better understanding of the dynamics of the system. This approach enables to, for instance, understand the air flow requirements of the air pipes, or the exergy content of the storage bed. As regards the technical constraints of the charging and discharging cycles, they provide valuable data concerning the expected operability of the asset. The developed approach additionally facilitates simulations with other working temperatures, materials, and so on. The great majority of the equations are a contribution of this thesis project and only a few constraints, mainly from the unit commitment, have been obtained from the Literature.

Thirdly, the overarching goal of the thesis required the evaluation of the storage technology for any kind of energy input and output, i.e. heat or electricity. The versatility of the model allows the use of any input signals, namely, any power supply source, district heating demand, and high-temperature heat demand. Similarly, the electricity and heat prices can be varied to observe their effect on the storage. The equations are presented in such a way that the desired level of granularity can be chosen by deciding the length of the time steps, and the simulation horizon can be tailored to adjust the level of uncertainty.

Lastly, the need to carry out multiple simulations with different inputs and conditions demanded a short computational time. In view of this, the model is formulated with linear equations that, due to the lower time requirements, enabled the addition of more constraints and model components. Despite the fact that some non-linear terms could have increased the accuracy of some thermodynamic behaviours, first attempts revealed that such approach would have resulted in very long simulation times (on the day(s) scale). This conclusion coincides with the findings of previous academic studies about programming-based models.

2. Which is the most promising energy market for the integration of ETES into the future energy system and what future developments will have to take place to open up new markets?

The research has included the investigation of three main energy markets or applications: the sale of electric power to the day-ahead market, the sale of high-temperature heat to an industry, and the sale of heat as a by-product of power generation to a district heating network (DHN).

The main conclusion from the results is that, due to the low investment needs and due to the high discharging efficiency, the application that currently yields the largest profit is the sale of high-temperature heat to an industry. Under such application, the minimum selling price to cover the investment is already in the range of natural gas commodity prices, which at the present time can be considered the main competitor.

Regarding the other two remaining applications, several market developments will have to take place to enable the implementation of ETES. In order for the business model to be based exclusively on electricity arbitrage, it has been demonstrated that the volatility of the electricity prices will have to reach very high levels. Additionally, the analysis has shown that this is the case for virtually all electricity storage technologies. Despite the fact that a high penetration of renewable energy sources could increase the volatility of prices, it is likely that market mechanisms would simultaneously emerge to dampen the price oscillations. Thus, the electricity arbitrage application would have to be in place along with other incentives, such as high renewable power curtailment, high imbalance penalties, or provision of grid services. The likelihood of these conditions will increase due to the high renewable power shares targets of many economies. If the sale of heat to a DHN is added to electricity arbitrage, the business case significantly improves. However, the minimum heat selling price is still high when compared to natural gas. Consequently, in order for ETES to be competitive in this respect, incentive schemes for low carbon-heat such as high CO₂ prices would have to be in place.

This conclusion is in line with the results found in the Literature, which point to P₂H as the most promising application for electrothermal storage. Notwithstanding, the present research includes a more granular assessment and an exhaustive sensitivity analysis of the results to the demand and price conditions. Regarding the applications involving electricity generation, also similar conclusions to previous academic studies have been reached. Previous authors have determined that electrothermal storage could have a business case based on electricity arbitrage, only along other purposes such as grid extension avoidance. Additionally, it has been confirmed that the business case in this application can improve with DHN, since the technology can leverage from the temporal correlation of high wind speeds (i.e. power supply) and high heating demand.

3. Which are the most relevant boundary conditions of the heat and electricity sectors that SGRE developers should consider for the commercial positioning of ETES?

Two main boundary conditions of the heat and power sectors have been considered in this thesis: selling prices and demand levels. Multiple sensitivity analysis have been carried out on the day-ahead electricity prices, on the district heating price and demand, and on the industrial heat price and demand. The results indicate that the revenues are more dependent on the prices than on the level of demand.

Regarding the day-ahead electricity price, it has been proven that the average is the most determinant component. The results show that if ETES is installed for a P₂H application, the higher the average electricity price, the lower the heat sales and revenues. This effect takes place because when the average electricity price is increased, the income from this revenue stream increases with respect to the one from heat sales. Thus, the installation of ETES for supplying heat to a thermal sink becomes more trivial and the business case worsens. This

has been demonstrated by comparing the profitability of ETES in Germany and Spain, which are countries with very different average day-ahead prices, and by several sensitivity analysis. On the contrary, when electricity arbitrage is the only revenue stream and there are no heat sinks, a high average price yields larger revenues and the business case improves.

As regards the electricity price volatility, it has been demonstrated that the daily fluctuations have to be very large in order to improve the business case. The fluctuations with the smaller periodicities (i.e. periods of 12 and 24 hours) are the ones that have a major impact on the revenues due to the charging and discharging times of the storage (i.e. 6 hours and 24 hours). This means that larger intra-day price fluctuations are beneficial due to the increase in revenues from electricity arbitrage: the system can charge power at lower prices compared to the selling prices. This has been demonstrated with the sensitivity analysis performed on each price coefficient, and had a positive effect in every single application. Additionally, it has been demonstrated that the more frequent component of the price (i.e. period of 12 hours) is the one with the largest impact on the storage cycles: bigger fluctuations lead to more cycling. This should be taken into account for the wear of the system components, which may affect the operational and maintenance costs. It is difficult to predict which generation fleet or market developments will increase daily fluctuations of prices, nevertheless, it has been suggested that markets with large shares of solar energy could have this characteristic.

With respect to the extraction of heat from the steam cycle for district heating, both the selling price and the demand have been analyzed. Regarding the break-even price to cover the investment of the steam cycle, it was found to be high, and especially when compared to other competitor technologies. This is a result of the low efficiency of the Rankine cycle, which requires large electricity price fluctuations to leverage from them. An initial estimation of the effect of improving such steam generation efficiency resulted in modest revenue improvements. Consequently, a more detailed analysis of the required costs for the enhancement of the system should be carried out and compared to the increase in revenues. With respect to the demand, it was found that the simultaneity of high electricity prices and demand is beneficial for the revenues due to the simultaneity of outputs. Moreover, having a high demand over the whole year is very relevant, which is not the case in many cities where the demand drops significantly in the summer. Thus, this application should also be considered for other heat sinks, such as for instance an industry with lower temperature requirements.

Lastly, the analysis of the sale of high-temperature heat to an energy-intensive industry was also performed. The obtained break-even price of heat was low compared to the average electricity price. This is a result of, first, the high volatility and low average of the German electricity price, and second, the lower cost and higher efficiency of the discharging cycle (compared to the Rankine cycle). The first condition is likely to improve further due to a large penetration of renewables, thus, it can be expected that the business case will also continue improving. With respect to the demand, a high average demand and large fluctuations were estimated to be the optimal conditions. The correlation of the

demand fluctuations with the price fluctuations was also found to have an impact on the economics; if high heat demand periods coincide with low electricity prices, the revenues from 'P₂H arbitrage' are maximized. Markets with large shares of solar power could also be attractive in this respect.

7.2 RECOMMENDATIONS FOR FUTURE WORK

In the course of this thesis several areas of improvement of the model and the analysis have been identified. The main recommendations for future investigations are the following:

Applications of ETES

An overview of all the potential applications of ETES has been provided. The three that were considered the most relevant have been included in the model and studied in more detail. Notwithstanding, the system conditions may evolve in a way that other applications emerge as more promising. Consequently, a deeper market analysis, including an investigation of different regulatory frameworks, would be beneficial in order to determine which applications should also be studied in depth next. As regards the model, any application could be added: grid services, imbalance and curtailment mitigation, industrial waste heat recovery, increased flexibility for power generation, and retrofit of polluting power plants. The first two would require the formulation of additional constraints, such as for instance minimum energy reserves or a new imbalance price input curve. The remaining would entail a detailed evaluation of the reduction of fuel usage, as well as of the investment costs and savings from existing equipment.

Model formulation

The linearization of the optimization problem decreased the computational time, nevertheless, this was at the expense of the simplification of some constraints. To begin with, the model does not currently differentiate among a cold start, a warm start, or a hot start. Such classification would allow to tailor the start-up times and costs to each condition. Secondly, the state of charge of the storage has been modelled by means of state variables. The corresponding constraints could be modified and expressed in relation to the temperatures inside the packed bed, which vary with time. Similarly to the energy content, the exergy losses have been approximated by a linear function and could be expressed as a function of the temperatures instead. Lastly, the efficiency of the steam cycle has been modelled as a constant value. It is known that the efficiency actually evolves in time and depends on the output power. Thus, a dynamic efficiency would also improve the accuracy of the results.

Analysis of the boundary conditions

The spectral analysis has been performed using some representative curves for each revenue stream due to the time constraints. Consequently, additional analysis should be carried out with more heterogeneous boundary conditions (e.g. from developing countries) in order to diversify and compare the results for each input. Regarding the modelling of the high-temperature heat demand, all the tested demand profiles were continuous and non-intermittent. It is considered that the analysis should be expanded to batch process with periods of no demand. Likewise, the sensitivity of the results to changes in the supply power should also be evaluated. Other commercial applications such as the supply of power with a power purchase agreement should also be considered. Lastly, it would be interesting to carry out a thorough analysis of the relationship between the design of the storage and the different boundary conditions.

BIBLIOGRAPHY

- [1] IRENA. *Electricity Storage and Renewables: Costs and Markets to 2030*. International Renewable Energy Agency (IRENA), Paris, 2017.
- [2] A. Bloess, W.P. Schill, and A. Zerrahn. *Power-to-heat for renewable energy integration: A review of technologies, modeling approaches, and flexibility potentials*. *Applied Energy*, 212:1611–1626, 2018.
- [3] Clingendael International Energy Programme. *European Union Industrial Energy Use with a Focus on Natural Gas*. CIEP, the Netherlands, 2017.
- [4] Yatich T. Shah. *Thermal Energy: Sources, Recovery, and Applications*. CRC Press, 2018.
- [5] I. Sarbu and C. Sebarchievici. *A Comprehensive Review of Thermal Energy Storage*. *MDPI*, 10:191, 2018.
- [6] International Energy Agency. *Industrial sector energy consumption*. IEA, Paris, 2016.
- [7] International Renewable Energy Agency. *Power System Flexibility for the Energy Transition*. IRENA, Paris, 2018.
- [8] EU Climate Action. Available: https://ec.europa.eu/clima/citizens/eu_en.
- [9] European Commission. *Support schemes*, . [Online]. Available: <https://ec.europa.eu/energy/en/topics/renewable-energy/support-schemes> [Accessed 10 June 2019].
- [10] Agora Energiewende. *Electricity Storage in the German Energy Transition*. Agora Energiewende, Berlin, 2014.
- [11] L. van Nuffel, J. Gorenstein Dedecca, T. Smit, and K. Rademaekers. *Sector coupling: how can it be enhanced in the EU to foster grid stability and decarbonise?* Brussels, 2018.
- [12] K.K. Cao, A.N. Nitto, E. Sperber, and A. Thess. *Expanding the horizons of power-to-heat: Cost assessment for new space heating concepts with Wind Powered Thermal Energy Systems*. *Energy*, (164):925–936, 2018.
- [13] P. H. Grunewald, T. T. Cockerill, M. Contestabile, and P. Pearson. *The socio-technical transition of distributed electricity storage into future networks. System value and stakeholder views*, *Energy Policy*, 2012.
- [14] P. H. Grunewald. *Electricity storage in future GB networks - a market failure?* BIEE 9th Academic Conference, Oxford, 2012.

- [15] A. Zucker, T. Hinchliffe, and A. Spisto. *Assessing storage value in electricity markets - A literature review*. European Commission Joint Research Centre, Luxembourg, 2013.
- [16] AH.K. Ringkjøb, P. M. Haugan, and I. M. Solbrekke. *A review of modelling tools for energy and electricity systems with large shares of variable renewables*. *Renewable and Sustainable Energy Reviews*, 96:440–459, 2018.
- [17] Aalborg University. Energyplan - advanced energy system analysis computer model. [Online]. Available: <https://www.energyplan.eu/>. [Accessed 9 May 2019].
- [18] H.M. Henning and A. Palzer. *A comprehensive model for the German electricity and heat sector in a future energy system with a dominant contribution from renewable energy technologies - Part I:Methodology*. *Renewable and Sustainable Energy Reviews*, Freiburg, 2013.
- [19] M. Sameti and F. Haghighat. *Optimization approaches in district heating and cooling thermal network*. *Energy and Buildings*, 140:121–130, 2017.
- [20] D. Olsthoorn, F. Haghighat, and P. A. Mirzaei. *Integration of storage and renewable energy into district heating systems: A review of modelling and optimization*. *Solar Energy*, 136:49–64, 2016.
- [21] X. Liu, J. Wu, N. Jenkins, and A. Bagdanavicius. *Combined analysis of electricity and heat networks*. *Applied Energy*, 162:1238–1250, 2016.
- [22] J. Després. *Modélisation du développement à long terme du stockage de l'électricité dans le système énergétique global*. 2015.
- [23] Henrik Lund, Finn Arler, Poul Alverg Østergaard, Frede Hvelplund, David Connolly, Brian Vad Mathiesen, and Peter Karnøe. *Simulation versus Optimization: Theoretical Positions in Energy System Modelling*. *Energies*, 10, 840, 2017.
- [24] Chung-Yang Huang, Chao-Yue Lai, and Kwang-Ting Cheng. *Electronic design automation : synthesis, verification, and test*. 2009.
- [25] Torben Ommen, Wiebke Brix Markussen, and Brian Elmegaard. *Comparison of linear, mixed integer and non-linear programming methods in energy system dispatch modelling*. *Energy*, 74:109–118, 2014.
- [26] L. Hughes. *Meeting residential space heating demand with wind-generated electricity*. *Renewable Energy*, 35(8):1765–1772, 2016.
- [27] X. Chen, X. Lu, M. B. McElroy, C. P. Nielsen, and C. Kang. *Synergies of Wind Power and Electrified Space Heating: Case Study for Beijing*. *Environmental Science Technology*, 3(48):2016–2024, 2014.

- [28] P. Li, H. Wang, Q. Lv, and W. Li. *Combined heat and power dispatch considering heat storage of both buildings and pipelines in district heating system for wind power integration*. *Energies*, 10(893), 2017.
- [29] Z. Li, W. Wu, M. Shahidehpour, J. Wang, and B. Zhang. *Combined Heat and Power Dispatch Considering Pipeline Energy Storage of District Heating Network*. *IEEE Transactions on Sustainable Energy*, 7(1):12–22, 2016.
- [30] P. Steffes P.E. *Grid-Interactive Electric Thermal Storage (GETS) Space Water Heating*. Steffes, North Dakota.
- [31] R. Renaldi, A. Kiprakis, and D. Friedrich. *Optimisation of Thermal Energy Storage Integration in a Residential Heating System*. *SusTEM 2015*, 2015.
- [32] T. Okazaki, Y. Shirai, and T. Nakamura. *Concept study of wind power utilizing direct thermal energy conversion and thermal energy storage*. *Renewable Energy*, (83):332–338, 2015.
- [33] G. Manfrida D. Fiaschi and, K. Petela, and L. Talluri. *Thermo-Electric Energy Storage with Solar Heat Integration: Exergy and Exergo-Economic Analysis*. *Energies*, 12(4), 2019.
- [34] S. Henchoz, F. Buchter, D. Favrat, M. Morandin, and M. Mercangoz. *Thermoeconomic analysis of a solar enhanced energy storage concept based on thermodynamic cycles*. *Energy*, 45(1):358–365, 2019.
- [35] J. I. Burgaleta, S. Arias, and D. Ramirez. *GEMASOLAR, the first power thermosolar commercial plant with molten salt storage*. Vizcaya.
- [36] J. Spelling R. Guédez, B. Laumert, and T. Fransson. *Optimization of Thermal Energy Storage Integration Strategies for Peak Power Production by Concentrating Solar Power Plants*. *Energy Procedia*, 49:1642–1651, 2014.
- [37] K. Risthaus and R. Madlener. *Economic Analysis of Electricity Storage Based on Heat Pumps and Thermal Storage Units in Large-Scale Thermal Power Plants*. *Energy Procedia*, 142:2816–2823, 2017.
- [38] M. Richter, G. Oeljeklaus, and K. Görner. *Improving the load flexibility of coal-fired power plants by the integration of a thermal energy storage*. *Applied Energy*, 263:607–621, 2019.
- [39] D. Li, W. Zhang, and J. Wang. *Flexible Operation of Supercritical Power Plant via Integration of Thermal Energy Storage*. *Power Plants in the Industry*, 2018.
- [40] M. Richter, F. Möllenbruck, F. Obermüller, A. Knaut, F. Weiser, H. Lens, and D. Lehmann. *Flexibilization of steam power plants as partners for renewable energy systems*.
- [41] Philipp Vinnemeier, Manfred Wirsum, Damien Malpiece, and Roberto Bove. *Integration of heat pumps into thermal plants for creation of large-scale electricity storage capacities*. *Applied Energy*, 184:506–522, 2016.

- [42] D. Gibb, M. Johnson, J. Romani, J. Gasia, L. F. Cabeza, and A. Seitz. *Process integration of thermal energy storage systems - Evaluation methodology and case studies*. *Applied Energy*, 230:750–760, 2018.
- [43] M. Aneke and M. Wand. *Energy storage technologies and real life applications – A state of the art review*. *Applied Energy*, 179:350–377, 2016.
- [44] IRENA. *Thermal Energy Storage - Technology Brief*. International Renewable Energy Agency (IRENA) and IEA-ETSAP, 2013.
- [45] L.F. Cabeza. *Advances in Thermal Energy Storage Systems*. 2015.
- [46] G. Hailu. *Seasonal Solar Thermal Energy Storage. Thermal Energy Battery with Nano-enhanced PCM*. IntechOpen, 2018.
- [47] Ibrahim Emir Dincer and Marc A. Rosen. *Thermal energy storage : systems and applications*. Hoboken, N.J., Wiley, 2011.
- [48] International Energy Agency. *Renewables 2018. Market analysis and forecast from 2018 to 2023*. IEA, Paris, 2018.
- [49] European Energy Research Alliance. *Low-Temperature Sensible Heat Storage*. European Energy Research Alliance, Brussels, 2018.
- [50] B. D’Aguanno, M. Karthik, A. N. Grace, and A. Floris. *Thermostatic properties of nitrate molten salts and their solar and eutectic mixtures*. *Scientific Reports*, pages 2045–2322, 2018.
- [51] Siemens AG. *Siemens - Concentrated Solar Power*. [Online]. Available: <https://new.siemens.com/global/en/products/energy/power-generation/steam-turbines/concentrated-solar-power.html>. [Accessed 9 April 2019].
- [52] X. Py, N. Sadiki, R. Olives, V. Goetz, and Q. Falcoz. *Thermal energy storage for CSP (Concentrating Solar Power)*. *The European Physical Journal Conferences*, 148, 2017.
- [53] International Energy Agency. *Market Report Series: Renewables 2018*. IEA, Paris, 2018.
- [54] International Energy Agency. *Technology Roadmap: Concentrating Solar Power*. OECD/IEA, Paris, 2010.
- [55] MAN Energy Solutions. *A tale of fire and ice*. [Online]. Available: <https://www.man-es.com/discover/a-tale-of-fire-and-ice> [Accessed 14 December 2019].
- [56] Malta Inc. *Malta’s Electro-Thermal Energy Storage System*. [Online]. Available: <https://www.maltainc.com/our-solution>. [Accessed 10 October 2019].

- [57] Siemens Gamesa Renewable Energy. [Online]. Available: <https://www.siemensgamesa.com/en-int/products-and-services/hybrid-and-storage/thermal-energy-storage-with-etes>. [Accessed 29 March 2019].
- [58] Eva Thorin. *Basics of Energy. Reference Module in Earth Systems and Environmental Sciences*, 2014.
- [59] Marc A. Rosen. *The exergy of stratified thermal energy storages. Solar Energy*, 71(3):173–185, 2001.
- [60] A. Keshavarz, M. Ghassemi, and A. Mostafavi. *Thermal Energy Storage Module Design Using Energy and Exergy Analysis. Heat Transfer Engineering*, 24:3:76–85, 2003.
- [61] R. K. Rajput. *A textbook of engineering thermodynamics*. Firewall Media, 2010.
- [62] P.G. Bergan and C.J. Greiner. *A new type of large scale thermal energy storage. Energy Procedia*, (58):152–159, 2014.
- [63] Ç. Boles. *Vapor and combined power cycles. Thermodynamics*, 1998.
- [64] Eurostat. *Combined heat and power (CHP) generation. Directive 2012/27/EU of the European Parliament and of the Council*, 2017.
- [65] European Commission. *Horizon 2020*. [Online]. Available: <https://ec.europa.eu/programmes/horizon2020/en/news/harnessing-full-power-renewable-energy-hydrogen>. [Accessed 5 April 2019].
- [66] IRENA. *Renewable Capacity Statistics 2018*. International Renewable Energy Agency (IRENA), Abu Dhabi, 2018.
- [67] Europe Beyond Coal. *Overview: National coal phase-out announcements in Europe*. 2018.
- [68] M. Raunbak, T. Zeyer, K. Zhu, and M. Greiner. *Principal Mismatch Patterns Across a Simplified Highly Renewable European Electricity Network. Energies*, 1934(10), 2017.
- [69] Monitor Deloitte. *Los retos y necesidades de las redes eléctricas para la integración eficiente de la nueva generación renovable de la transición*. Deloitte Consulting, S.L.U., 2018.
- [70] B. Burger. *Electricity production from solar and wind in Germany in 2014*. Fraunhofer Institute for Solar Energy Systems ISE, Freiburg, 2014.
- [71] European Network of Transmission System Operators for Electricity. *Electricity Balancing in Europe. An overview of the European balancing market and electricity balancing guideline*. Entso-e, Brussels, 2018.
- [72] European Network of Transmission System Operators for Electricity. *Survey on ancillary services procurement, balancing market design 2017*. Entso-e & Wgas, 2018.

- [73] European Commission. *Communication on an EU strategy for Heating and Cooling – the contribution from heating and cooling to realising the EU’s energy and climate objectives*. EC, Brussels, 2015.
- [74] The Parliamentary Office of Science and Technology. *Carbon Footprint of Heat Generation*. Houses of Parliament - Parliamentary Office of Science and Technology, London, 2016.
- [75] Renewable Energy Policy Network for the 21st Century. *Energy Systems Integration and Enabling Technologies. A comprehensive annual overview of the state of renewable energy*. REN21, 2018.
- [76] International Energy Agency. *Linking Heat and Electricity Systems*. OECD/IEA, Paris, 2014.
- [77] J. Kessen. *District Heating in the Danish Energy System*. GronEnergi.
- [78] D. Dorien Bennink and J.H.B. Jos Benner. *Inzicht in de belangrijkste cost drivers van warmleveranciers in Nederland*. CE Delft, 2019.
- [79] Andreas Schroder, Friedrich Kunz, Jan Meiss, Roman Mendelevitch, and Christian von Hirschhausen. *Current and Prospective Costs of Electricity Generation until 2015*. DIW Berlin, 2013.
- [80] Germán Andrés Morales-España. *Unit Commitment. Computational Performance, System Representation and Wind Uncertainty Management*. Doctoral thesis. 2014.
- [81] Sven Werner. *European District Heating Price Series*. Energiforsk, 2016.
- [82] Alexander Zaczek. *Master thesis. Modeling of CHP-based local heating networks in order to cover the positive residual load*. Technische Universitat Hamburg-Harburg, 2016.
- [83] Intercontinental Exchange. *Dutch TTF Gas Futures*. [Online]. Available: <https://www.theice.com/products/27996665/Dutch-TTF-Gas-Futures/data?marketId=5132981span=3>. [Accessed 1 December 2019].
- [84] American Geosciences Institute. *What are the energy-related carbon dioxide (CO₂) emissions by source and sector for the United States?* [Online]. Available: <https://www.americangeosciences.org/critical-issues/faq/what-are-energy-related-carbon-dioxide-co2-emissions-source-and-sector-united-states>. [Accessed 20 November 2019].
- [85] Andrei Marcu, Emilie Alberola, Jean-Yves Caneill, Matteo Mazzoni, Stefan Schleicher, Charlotte Vailles, Wijnand Stoefs, Domien Vangenechten, and Federico Cecchetti. *2019 State of the EU ETS Report*. European Roundtable on Climate Change and Sustainable Transition, 2019.

A

REFERENCE CASE

This appendix includes the methodology for the calculation of the revenues of the *reference case* without storage. The results obtained from these calculations have been used to obtain the relative NPV, which indicates whether an investor would profit from installing ETES or not.

Table A.1: Revenue calculation for the reference case without storage

Input type	Revenue streams	Condition	Condition	Revenue	
$P_{\text{supply}}(t)$	$R_{\text{el}}(t), R_{\text{th}}(t)$	1	2	reference case	
Heat	Heat		$P_{\text{supply}}(t) > D_{\text{th}}(t)$	$D_{\text{th}}(t) R_{\text{th}}(t)$	
			$D_{\text{th}}(t) > P_{\text{supply}}(t)$	$P_{\text{supply}}(t) R_{\text{th}}(t)$	
	Electricity			$\eta_{\text{el}} P_{\text{supply}}(t) R_{\text{el}}(t)$	
	Heat and electricity	$\eta_{\text{el}} R_{\text{el}}(t) > R_{\text{th}}(t)$			$\eta_{\text{el}} P_{\text{supply}}(t) R_{\text{el}}(t)$
Electricity	Heat		$P_{\text{supply}}(t) > D_{\text{th}}(t)/\eta_{\text{th}}$	$D_{\text{th}}(t) R_{\text{th}}(t) + \eta_{\text{el}} [P_{\text{supply}}(t) - D_{\text{th}}(t)] R_{\text{el}}(t)$	
			$D_{\text{th}}(t)/\eta_{\text{th}} > P_{\text{supply}}(t)$	$P_{\text{supply}}(t) R_{\text{th}}(t)$	
	Electricity			$P_{\text{supply}}(t) R_{\text{el}}(t)$	
	Heat and electricity	$R_{\text{el}}(t) > \eta_{\text{th}} R_{\text{th}}(t)$			$P_{\text{supply}}(t) R_{\text{el}}(t)$
		$\eta_{\text{th}} R_{\text{th}}(t) > R_{\text{el}}(t)$			
			$P_{\text{supply}}(t) > D_{\text{th}}(t)/\eta_{\text{th}}$	$D_{\text{th}}(t) R_{\text{th}}(t) + [P_{\text{supply}}(t) - D_{\text{th}}(t)/\eta_{\text{th}}] R_{\text{el}}(t)$	
			$D_{\text{th}}(t)/\eta_{\text{th}} > P_{\text{supply}}(t)$	$\eta_{\text{th}} P_{\text{supply}}(t) R_{\text{th}}(t)$	

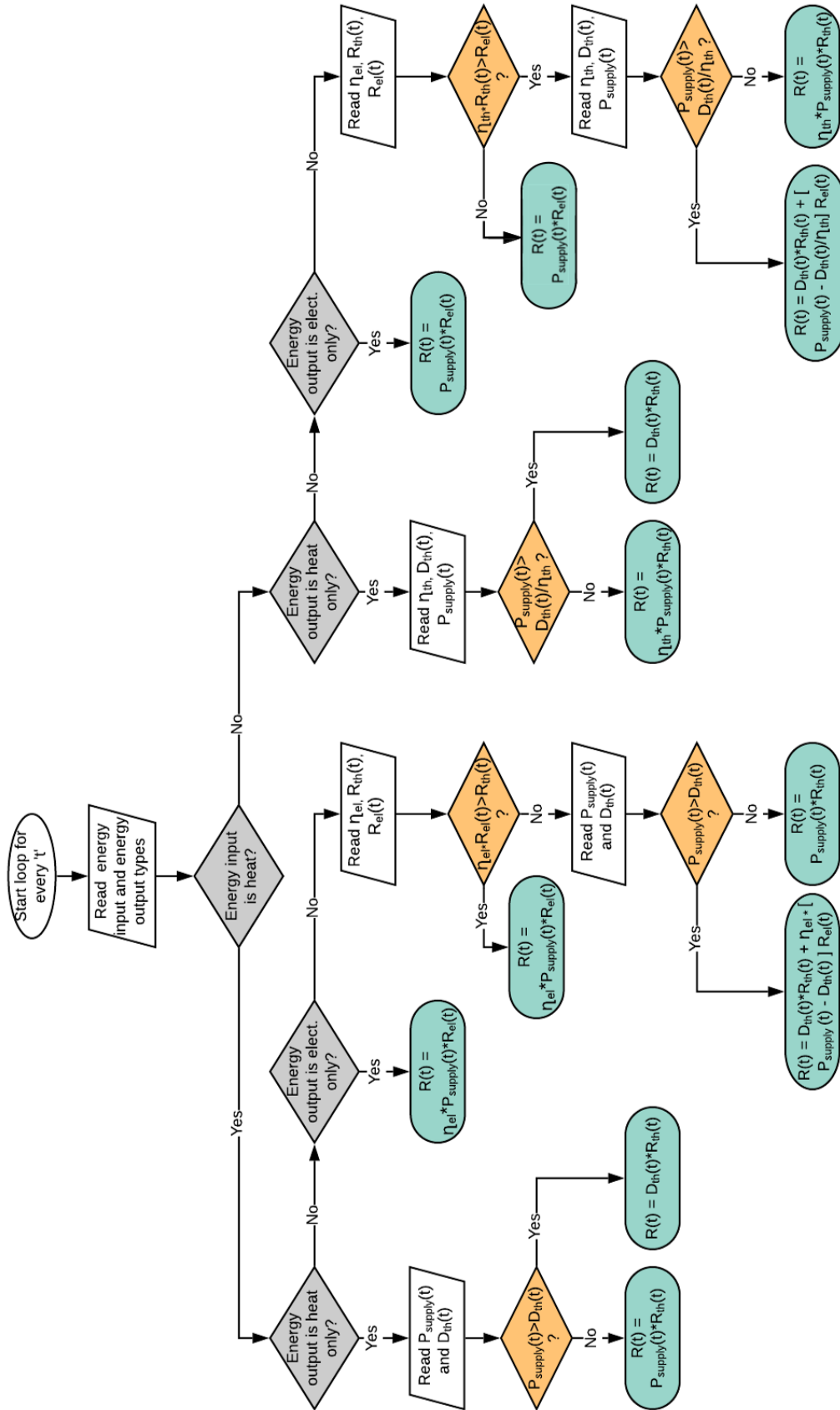


Figure A.1: Flow chart with the process calculation of the revenues of the reference case

B | FOURIER ANALYSIS

The prevailing yearly frequencies for the German and Spanish electricity day-ahead markets are shown below. These frequencies have been obtained from historical data from the year 2014 until the year 2018, and they have been used in the creation of the artificial signals.

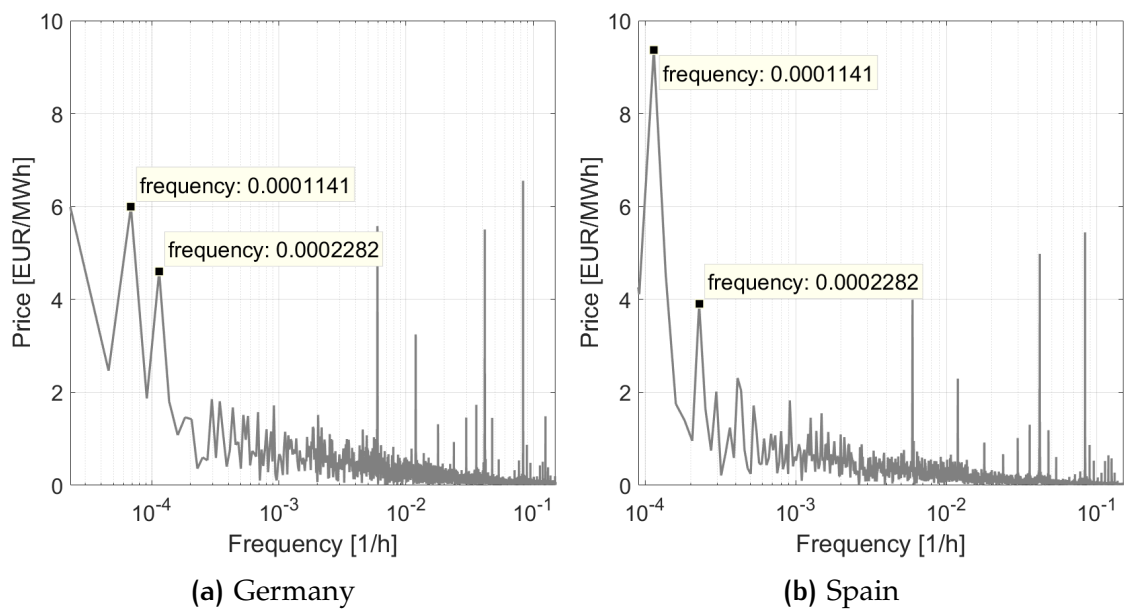


Figure B.1: Spectral density of the day-ahead market prices of Germany and Spain, from 2014 to 2018

C

ADDITIONAL SIMULATION RESULTS

C.1 POWER-TO-HEAT

The following figures depict additional simulation results of Case 3.

Constant heat demand profile analysis

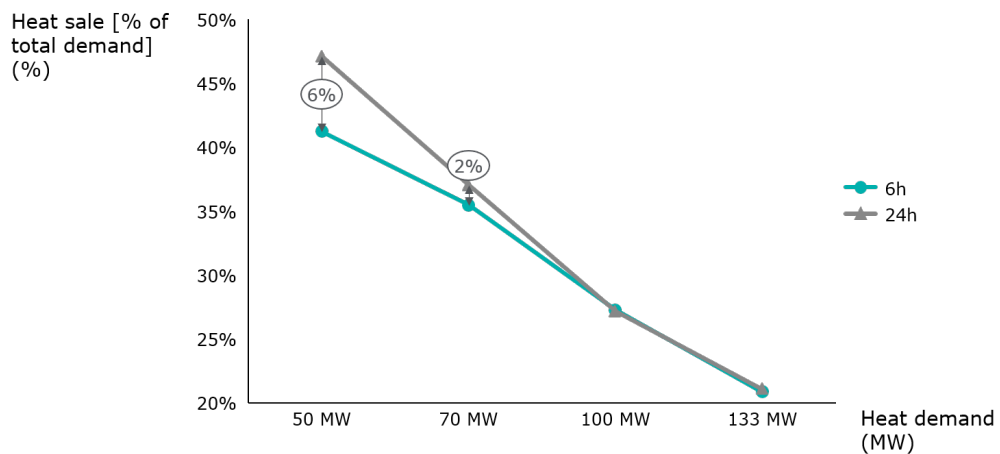


Figure C.1: P2H: sensitivity analysis of the heat sales to changes in the constant heat demand level, for two different storage capacities

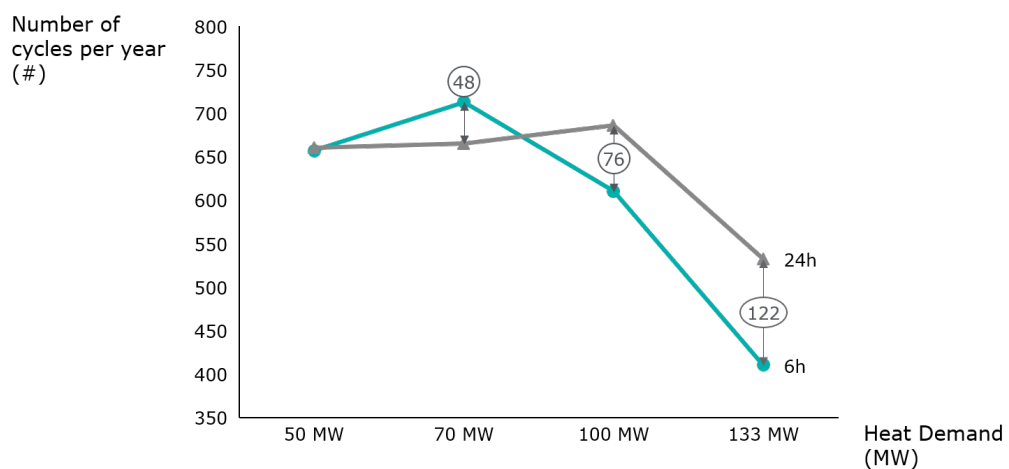


Figure C.2: P2H: sensitivity of the number of cycles to changes in the constant heat demand level, for two different storage capacities

Variable heat demand profile analysis

The following two plots show the variation in the heat sales to an industry, as well as in the storage cycles, for different standard deviations of demand.

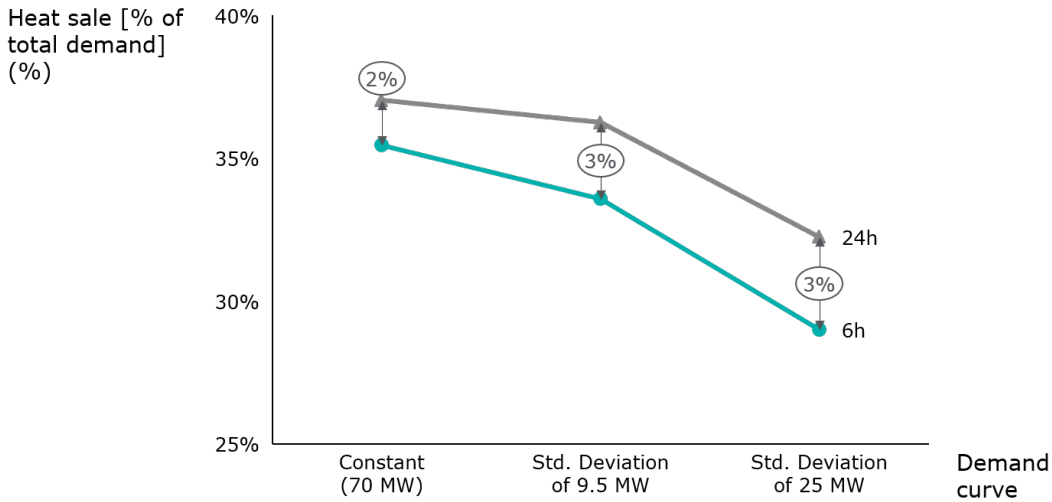


Figure C.3: P2H: sensitivity of the heat sales to the variability of the heat demand, for two different storage capacities

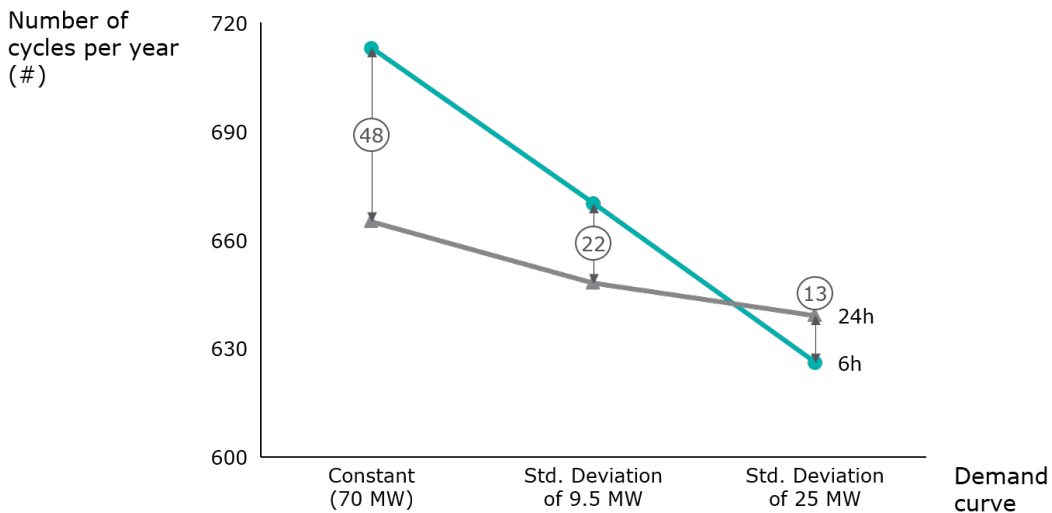


Figure C.4: P2H: sensitivity of the number of cycles to the variability of the heat demand, for two different storage capacities

Phase shift analysis

The following two plots show the variation in the heat sales to an industry, as well as in the storage cycles, for different phase shifts between the heat demand and the electricity prices.

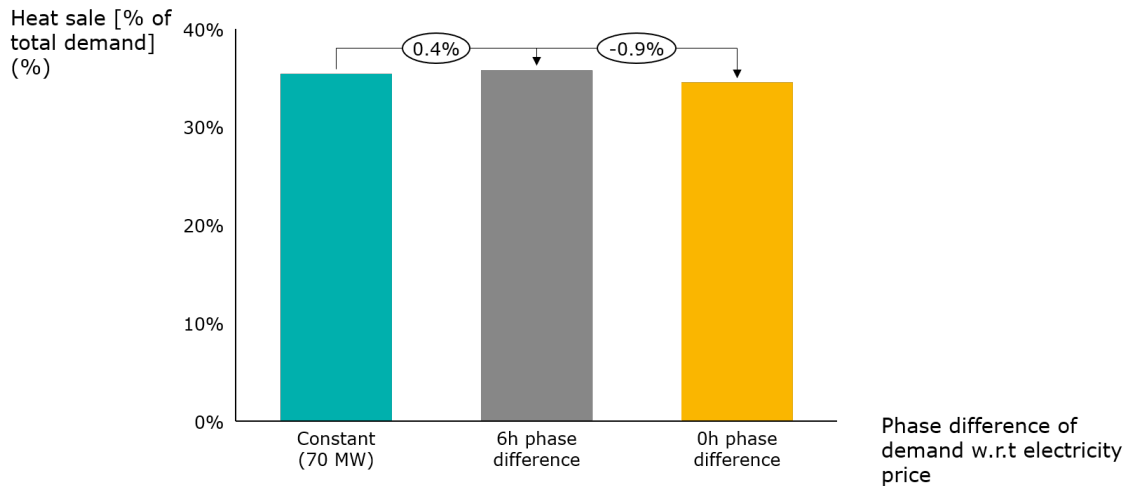


Figure C.5: P2H: sensitivity of the heat sales to the phase shift between the heat demand and the electricity price, for a 6h storage

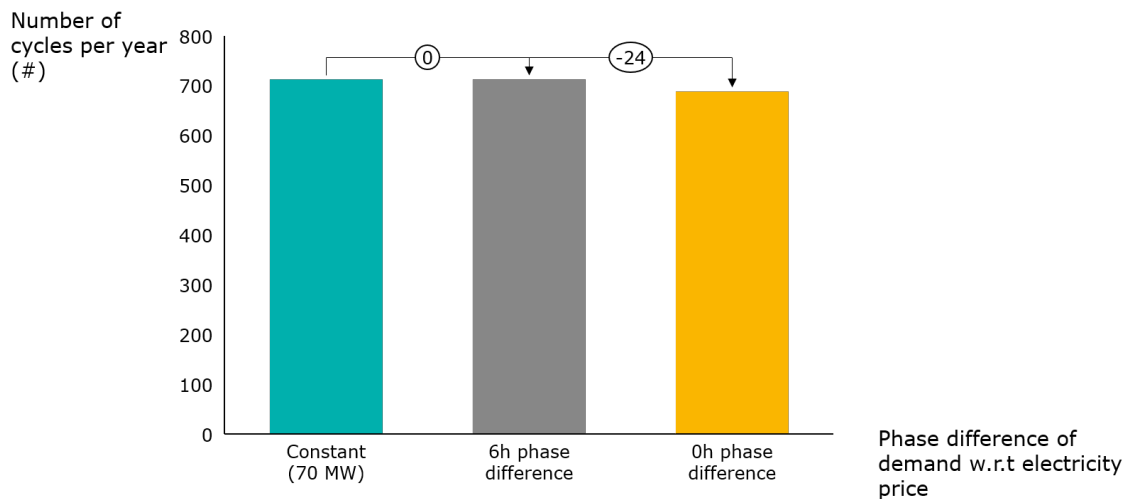


Figure C.6: P2H: sensitivity of the number of storage cycles to the phase shift between the heat demand and the electricity price, for a 6h storage

C.2 POWER-TO-HEAT-AND-POWER

Rankine cycle efficiency

In order to observe how the efficiency analysis changes with a larger DHN price, the same study was done with a district heating price of 55 €/MWh and the same industrial heat price of 35 €/MWh. The NPV results are shown in Figure C.7, and the amount of power discharged to each application is presented in Figure C.8.

1. Due to the larger price all NPV increase and turn positive for all efficiencies, with the only exception of the 6h storage and an efficiency of 36.8%.

- The change in NPV per change in the Rankine cycle efficiency smoothens, mainly in the 24h storage. This can be explained by looking at the sales graph, where it is observed that the extra increase in electric power sales (i.e. from 13% under a 50€/MWh price to 14% for 55€/MWh) is balanced out by a larger decrease in the DHN sales (from -5% to -6%).

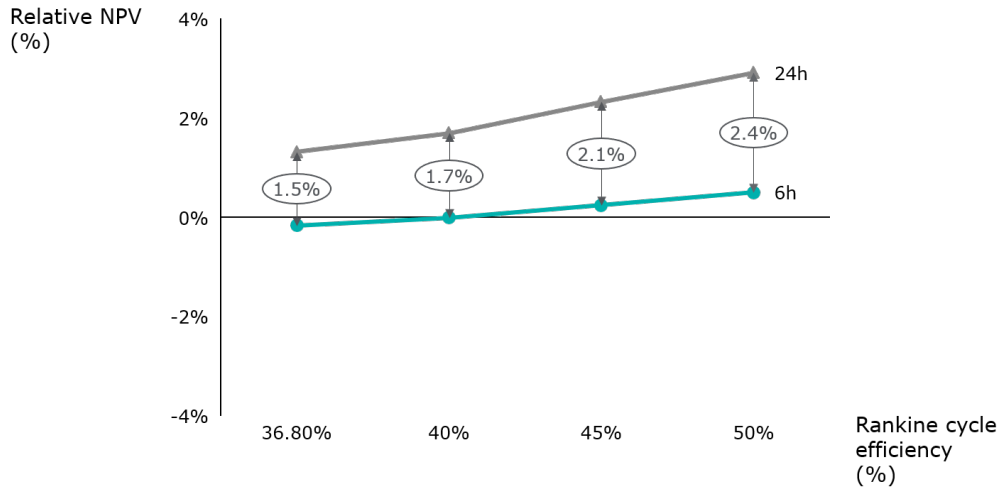


Figure C.7: P2H&P: sensitivity analysis of the NPV to changes in the Rankine cycle efficiency, for a higher DHN price

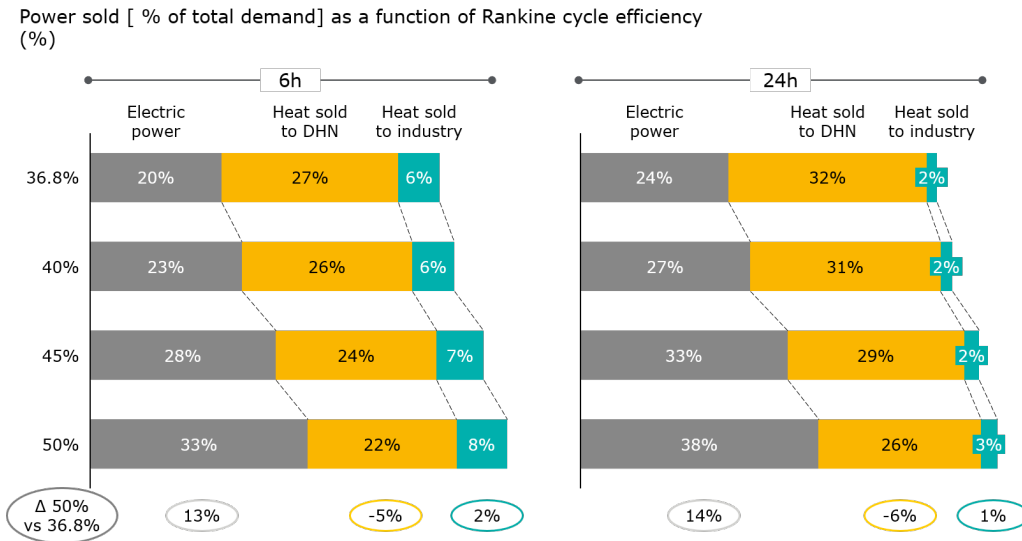


Figure C.8: P2H&P: sensitivity analysis of the electric and thermal discharged powers to changes in the Rankine cycle efficiency, for a higher DHN price

Lastly, the same exercise was done for a larger high-temperature heat price of 40 €/MWh (Figures C.9 and C.10). It is noticed that:

- The results improve in a lower magnitude than with the increase in the DHN price.

2. Additionally, the 6h results improve more compare to those of the 24h storage.
3. As it was expected, the heat sales to industry remain nearly constant and the electric power sales increase, but in a lower scale.

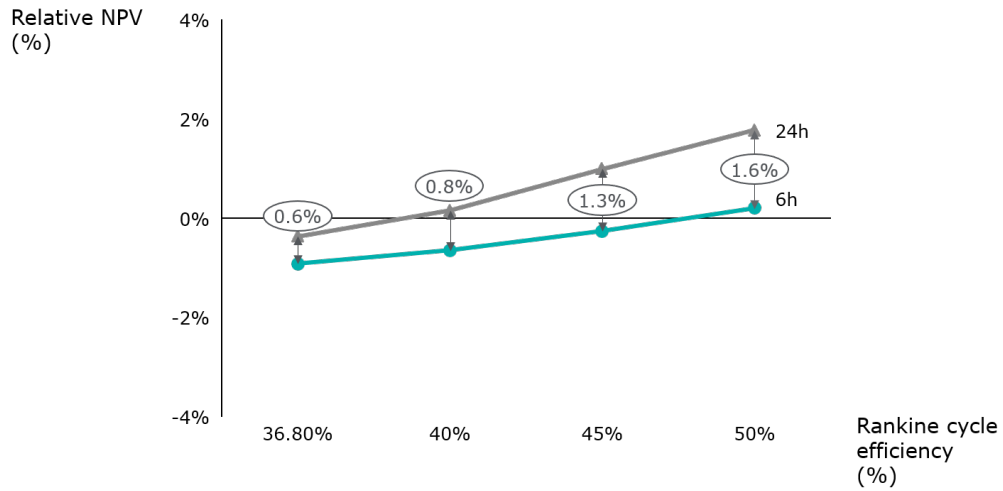


Figure C.9: P2H&P: sensitivity analysis of the NPV to changes in the Rankine cycle efficiency, for a higher industrial heat price

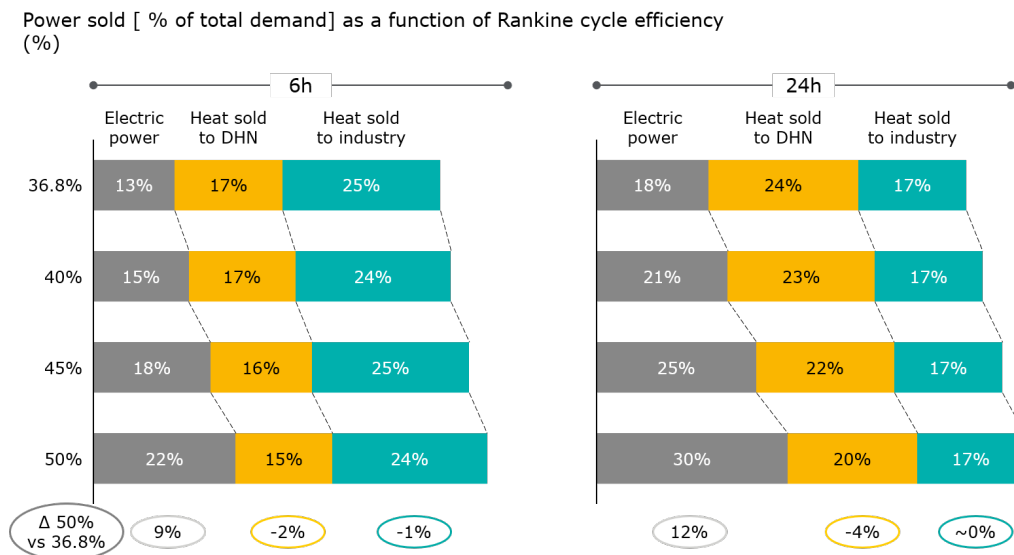


Figure C.10: P2H&P: sensitivity analysis of the electric and thermal discharged powers to changes in the Rankine cycle efficiency, for a higher industrial heat price

